The use of Stable Isotopes in the Investigation of Factors Affecting the Degradation of Phenol in Soil

Zöe Billings

A thesis submitted to the University of York for the degree of Doctor of Philosophy in the Department of Biology.

March 2007.

Abstract

Bioremediation is a rapidly developing area of environmental biology, offering a cost effective method for large-scale contaminant removal. Many current methods of bioremediation involve the use of culturable organisms. Cultureable organisms account for only a small fraction of the microorganisms present in the soil, and thus potentially environmentally relevant organisms may be going unnoticed that may offer more efficient results. Stable isotopes offer the potential to examine the role of unculturable organisms in bioremediation, with isotopic labelling of the lipid biomarkers, PLFAs, enabling organisms assimilating the label to the group level to be identified. DNA-SIP provides greater resolution of which organisms can be identified to the species level, whilst RNA-SIP further increases the resolution towards those species metabolically active independent of cell replication. The pollutant phenol's degradation pathways have been extensively studied. Culturable phenol degraders have been identified and here stable isotopes were used to examine what factors affect its degradation, encompassing the unculturable organisms.

Field studies demonstrated that additions of nitrogen (N) and biocide do not affect the rate at which phenol is mineralized over a 24 hour period in soils, only lime (L) additions resulted in soils responding initially significantly slower to the addition of phenol, with a lower cumulative phenol-derived CO_2 flux over 48 hours, tending towards significance. These differences became significant in treatments where vegetation was removed. PLFA analyses demonstrated only certain organisms were assimilating the phenol. Conversely, while control soils dominated the mineralization of phenol, the assimilation into PLFAs was dominated by the limed soils, by Gram-negative and fungal lipid biomarkers.

A second study in the laboratory revealed that differences in mineralisation seen in the field were not carried through into the laboratory. The differences in assimilation however, were robust and prominent in both the laboratory and field experiments. These results suggest that C limitation is a driving factor in reducing the mineralisation rates in the limed soil, whilst it is a community shift of microorganisms responsible for the differences in C assimilation from phenol.

Contents

Chapter 4. Nucleic acid and PLFA SIP; tools for identifying *in situ* phenol degraders in soils. **74-108**

List of Figures

List of Tables

List of Plates

Acknowledgements.

I wish to express my deepest gratitude to my two supervisors, Professor Phil Ineson and Dr Paul Chamberlain for all aspect in the production of this thesis. Phil has been a great source of enthusiasm and discussion throughout my four years, as well as being hugely practical, and Paul has been a great help and support during, and after, my time spent at CEH Lancaster, sharing his knowledge of PLFAs with me.

I also wish to thank several people for their help and support during the fieldwork campaigns, none of which have gone smoothly! Harry Vallack has provided a great deal of assistance during fieldwork at Sourhope, as has Dr Lisa Cole and Alison Grice. At the site Gordon Common has been invaluable in assisting with the practicalities of carrying out fieldwork in an area which is not the most hospitable and providing me with data from the weather station at the field site at Sourhope.

Mike Speed and his colleagues at Pro Vac have been extremely supportive, after constructing the worlds first mobile laboratory, assisting with the occasional (i.e. any time I go near it) problems and have always been eager to try and solve problems, even long range. Geoff Stimson from the biology manual workshops has been very helpful throughout my time at York, as have Steve Howarth and Trevor Illingworth from the biology electronics workshops.

The support and friendship of many members of the research teams has made my thesis all the more enjoyable, namely Andreas Heinemeyer, Lisa Cole, Tim Morrissey, Richard Skinner, Iain Hartley (thanks for all your help constructing the laboratory incubator!), Jo Leigh, Joana Zaragoza Castells. I also thank my family for their unwavering support throughout this thesis and for believing in me.

This work was supported by a NERC CASE studentship.

Declaration

No portion of the work in this thesis has been submitted in support of an application for another degree or qualification of this or any other institute of learning

Zöe Billings

Chapter 1. Introduction

1.1 Unculturable microbial populations and their role in biodegradation

A culturable microorganism is defined as one that can be grown and maintained on culture medium in the laboratory, with different organisms requiring different, and sometimes complex, media to grow successfully in the laboratory. Unculturable microorganisms are those that cannot, to date, be cultured in the laboratory away from their natural habitat.

Common methods of culturing microorganisms that degrade a particular substrate involve providing the substrate of interest as the only C or N source available to a dilution of putative microorganisms, derived as a suspension from an environmental sample. The organisms which subsequently grow on or in the culture medium are assumed to utilise the substrate of interest as their C or N source, and so can be identified as putative degraders of that substrate.

The vast majority of microorganisms present in the soil are not culturable in the laboratory, and the use of traditional culturing and identification methods alone ignores a huge and potentially very important range of microorganisms; the circularity is that only culturable organisms, making up only a small fraction of organisms present in the soil (Torsvik *et al.*, 1990), are only ever going to be identified. This inability to assess and realise the full potential of unculturable microbial populations is a recurring problem in the understanding, and application, of advances in the study of microbial ecology is the (Watanabe, 2001).

The relatively recent development of alternative molecular biological approaches is pushing through this traditional research barrier (see Watanabe and Baker, 2000). Modern molecular techniques have shown that microbial populations in the natural environment are much more diverse than microorganisms thus far isolated in the laboratory, (Boschker *et al.*, 1998), yet developments in environmental biotechnology have been largely dependent on studies with pollutant-degrading bacteria isolated using conventional culture methods (Watanabe and Baker, 2000). Researchers have now started to use molecular methods to analyse microbial populations relevant to pollutant degradation in the environment (see section 1.1.2). These techniques can be used

either individually, or in combination with other molecular ecological and physiological methods for identifying so-called, environmentally relevant microorganisms (ERMs) Watanabe and Baker (2000). The conclusion is that information provided by such analyses will aid in the evaluation of the effectiveness of bioremediation and will lead to the formulation of strategies to accelerate bioremediation techniques (Watanabe, 2001).

The increasing application of bioremediation approaches as a cost effective method for large scale contaminant removal is becoming one of the most rapidly developing fields of environmental restoration (Mishra *et al.*, 2001). A number of bioremediation strategies have been developed for the treatment of contaminated wastes and sites, utilising microorganisms to reduce the concentration and toxicity of various chemical pollutants in the environment. In particular, recent advances in the molecular genetics of biodegradation are opening up new techniques for the *in situ* treatment of environmental contaminants (Mishra *et al.*, 2001). With the large number of unculturable organisms present in ecosystems, it is therefore important that the potential of these organisms to be used in bioremediation research is explored. Methods to measure how such populations degrade substrates are of great use in determining the extent of their impact in such studies.

1.1.1 Traditional techniques for estimating microbial populations in soil

There are numerous traditional techniques available to quantify microbial growth and biomass. These traditional techniques are divided into four board categories: direct, microbial, respirometric and biochemical.

1.1.1.1 Direct methods

Direct method involves the counting of organisms, using a microscope, without subsequent growth or enrichment steps. The results are open to subjective interpretation and offer little resolution in terms of identifying the organism.

1.1.1.2 Microbial methods

Microbial methods are the most common traditional method and include plate counts and most probable number estimations

The agar plate technique, pioneered by Clarke (1965) is a common method, requiring a suspension of soil microorganisms to be plated onto growing medium in a dilution series and incubated for several days. The numbers are then counted on a dilution plate offering good resolution and the population estimated from that figure. The recipe for the medium can be adjusted to provide different nutrients, and alter the carbon source for example, however putative degraders may still be able to grow and the choice is limited by the available media and conditions that can be replicated.

Direct observation can be used in the most probable number method (MPN), first used by Alexander (1965), when aliquots of a soil suspension are diluted or alternatively, changes in a chemical or biological indicator can be used. The number of microorganisms present in the original sample can then be estimated using statistical tables, however it has been shown by Atlas (1982) that with a small number of replicates, the validity decreases. The aforementioned traditional techniques do however rely on the organisms being culturable, a pre requisite which, as highlighted above, will exclude a high percentage of the soil microorganisms.

1.1.1.3 Respirometric methods

Respirometric methods utilise organisms' ability to remove or produce specific gases, including O_2, CO_2 and methane. The technique was pioneered by Wallis and Wilde (1957) to measure total CO_2 production from a forest soil. Whilst this doesn't give a measurement of biomass, it does indicate the level of microbial activity.

Since then more complex techniques have developed including the fumigation incubation method (Jenkinson and Powlson 1976). Whereby soil samples are fumigated with chloroform vapour to kill the microbial population. The choloroform vapour is then removed and a small sample of untreated soil is

added to the fumigated soil, which is then incubated. The amount of CO_2 evolved by unfumigated control samples is subtracted from the CO_2 evolved by the fumigated samples, giving an indication of the amount of CO_2 being evolved by the microbial mineralisation of the killed population. The population's size can then be estimated.

Substrate induced respiration (SIR) was pioneered by Anderson and Domsch (1974) and involves the addition of a substrate to soil to increase respiration. The evolved CO_2 can then be measured and estimations of population size can be made, using the values from known populations as calibration. This method was further developed by Anderson and Domsch (1978) to allow SIR response to be related to microbial biomass by calibrating their method with Jenkinson and Powlson's fumigation method (1976).

1.1.1.4 Biochemical methods

Biochemical techniques involve the measurement of cell constituents, products or reactions mediated by a constituent part of the cell. Cell constituents measured include protein determination (Lowry 1951; Bradford 1976), however this is unsuitable for environmental samples (Atlas 1982), as the relative levels of protein in such samples can vary due to changes in population state and micro environments within the soil, rather than just population size.

Fatty acids and lipopolysaccharides, including phospholipid fatty acids (PLFAs) can be used as a measure of both population sie and cell type as different cell types contain different specific fatty acids in their cell membrane (Zelles *et al.* 1992).

1.1.2 Molecular methods

Molecular methods enable a large range of soil microorganisms to be included, being independent of culturing. DNA or RNA extraction provides a specific measurement of microbial populations within soil samples. Functional gene probes can be used identify key enzymes involved in a function of interest through highly conserved regions in their gene sequences. Primer sets are used to amplify these conserved regions of DNA (McDonald *et al.*, 1996), however these rely on the gene sequence for the function of interest having already been identified.

Soil samples undergo thermal shock, a sonic bath or microwave energy to lyse the cells. The DNA is then amplified using polymerase chain reaction (PCR) and visualised by electrophoresis on agarose gel containing ethidium bromide (Picard *et al.* 1992). Comparison of the band pattern with known microorganisms then allows microbes present to be identified. Picard *et al.* (1992) used this method to estimate the number of bacteria present in a soil sample. It is reliant on the primers being available for all the organisms of interest, otherwise they are excluded from the estimation.

More recently denaturant-gradient gel electrophoresis (DGGE) has been developed, which involves running proteins across a varying urea concentration in order to investigate their unfolding/refolding in the presence of a chaotropic agent. This enables the separation of DNA products from polymerase chain reaction which are of similar size, and thus would not separate during traditional agarose gel electrophoresis. DGGE separates DNA fragments based on sequence differences that result in differential denaturing characteristics of the DNA. Resulting sequences can be matched to a library of known phylogenies, however the number of proteins to which this has been applied is limited (Gianazza *et al.*, 1998)

Other modern methods to examine entire microbial populations include probing PLFAs (Boschker *et al.,* 1998) and nucleic acids (Radajewski *et al.,* 2000) with stable isotopes and, most recently, bioluminescence, whereby luminescence-based bioassays are used to measure ecotoxicity, and has been found to offer complementary applications to traditional testing techniques (Trott *et al.,* 2007).

1.2 The history of SIP using PLFAs

1.2.1 SIP

Stable isotopes of the same element differ only in the number of neutrons, they share the same chemical characteristics and behave almost identically, with fractionation occurring due to the slight variation in the overall mass. Unlike radioisotopes, which degrade, stable isotopes remain and do not pose any additional health risk. Stable isotope probing (SIP) involves the use of a stable isotope biomarker to trace substances and establish functional transfers through a system. It provides a unique method of being able to directly link an organism to a function, reducing the possibility that putative organisms are falsely linked to a particular process. The main advantage of stable isotopes over radioisotopes is that they can be freely used in field situations, since they do not pose any safety or contamination concerns, other than the inherent ones associated with the compound under study. The use of radio labelled substrates (for example, ^{14}C) in the field is greatly restricted due to safety and environmental regulations. The location of the SI and it's subsequent metabolism can be tracked both in the environment and within the organisms using the compound as part of it's metabolism (using IC-GC-IRMS) with different parts of the cell retaining the SI, including cell membranes and nucleic acids.

Biomarkers are compounds that are unique to a limited number of organisms, with the presence or absence of such biomarkers indicating that an organism is active. In order to give an accurate indication of activity, a biomarker must quickly disappear from the system after cell death (White *et al.*, 1979). Phospholipid fatty acids (PLFAs) are specific cell membrane components of microorganisms and account for a large proportion of the cell biomass and, as such, can be used to investigate and evaluate the activity of microbial communities (Zelles, 1999). Different phylogenies tend to have distinct PLFA 'fingerprints' and a labelled PLFA trace fingerprint can be compared to the known library of PLFA fingerprints and a phylogeny accordingly assigned.

The linking of these techniques to label PLFA's with SI's is an extremely versatile approach as, not only can it be used safely either in the laboratory or the field due to the absence of radioactive isotopes and associated restrictions, but

also the label can be introduced to the system of interest in a number of ways. For example, label can be presented as a gas, e.g. $^{13}CO_2$, entering the system photosynthetically via a plant (Staddon, 2004), or alternatively it may be introduced as a compound, presented in solution (Padmanabhan *et al.*, 2003). It is also possible to prepare labelled biologically-derived materials, such as litter, for decomposition studies, and there is a growing wide range of commercially manufactured compounds available (e.g. 99% $^{13}C_6$ phenol, Cambridge Isotope Laboratories, UK). These compounds tend to be expensive, but IC-GC-IRMS is a highly sensitive precision instrument and can detect and measure very small isotopic changes, thus reducing the amount of substrate needed.

1.2.2 Development of the SIP/ PLFA technique

Boschker *et al.* (1998) first used a stable isotope (^{13}C) to directly link a microbial population to a biogeochemical process, using this approach. Active microorganisms turn over their cellular components, including cell membranes, and Boschker *et al.* (1998) showed that, by adding a substrate with an isotopic label, the organisms responsible for degrading either a part or a whole substrate incorporated the stable isotope label into the PLFAs. The PLFAs were then extracted and analysed using an individual compound gas chromatograph, coupled to an isotope ratio mass spectrometer (IC-GC-IRMS). Boschker *et al.* (1998) used this method to identify the degraders of ^{13}C acetate as being similar to *Desulfoltomaculum acetoxidans,* a Gram-positive bacterium, rather than the more studied Gram-negative *Desulfobacter* species, suggesting that the focus of research should include these Gram-positive bacteria in future work. In a second experiment, further pioneering this technique, Boschker *et al.* (1998) also added ^{13}C methane to the top layer of a freshwater sediment. The organisms that assimilated the methane and incorporated the label in to their PLFAs were identified as belonging to the type 1 genera *Methylobacter* and *Methylomicrobium*, therefore unambiguously linking these organisms to the process of methane assimilation. Since 1998 this technique has been widely used with ^{13}C both in the laboratory and in the field, utilising both natural variations in isotopic signal in compounds (Hinrichs *et al.,* 1999), or introducing a strong label into the environment (Staddon, 2004)..

Carbon is not the only element to have been successfully used as an isotopic label in PLFAs. Alexandrino *et al.* (2001) used deuterated styrene ($^2H_8$) to characterise styrene degrading populations from biofilters used for waste gas treatment. After three days incubation with $^2H_8$ styrene, the PLFAs in the degraders contained up to 90% dueterated molecules, with the largest amount of label incorporated into an organism with a *Pseudomonas* – like fatty acid profile in the experimental biofilter. However, in the full scale biofilter, the labelled PLFAs suggested an unknown styrene degrader, whilst the absence of label in certain PLFAs indicated that organisms belonging to the species *Xanthomonas*, *Bacillus, Streptomyces* and *Gorgonia* were not responsible for the degradation of styrene.

It is important when examining degradation pathways that one can be confident the organism identified from the ^{13}C PLFA profile is the primary degrader, responsible for metabolism of the labelled substrate. The timing of the sampling is therefore crucial to ensure that secondary organisms (i.e. those which consume primary organisms or secondary products) are not misidentified as primary. The turnover of PLFA, and therefore incorporation of label, can be quite rapid, depending on the level of microbial activity; Pombo *et al.* (2002), for example, found detectable ^{13}C PLFA levels as little as 4 hours after incubation with a labelled substrate and, as mentioned above, Lu *et al.* (2004) found ^{13}C PLFA enrichment in samples taken within an hour after the end of a 6 hour $^{13}CO_2$ pulse.

1.2.3 Laboratory use of SIP / PLFA

Butler *et al.* (2003) pulse labelled annual ryegrass under $^{13}CO_2$ in a greenhouse at two stages of development, the stage of transition between active and rapid root growth, and during rapid root growth. They analysed the PLFAs from the rhizosphere and bulk soil, and found that the fungal biomarker 18:2(n-6) showed the fasted and highest incorporation of photo-assimilate, whilst the Gram-positive biomarkers i15:0 and a15:0 were most active during the first growth stage, and the Gram-negative biomarker, 16:1(n-5), were found during the second grown stage. Similarly, Lu *et al.* (2004) used a $^{13}CO_2$ pulse for 6 hours to establish the links between rice plant photo-assimilate and the rhizosphere

microbial communities. In this microcosm experiment, replicate microcosms were pulsed at six different development stages of rice, and were then sampled destructively within an hour of the end of the pulse. The mean $^{13}CO_2$ concentrations inside the chamber during the pulses were between 180 and 270 ppm, accounting for between 24 and 57% of the total CO_2 concentration inside the chamber. The incorporation of the ^{13}C into the PLFAs was seen immediately (within 1 hour) demonstrating the tight link between the photo-assimilate and microbial activity. A higher proportion of the ^{13}C was incorporated into the straight chain fatty acids, 16:0, 16:1(n-7), 18:1(n-7) and 18:1(n-9), than the branched chain fatty acids, with a seasonal increase in the total PLFAs, most notably 18:1(n-7), 18:1(n-9) and 16:0. These findings suggested that rice plants promoted increased microbial activity and specific shifts in the soil microbial community.

This method of label introduction has also been used to examine the different responses of an organism under different conditions and the resulting variations in the use of plant-derived C. Gavito and Olsson (2003) labelled *Plantago lanceolata* L. with $^{13}CO_2$, in a greenhouse experiment, to examine how arbuscular mycorrhizal fungi (AMF) allocate photo-assimilate under different inorganic and organic nutrient amendments. They used the 16:1(n-5) fatty acid biomarker to represent the AMF lipids being recognised as the dominant AMF-specific storage lipid. The incorporation of the label into this signature fatty acid, combined with measuring hyphal length density, demonstrated that the proliferation of the AMF extraradical mycelium occurred in all their amended treatments, relative to the unamended treatments.

Hanson *et al.* (1999) used the technique of labelling the PLFAs with a stable isotope tracer to identify the populations responsible for the degradation of toluene, a widespread pollutant. Toluene has been well studied in the laboratory and its biodegradation pathways have been characterised, although most of the work has been carried out using *Pseudomonas* species. The aim of Hanson *et al.* (1999) was to use labelled toluene to identify the native populations of toluene degraders in Yolo silt loam. This soil was collected from the field and transferred to microcosms, pulsed with ^{13}C toluene and the PLFAs extracted and analysed. Out of the 59 PLFAs detected, only 16 were labelled with ^{13}C and the results indicated that the degradation was carried out by a population with a similar

PLFA trace to the genera *Rhodococcus*, rather than *Pseudomonas,* and suggested further targeted research for possible bioremediation.

1.2.4 Field use of SIP

One example of field use is incorporating $^{13}CO_2$, via photosynthesis, into plants and following the signal as it transfers, as exudates, to the below-ground community. This results in a microbial community that may be highly labelled (Staddon, 2004); a contrasting example is the direct addition of highly labelled commercially produced substrates to soils (Padmanahban *et al.*, 2003).

The naturally low level of enrichment of ^{13}C in methane was utilised by Hinrichs *et al.* (1999) to examine methane consumption in marine sediments. They took sediment samples from a methane seep in Northern California and compared the lipid biomarkers in the sediments with those of control sediments. PLFA analyses showed that two ether lipids were present in the methane seep sediments, which were specific to archea, and were not present in the control samples. The authors looked at the level of ^{13}C in the archeal biomarkers, depleted by more than 70‰ relative to primary products, and concluded that the only source of C, depleted sufficiently in ^{13}C, was methane. These PLFA results, together with parallel gene surveys of small subunit ribosomal RNA (16S rRNA), suggested that the methane was consumed by archaebacteria that are phylogenetically distinct from known methanogens. This clearly demonstrated the use of ^{13}C PLFA approaches at natural abundance labelling.

Ostle *et al.* (2000) were the first to introduce in situ ^{13}C labelling to below-ground systems through the application of a pulse of $^{13}CO_2$ at 350 ppm, the photoassimilated ^{13}C entering the below-ground community by fixation in photosynthesis and subsequent exudation in plant roots. This provides the most direct approach to identifying which organisms in the below ground community directly utilise plant root exudates.

The introduction of a ^{13}C label into below-ground ecosystems via photosynthesis has also been successfully demonstrated in the field. In 2004, Treonis *et al.* used stable isotope probing to label grassland soils *in situ* with $^{13}CO_2$ for 5 hours at ambient concentration to identify which microbial groups were actively involved in the assimilation of root-derived C in limed grassland

soils. ^{13}C-enrichment of PLFAs was seen at 4 and 8 days after pulsing with $^{13}CO_2$, with the fungal biomarkers 18:1(n-9) 18:2(n-6), and Gram-negative bacterial biomarkers 16:1(n-7), 18:1(n-7) and 19:0cy showing the highest enrichment, turning over more rapidly than the Gram-positive bacteria biomarker lipids (a18:0, i15:0 and 16:0). Based on the ^{13}C-enrichment of these PLFAs, the conclusion was drawn that the imposed liming treatment had not affected the turnover rates of ^{13}C labelled C, or which organisms utilised the photo-assimilate.

The most widely used method for introducing a stable isotope into a system is to introduce a highly labelled, commercially produced, substrate. The ability to provide compounds at enrichment levels of up to 99% increases the probability of sufficient quantities of the label being incorporated into the biomarkers to be detectable. Whilst, as mentioned above, these compounds are relatively expensive, the high level of label means that the amount of substrate needed is small. In a temperate forest soil it has been demonstrated by Bull *et al.* (2000), using the techniques pioneered by Boschker *et al.* (1998) with $^{13}CH_4$ as the substrate, that PLFA profile labelling can be achieved at high enrichment and low concentration; this particular study revealed a novel methanotroph, similar to type 2 methanotrophs, as an important microorganism in atmospheric methane oxidation in these soils.

Pelz *et al.* (2001) combined tracing the incorporation of ^{13}C into cell fatty acids with whole cell hybridisation to identify toluene-assimilating populations in PHC-contaminated freshwater aquifers under sulphate reducing conditions. The highest ^{13}C-enrichment was found in the PLFA 16:1(n-5) and ^{13}C-enriched biomarkers, characteristic for the genera *Delsulfobacter* and *Desulfobacula* (cy17:0 and 10Me16:0), rather than the other sulphate-reducing general *Desulfovibrio* and *Synthrophobacter*, suggesting that it was the *Delsufobacter* and *Desulfobacula* responsible for the assimilation of toluene in PHC-contaminated freshwater aquifers. This was supported by whole cell hybridisation work and provided important information regarding the use of *Delsufobacter* and *Desulfobacula* populations in bioremediation of PHC-contaminated freshwater aquifers.

Crossman *et al.* (2005) used SIP, combined with PLFA and bacteriohopanoid analyses to characterise methane-oxidising bacteria in soil,

after incubating sieved forest soils with $^{13}CH_4$. They found evidence to suggest a novel population of methane-oxidising bacteria related to the type II culturable methanotrophs *Methlocapsa* and *Methylocella* genera of bacteria with 18:1(n-7) being enriched, but also finding enrichment of i17:0. Crossman *et al.* (2006) continued this work with methanotroph bacteria in soils, studying the effect of ammonium sulphate on the microbial population oxidising ambient methane in the field using SIP combined with PLFA analysis; they found that ammonium sulphate treatment reduced the amount of ^{13}C incorporation in the majority of PLFAs, with the exception of *i*17:0 in the presence of high concentrations of methane. This suggested a shift in the functional community, which could not have been detected using conventional non-isotopic apparatus.

The use of stable isotope as a tracer, to investigate either element fluxes through ecosystems or degradation pathways of xenobiotics, offers the potential to move away from the constraints of studying these processes using culturable organisms only, and also enables field studies outside the laboratory. However, the main limitation of the techniques, as pioneered by Boschker *et al.* (1998), is the resolution of the tool in identifying the populations of interest. While PLFA profiles can generally be matched to those in a microbial group, who share characteristic PLFA patterns, they rarely offer the means to identify the responsible organisms down to the species level. To this end, techniques that rely on the higher resolution provided by nucleic acids are currently being developed (Radajewski *et al.* 2000, Manefield 2002a).

1.3 SIP using nucleic acids

Radajewski *et al.* (2000) developed a technique which they specifically named stable isotope probing (SIP). This used the same principles as Boschker, whereby a substrate with a stable isotope label is added to the potential organisms of interest but, whereas Boschker *et al.* (1998) looked at the label incorporation into the PLFAs, Radajewski *et al.* (2000) used DNA as the incorporation biomarker. The semi-conservative nature of DNA replication was revealed by Meselson and Stahl (1958), based upon the ready incorporation of ^{15}N into microbial DNA, followed by density ultra-centrifugation. Radajewski *et al.* (2000) used SIP to identify the organisms responsible for the assimilation of methanol as a carbon

source in a temperate forest soil. The technique relies on the separation of ^{13}C labelled DNA from unlabelled ^{12}C DNA, by ultra-centrifugation using a self-forming gradient, such as CsCl. The heavier carbon isotope labelled DNA, when bound to ethidium bromide in the ultra-centrifuge tube, separates from unlabelled ^{12}C DNA, forming bands which can be removed by subsequent fractionation of the gradient down the centrifuge tube, See Fig. 1.1.

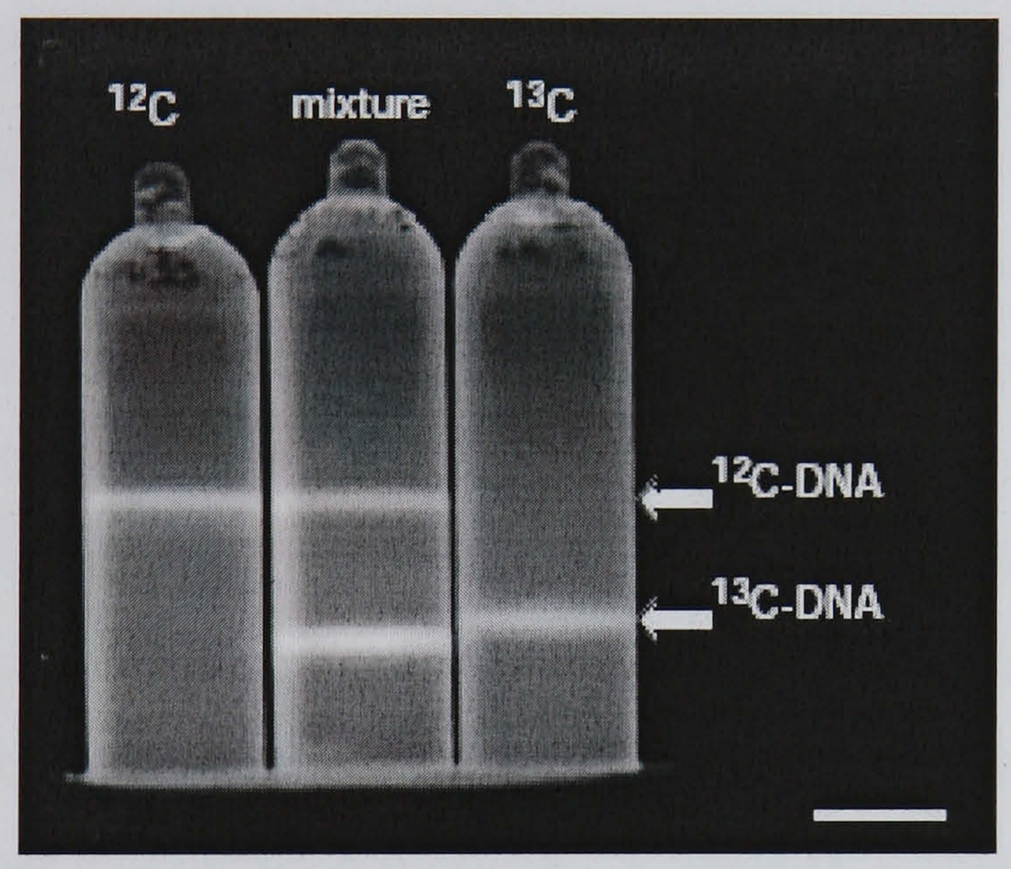

Figure 1.1 Equilibrium centrifugation of isotopically labelled DNA in CsCl/ethidium bromide density gradients, pure fractions and a mixture of the DNA extracted from a *M. extorquens* AM155 culture utilizing either ^{12}C- or ^{13}C-methanol as the sole carbon source. (Reproduced from Radajewski *et al.,* 2000)

Padmanabhan *et al.* (2003) used SIP to look at the *in situ* degradation of four compounds; glucose, phenol, caffeine, and naphthalene in the field using 16rRNA gene analysis of ^{13}C labelled DNA. Using general bacterial primers for PCR, together with cloning, they retrieved sequences from 11 bacterial genera with overlapping niches (6 glucose, 6 phenol, 4 caffeine and 3 naphthalene). They identified 10 of the genera as known isolates of chemo-organotrophs found in soil, water and sewage, whilst the 11^{th} was already known from environmental samples. These data demonstrated a high degree of similarity between organisms that are known pollutant degraders, determined using culture dependant studies,

and those found by culture independent methods; this indicates that, although much of the soil DNA is not identified and is not from culturable organisms, the environmentally important organisms involved in the degradation of these four compounds, on this occasion, were those which have already been isolated and cultured.

However, the use of nucleic acid SIP is not without limitations. The separation of the labelled and unlabelled i.e. heavy and light biomarkers relies on density gradient ultra-centrifugation and the biomarker must incorporate significant isotopic enrichment to achieve adequate separation. DNA is relatively slow to incorporate a strong signal relative to other cellular components and the incorporation of any enrichment is dependent on the organism actively replicating during the pulse (Manefield *et al.*, 2002a; Radajewski *et al.*, 2003). The use, therefore, of RNA as a biomarker poses obvious potential advantages over DNA. Due to its high turnover rate, RNA should incorporate a more rapid and stronger isotopic enrichment, leading to good separation from unlabelled biomarker during ultra-centrifugation. Also, because RNA replication is independent of cell replication, it offers a higher resolution of target organisms.

Manefield *et al.* (2002b) used stable isotope probing with RNA to examine organisms involved in the degradation of labelled phenol in an aerobic industrial bioreactor by adding $^{13}C_6$ phenol into the bioreactor containing heavily polluted waste water (> 200 μg phenolic compounds per ml). The bacterial RNA was subsequently extracted from the reactor, and the light, unlabeled RNA was separated from the heavy labelled by equilibrium density gradient centrifugation. RNA samples from the heavy fraction were then reverse transcribed and the resulting PCR products were subjected to DGGE, followed by cloning and sequencing. The bacterial strains developing in the bioreactor were *Pseudomonas putida* BS564 and *Pseudomonas chloroaphis* BS523, both strains being known and culturable phenol degraders. The bacterial sequences produced from the clones revealed that, rather than the mixed *Pseudomonas* species being responsible for the majority of the phenol degradation, the degradation was in fact dominated by a *Thauera* species, clearly illustrating the potential advantages of using SIP for determining the role of unculturables.

Prosser *et al.* (2006) have since reviewed the use of DNA-SIP as a tool for studying plant-microbe interactions, highlighting it's potential for studying specific interactions combined with the use of RNA-SIP.

1.4 The microbial degradation of phenol

Phenol (C_6H_6O; hydroxybenzene) is an aromatic hydrocarbon commonly extracted from the distillation of coal tar, and also synthetically produced through several processes, including the oxidation of cumene or toluene (van Schie and Young, 2000). Phenol also occurs naturally in all plant material, being a major constituent of lignin and, as plant material decays, the lignin is broken down and phenol is released. However, the amount released into the soil from natural sources is a fraction of that released from anthropogenic sources (van Schie and Young, 2000). Phenol is a common industrial pollutant, contaminating sites associated primarily, with the manufacture of plastics, the petrochemical industry, chemical storage, manufactured gas plants, the manufacture of steel, textiles and pharmaceuticals as well as sites involved with creosote and wood preserving (Guerin 1999).

Phenol is highly mobile in the soil environment and most commonly is transported into the soil environment through leaching into ground and surface water, for example it is discharged into the environment via wastewater effluent from a number of manufacturing processes, as well as the excessive use of pesticides (Jensen 1996). This leaching of phenol and phenolic compounds from industry presents a major biological problem, since many phenolics are known to be carcinogens and have been declared harmful pollutants. All industries that use or produce phenol will, at some point, inevitably release traces into the environment where it may taint potable water, producing an unpleasant aroma; it also reacts during chlorination or water, forming chlorophenols, which are suspected carcinogens (van Schie and Young 2000). Current methods of remediating areas contaminated with phenol include physiochemical processes, such as passing aqueous effluents containing phenol over activated charcoal, and also biological processes. With any of these processes there are also the associated risks of releasing secondary pollutants (Annadurai *et al.*, 2002, Chen *et al.*, 2002).

The concentration found on a background level in soil is poorly documented, which WHO (1994) suggested was due to phenol being unlikely to persist in soil because of rapid biodegradation or transport to either groundwater or air. This view was supported by the Agency for Toxic Substances and Disease Registry (ATSDR, 1998) who also considered that elevated soil concentrations of phenol are likely to be the result of localised spills of historic industrial use The WHO (1994) reported phenol concentrations up to 13 $mg.kg^{-1}$ from surveys of lake and river sediments across the USA

Phenol is acutely toxic to many organisms and it's relatively high water solubility (8.3g / 100 ml at 20°C) leaves aquatic ecosystems vulnerable. It is weakly acidic thus its ionised form is susceptible to electrophilic substitution chemical reactions, however the USEAP (1996) estimates that at a pH of 8, approximately 99 % of phenol will exist in the neutral form. Phenol has a relatively low vapour pressure, 48 Pa, at 20°C, resulting in it being a highly volatile substance, though, to a limited extent it can sorb to soil organic matter, reducing both its transport and volatilisation. (Environment Agency 2005)

Additionally, phenol has well known antimicrobial properties and is widely used as a topical antiseptic, with the main effect being on microbial cell membranes, disrupting them to increase fluidity and, potentially, resulting in cell death. However, a number of microorganisms have become resistant to the bactericidal effects of phenol, primarily as a result of changes in their cell membranes. These bacteria which are resistant to the bactericidal effects of phenol therefore offer a method of removing phenol contamination.

Phenol is degraded by organisms both aerobically and anaerobically, under both these conditions the half life of phenol in soil and groundwater ranges considerably. USEPA (1999) reviewed a wide range of studies, many of which were conducted under optimal laboratory conditions and estimated the half life of phenol in soil to be 3.5 days. Whereas Mackay *et al.* (2000) reported a range of aerobic degradation half-life values from under 24 hours to 23 days in soils. In groundwater the Environment Agency (2002) reported aerobic degradation half-life values in groundwater ranging between 10 and 100 days and anaerobic degradation half-life values from 50 to 300 days and suggested that aqueous concentrations of phenol above 0.5 gl^{-1} would prove toxic to phenol degrading organisms.

The aerobic pathway of phenol degradation is now firmly established and has been well documented. The first step in the pathway is the conversion of phenol to catechol, by the enzyme phenol hydroxylase using mono-oxygenase. A hydroxyl group is added, *ortho* or *para* to the existing hydroxyl group and the resulting catechol can then be degraded by either the ring being cleaved between or outside the two hydroxyl groups (see Fig. 1.2). Intradiol cleavage (the *ortho* pathway) converts catechol by cleaving between the two hydroxyl groups, using the enzyme 1,2-dioxygenase to form *cis*, *cis*-muconate, which enters the Krebs cycle after further conversion. This is the phenol degradation pathway generally utilised by eukaryotes. The extradiol pathway is utilised by prokaryotes for the degradation of phenol. Extradiol or *meta* cleavage (the α-keto acid pathway) of phenol occurs outside the two hydroxyl groups, adjacent to one of them, catalysed by catechol 2,3-dioxygenase, forming 2 hydroxomuconate semialdehyde. This is then oxidised to form *cis* 2-hydroxypenta 2,4-dienoate, then 4 hyroxy-2-oxovalerate, before being converted into pyruvate and acetaldehyde, and entering the TCA cycle (Schlegel, 1993). The intradiol pathway was illustrated by Neujahr and Gaal (1973) for *Trichosporon cutaneum*. These authors found that the addition of phenol to laboratory cultures of *Trichosporon cutaneum* resulted in activities 50–400 times higher than for non-induced cells, for phenol hydroxylase, catechol 1,2-oxygenase and cis,cis-muconate cyclase. The use of eukaryotes to degrade phenol on a commercial scale is currently an area of industrial development with Chang et al. (1998) reporting that in the yeast *Candida tropicalis* complete phenol inhibition of the fungus does not occur until 3,300 mgl^{-1} whilst Leitão *et al.*, (2007) also found *Penicillium chrysogenum*, a halotolerant fungus, capable of degrading phenol with no accumulation of toxic intermediates. Hinteregger *et al.*, (1992) found that the addition of phenol to laboratory cultures of *Pseudomonas putida EKII* resulted in high levels of catechol 2,3-dioxygenase as well as smaller amounts of 2-hydroxymuconic semialdehyde hydrolyase and catechol 1,2-dioxygenase, demonstrating it was the extradiol pathway being utilised. These pathways are shown in Fig. 1.2.

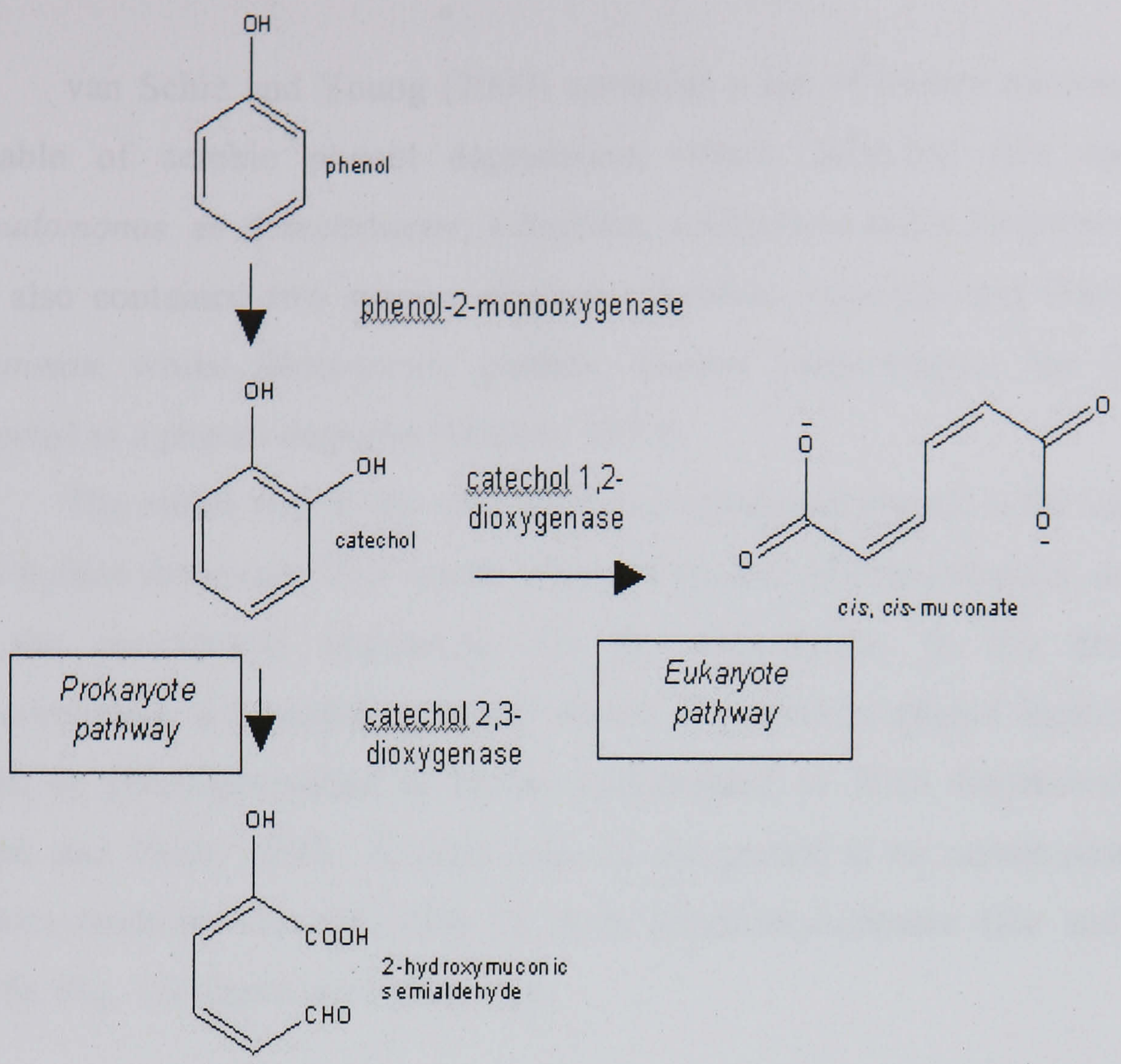

Figure 1.2 The aerobic pathways of phenol degradation.

van Schie and Young (2000) compiled a list of known microorganisms capable of aerobic phenol degradation, which identified five species of *Pseudomonas,* an *Acinetobacter,* a *Bacillus,* a *Ralstonia* and a *Streptomyces*. The list also contained two species of yeast; *Candida tropicalis* and *Trichosporon cutaneum,* whilst *Rhodotorula glutinis,* another yeast species, has also been reported as a phenol degrader (Walker, 1973).

The initial step in the anaerobic degradation of phenol is the conversion to 4-hydroxybenzoate. This can be achieved via one of two pathways, depending on the organism(s) responsible for the degradation. In the denitrifying *Pseudomonas*, a phosphate group is added to phenol by phenol kinase and the resulting phenylphosphate is further metabolised to form 4-hydroxybenzoate (Lack and Fuchs 1994). Another route is for phenol to be carboxylated by 4-hydroxybenzoate decarboxylase to form 4-hydroxybenzoate (He and Weigel 1995). Fig. 1.3 shows these pathways.

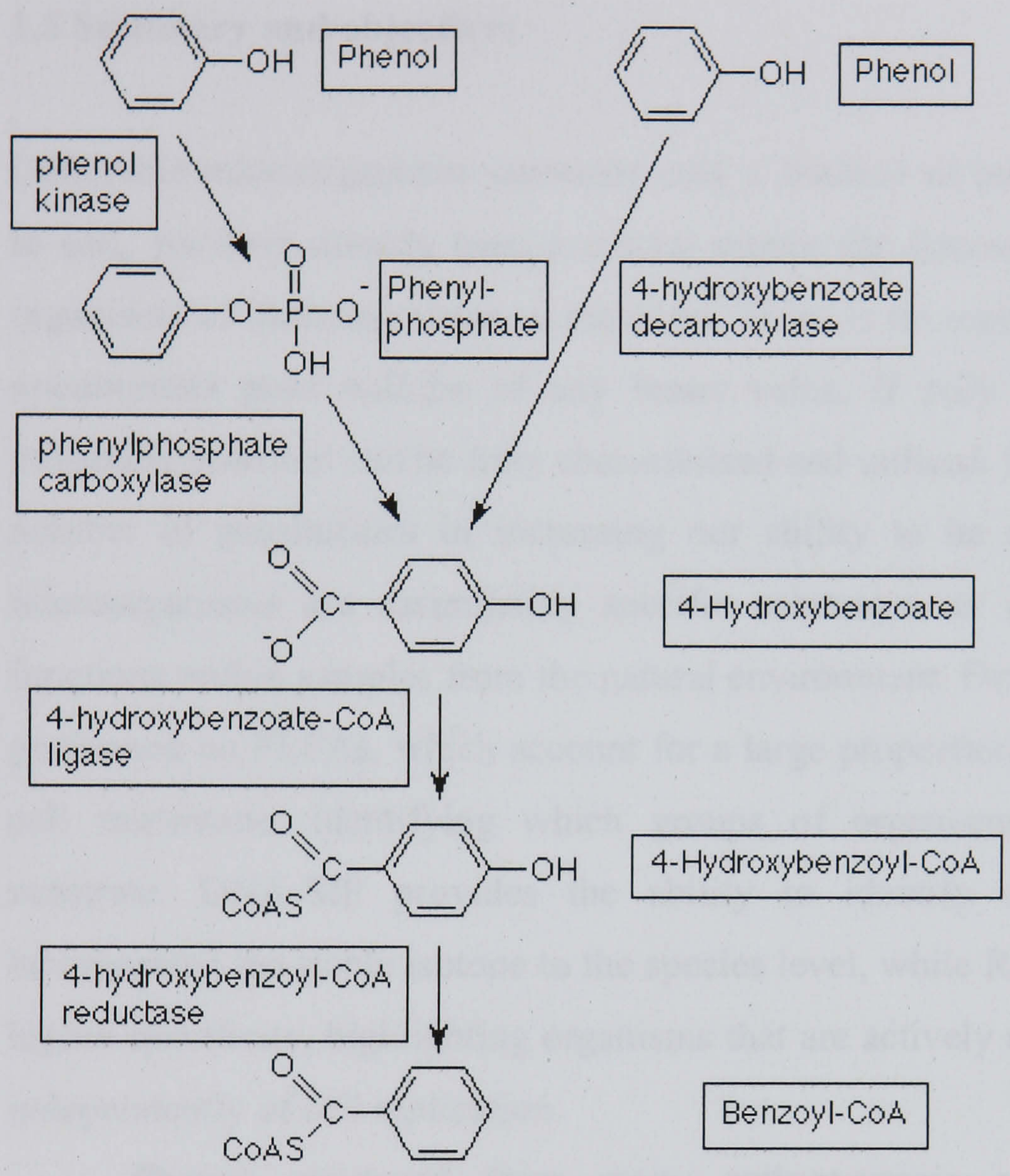

Figure 1.3 The anaerobic pathway for phenol degradation.

Known microorganisms, capable of anaerobic phenol degradation include bacteria from the *Thauera*, *Azoarcus*, *Desulfobacterium*, *Desulfomaculum*, *Desulfovibrio* and *Geobacter* genera (van Schie and Young 2000).

1.5 Summary and objectives

Culturable microorganisms represent only a fraction of microorganisms present in soil, yet have already been a crucial source for discovering and developing organisms of immense value to mankind. There is no reason to believe that the unculturable pool will be of any lesser value, if only the full genetic and metabolic potential can be fully characterised and utilised. Stable isotopes offer a number of possibilities in increasing our ability to be able to detect which microorganisms are assimilating specific substrates, or carrying out specific functions within samples from the natural environment. For example, SIP can be performed on PLFAs, which account for a large proportion of a microorganisms cell membrane, identifying which groups of organisms are assimilating a substrate. DNA-SIP provides the ability to identify organisms that have incorporated the stable isotope to the species level, while RNA-SIP enables even higher specificity, highlighting organisms that are actively assimilating the label, independently of cell replication.

Phenol, produced from many anthropogenic sources, presents an important environmental problem, particularly when spillages or leakages from industry occur. Methods for remediation of areas contaminated by phenol are needed, particularly utilising techniques which are effective at destroying the molecule without the risk of creating secondary pollutants. Within this context, SIP offers the potential of identifying novel phenol degraders, which may in turn, be utilised in the bioremediation of phenol. This study aims to utilise the ^{13}C stable isotope of C in the field, to examine both the factors and organisms which are important in controlling the degradation of phenol in soils.

The specific hypotheses to be tested in this thesis were:

1. **The experimental treatments at Sourhope affect the degradation of substances applied to the soil.**
2. **The effect of treatments on the soil populations will be robust and not affected by vegetation.**
3. **The microbial community will not respond universally to the addition of phenol.**
4. **The behaviour of soils in laboratory incubations will complement *in situ* responses to phenol addition.**

2. Examining the impact of lime, nitrogen and biocide on the degradation of substrates *in situ* using stable isotopes

2.1 Introduction

In 1997 the NERC Thematic Research Programme 'Biological Diversity and Function in Soils' established at an experimental upland grassland site on the Scottish borders, at Sourhope (55°28'32"N, 2°14'43"W, OS grid ref NT855197). There were six main aims of the programme. Firstly to quantify the taxonomic and metabolic diversity of key groups in the soil biota in a single ecosystem, sufficient to provide a basis for an experimental programme to determine the role of soil diversity in ecosystem processes. Secondly, to extend taxonomic understanding of the soil biota, especially by using isolation and molecular techniques to examine hitherto poorly characterised groups. The third aim was to characterise the roles played by all major groups within the soil biota (including root–microbe associations) in ecologically important processes in carbon (C) and nitrogen (N) cycles in soil, including the development of C sinks, determining the pathways and rates of movement of C through components of the soil foodweb. The fourth aim was to determine (both experimentally and by comparison of contrasting sites) the extent to which depauperation of the soil biota would reduce the ability of the soil to provide essential ecosystem services, including the ability to cope with anthropogenic inputs. The penultimate aim was to conduct parallel manipulations of major taxonomic groups of soil biota under controlled conditions. Finally, there was the sixth aim of determining the extent to which indicators of soil biodiversity can be used as measures of soil ecosystem resilience, relevant to land use management.

Consequently, the Sourhope site has been the centre of extensive soil biological research over the last decade, resulting in a wealth of information on the abiotic and biotic status of this area of the UK uplands. Such upland grassland habitats represent a large proportion of hill ground in the UK and previous work, particularly by Bardgett *et al.* (1996, 1997), has demonstrated that, compared to improved grasslands, unimproved grasslands (such as Sourhope) have a greater microbial diversity, making it more suitable for experiments examining the above- and below-ground communities. The

Sourhope site (see Plate 1), had not been subject to any additions of lime or fertilizer in recent history, and fencing has excluded grazing animals from the site since summer 1998. The treatments applied to the site were designed to be similar to those applied for pasture improvement or to specifically alter soil biodiversity, resulting in four experimental treatments: lime ($CaCO_3$, 600 g m^{-2} y^{-1}), N (12 g m^{-2}, twice a year), N and lime (same quantities as for individual applications) and biocide (Dursban 1.5 litres per hectare, 5 times a year, 36 cm^3 in 10 litres water per plot). There were also two Control treatments, Control 1 and Control 2 which were identical (there being two purely to enable enough Control treatment area for all experiments) and had no additional treatments.

Fitter *et al.* (2005) reviewed the findings from the experiments conducted at Sourhope focusing on biodiversity and ecosystem functioning in soils. Combining results from various studies at the site, Fitter *et al.* (2005) provided an overview of the high level of diversity of "small" organisms present at Sourhope with over 100 bacterial species (McCaig *et al.*, 2001), 365 protozoan species (Finlay & Fenchel 2001), ca. 140 species of nematode (Floyd *et al.*, 2002) and 24 distinct types of arbuscular mycorrhizal fungi (AMF) (Vandenkoornhuyse *et al.*, 2002). Interestingly, despite the extreme diversity of "small" organisms at Sourhope, this was not the case for the larger soil organisms (Davidson *et al.*, 2002).

Stable isotopes have already been used extensively at the site; $^{13}CO_2$ pulse labelling has also been utilised at Sourhope, with highly enriched $^{13}CO_2$ at ambient concentration being used to trace the path of atmospheric C through the ecosystem (Staddon, 2004). Ostle *et al.* (2002) found that within 48 hours of the pulse, over 70% of the labelled C had been returned either through respiration or as plant exudates, Johnson *et al.* (2002) detected labelled C in AMF as little as an hour after a short pulse of $^{13}CO_2$. Chapter 2 describes the application of a ^{13}C-phenol pulse to the soil surface in four treatments at Sourhope (Control, L, N and B) in order to determine the way in which the treatments influenced the degradation of an anthropogenically produced substrate applied *in situ*. Using the same approach the application of ^{13}C-glucose to the soil surface in the same four treatments under investigation, to determine if the treatments had the same influence on the degradation of a more natural C source. Finally, a $^{13}CO_2$ pulse

was applied to a darkened area of soil in Control and L treatments to determine if the chemical differences in the treatments influenced the return of the gas.

The experiment described in this Chapter coincided with a major fieldwork campaign at the site, with a number of research groups working towards common objectives. Due to delays in its construction a new custom built mobile laboratory was deployed without extensive pre-testing and the work described here was the first experiment using the mobile laboratory. The unique opportunity of working in a campaign with other research teams during this campaign was felt to negate the potential risks of commissioning the laboratory in the field, when relatively untested.

2.1.1 The mobile laboratory: research and development

In 2000 the UK Natural Environment Research Council (NERC) agreed to fund the construction of a unique field-based laboratory system for the *in situ* determination of carbon-13 stable isotope composition of CO_2 air and soil fluxes. The system comprised a customised gas chromatograph isotope ratio mass spectrometer (GC-IRMS) dedicated for $^{13}CO_2$ determination, customised to work under field conditions, with continuous gas flow through 16 air sampling lines, designed to work automatically, without user intervention, allowing semi-continuous sampling for periods of up to several days.

The resulting laboratory was the first mobile GC-IRMS ever to be constructed and involved the design and commissioning of an appropriate mobile housing for the GC-IRMS. The structure of the laboratory itself was a modified twin-axle trailer unit (Indespension Ltd., Bolton, U.K.) fitted with temperature controlled heaters and wall extraction fans to maintain constant laboratory temperature (ca. 15°C) for optimum GC/GC-IRMS operation. Reliable laboratory temperature regulation over a wide range of ambient conditions was possible, given adequate insulation and correct positioning of fans, heating and cooling systems within the laboratory. The laboratory had side and rear access doors, containing fixed conventional laboratory benching and anti-vibration mats to protect sensitive turbo-pumps and computers during transport.

The GC-IRMS itself was constructed by Pro Vac Services (Crewe, UK), based around a standard laboratory gas chromatograph (GC) coupled to an

isotope ratio mass spectrometer (IRMS), with a flow rate of ca. 3.6 cm^3 min^{-1}, configured to automatically monitor CO_2, via 16 sequentially scanned input ports. The GC operated at a temperature of, 60°C and contained a 30 m fused silica plot column (Restek International) the IRMS was custom-made by Pro Vac services (Crewe, UK) being specifically customised to enable towing of the equipment over rough terrain. Modifications to the construction of the GC-IRMS included the permanent welding of the field magnet into place, silicone embedding of electronic components and ready access to vulnerable components to be removed during transit. Fig. 2.1 shows a flow diagram of the mobile laboratory components.

Due to the laboratory being utilised in the field, it was also necessary to provide an adequate and reliable supply of electricity. A 4 kW diesel generator carried on a separate vehicle was used to generate electricity on site, supplied to the laboratory via a 240V distribution board with residual circuit breaker (RCB) and conventional 13 amp sockets. During operation the generator was parked at a considerable distance from any experimental plots (usually 100 m) to prevent contamination with exhaust gases. A metal protected power cable was used to distribute the power.

The raw data produced by the GC-IRMS in the form of a time-indexed (1 Hz) digital data stream showed the amplified mV signals for the three mass collectors (beam 44, 45 and 46; see Fig.2.2). A custom designed computer program written in SAS software (V8 2000 SAS Institute Inc) structured the data, integrating the area underneath each of the mass peaks to calculate the amounts of ^{12}C and ^{13}C in each injected gas sample.

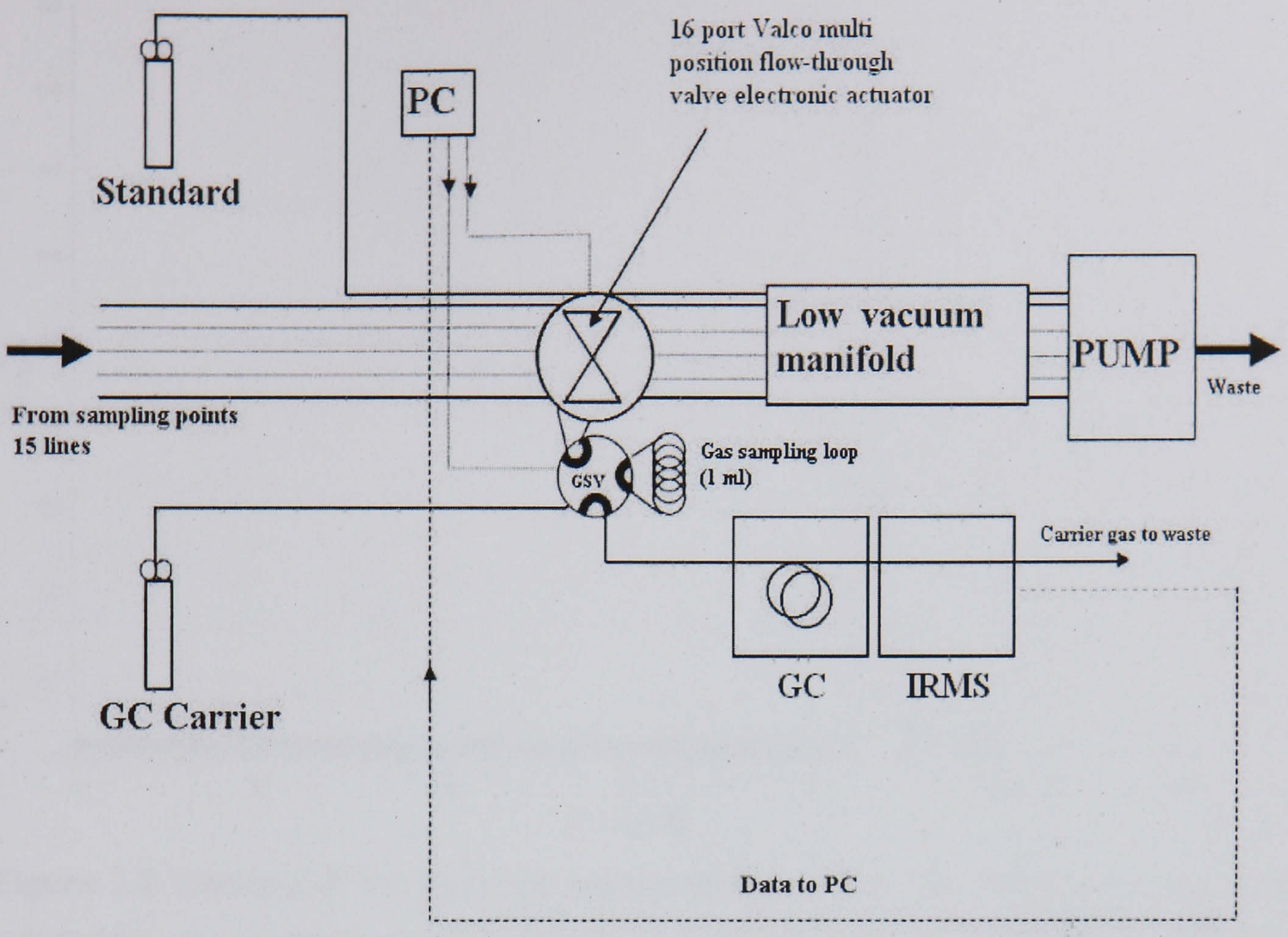

Figure 2.1 Schematic of the GC-IRMS in the mobile laboratory showing air from each of 15 sample lines being drawn though a manifold to waste. Note the 16 port Valco multi-position flow-through valve electronic actuator which sampled each line in turn, diverting it to a sample loop, 1 cm^3, prior to being injected into the GC and IRMS. Results were recorded on the PC.

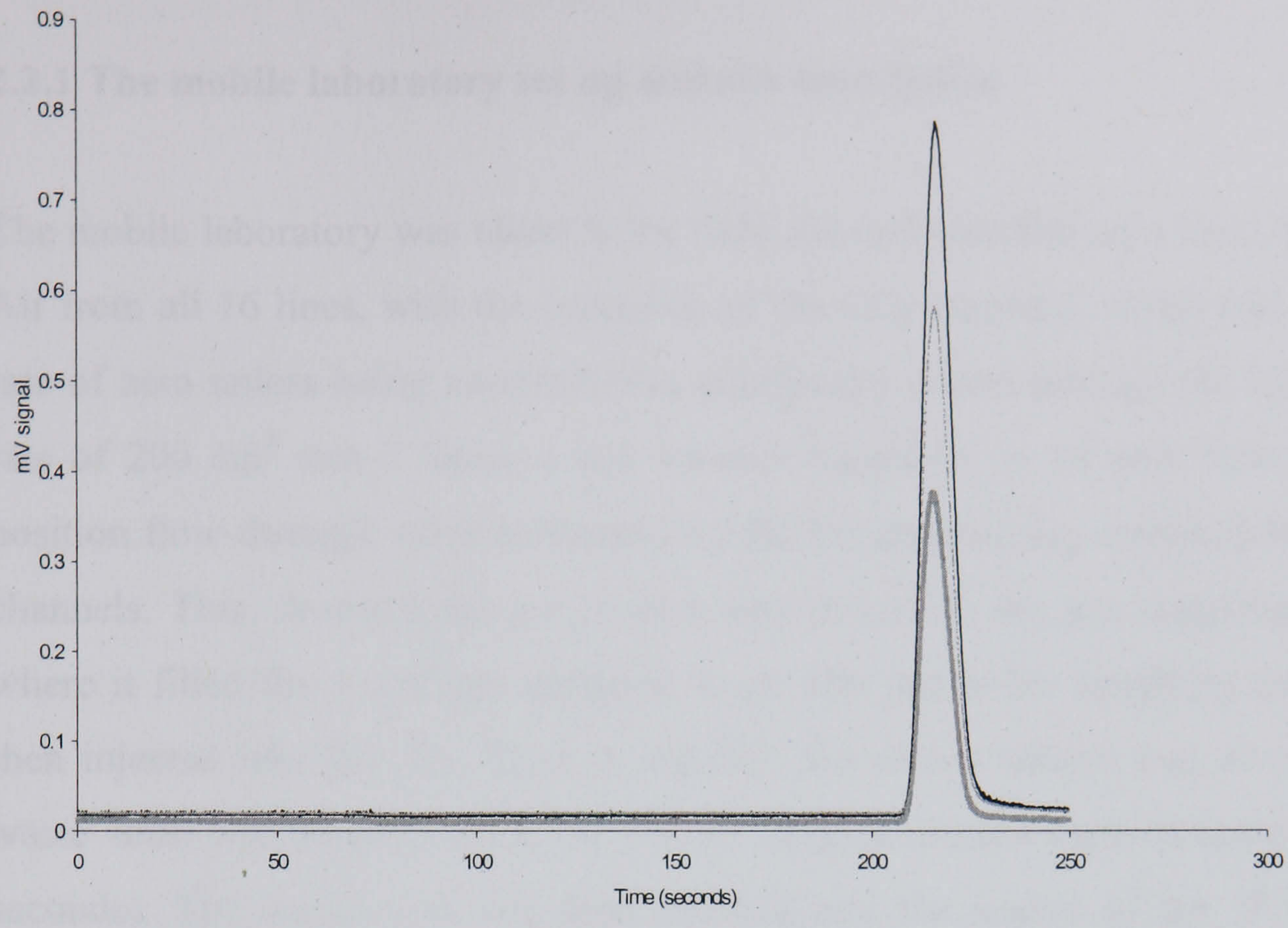

Figure 2.2 Example of the Millivolt signals produced from the three collectors in the GC-IRMS, after amplification (- mass 45, - - mass 46, - mass 44). This shows a trace for a normal (natural abundance) air sample, using a sample run of 250 seconds.

Prior to use in the field, air was injected into the GC-IRMS system via a Valco gas sampling valve (GSV) and the efficiency of a range of sample loops of different sizes was tested. It was found that, from a range of sample loop sizes from 0.25 to 2 $cm^{3,}$ a loop size of 1 cm^3 produced the largest analytical peaks, with minimum peak broadening; hence, a sample loop size of 1 cm^3.was used for all the mobile laboratory measurements described here (data not shown).

2.2 Methods

2.2.1 The mobile laboratory set up and site description

The mobile laboratory was taken to the field site and installed on a level surface. Air from all 16 lines, with the exception of the CO_2 standard, which had a flow rate of zero unless being sampled, was continually drawn through the lines at a rate of 200 cm^3 min^{-1} using a low vacuum manifold. A 16 port Valco multi position flow-through valve controlled by the PC sequentially switched between channels. This, diverted the gas in each line in turn to the gas sampling valve where it filled the 1 cm^3 gas sampling loop. The gas in the sampling loop was then injected into the GC. Once in the GC, the carrier stream was directed to waste until immediately prior to carbon dioxide elution (approximately 140 seconds). The carrier gas was then directed into the source of the IRMS for $^{13}CO_2$ isotope analysis, with mass beams 44, 45 and 46 being measured and recorded. Data from the IRMS were stored on a PC with each single analysis taking a total of ca. 5 minutes.

Closed-top chambers, diameter 20 cm, used for the experiment were made from Perspex, with a height of 30 cm. An inlet hole was situated on the side of the chamber, 3 cm from the bottom to which an air inlet pipe was connected, allowing air to be drawn into the chamber from a height ca. 1 m above ground (see Plate 2). The outlet hole was 2 cm from the top of the chamber on the opposite side to the inlet, to which PTFE tubing, with an internal diameter smaller than the inlet tube, was connected; this tubing then ran to the mobile laboratory in the field. Chambers were sealed onto the rings using sections of rubber car tyre inner tube.

Sampling of gases up to 100 m radius from the GC-IRMS was achieved using PTFE tubing connected to flow-through chambers (see below) secured to the ground, previous work by McNamara *et al.* (2002) had established that there is no isotopic fractionation in a flow through line system of this design and length. Results of the analyses were automatically integrated, processed and digitised for storage on a hard disc.

The work was conducted at the Natural Environment Research Council (NERC) funded experimental Sourhope field site in the Scottish borders, UK., using the established biodiversity manipulation plots at the site (see section 2.1).

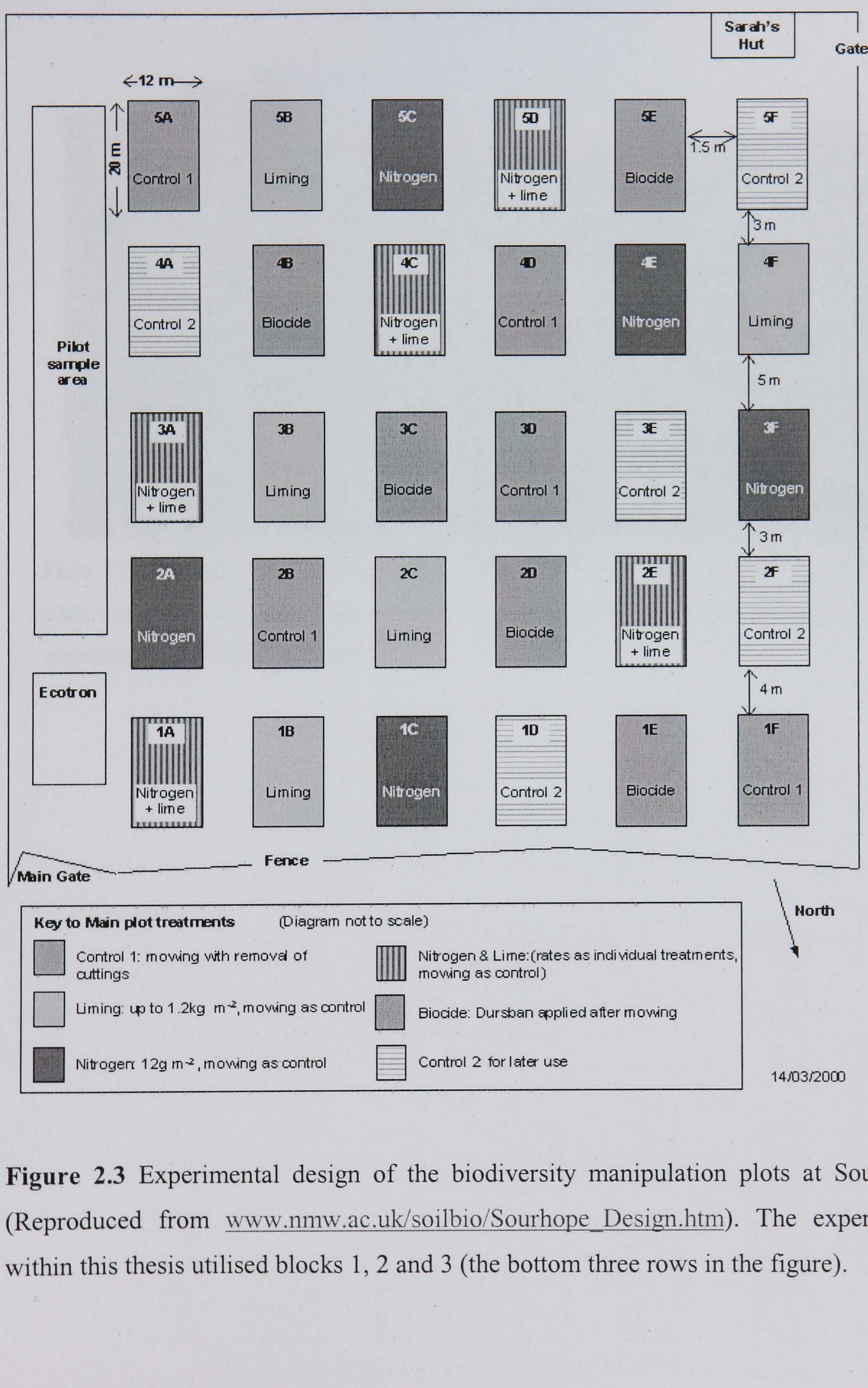

Figure 2.3 Experimental design of the biodiversity manipulation plots at Sourhope. (Reproduced from www.nmw.ac.uk/soilbio/Sourhope_Design.htm). The experiments within this thesis utilised blocks 1, 2 and 3 (the bottom three rows in the figure).

Plate 1 Photograph of the field site at Sourhope with the mobile laboratory in place. The plate shows the slope of the plots and the positioning of the chambers, the height of the vegetation and the 'rigs and furrows'.

2.2.2 *In situ* degradation of phenol monitored using $^{13}CO_2$

To measure the degradation of phenol in the field, $^{13}C_6$ phenol (Cambridge Isotope Laboratories, UK 99%, 50 ppm) in water, 300 cm^3, was applied within 10 cm sections of 20 cm diameter drainage pipe, set into the ground (see Fig. 2.4) to the soil surface (314 cm^2) in each of the rings in 12 treated plots, four different treatment plots, and three replicate blocks of each treatment. An equal volume of water without phenol was added to other plots to provide two "natural abundance" chambers. The treatments were; control, lime (L) (600 g m^{-2} y^{-1}), nitrogen (N) (12 g m^{-2}, twice a year) and biocide (B) (Dursban 1.5 litres per hectare, 5 times a year, 36 cm^3 in 10 litres of water per plot). The mineralisation of phenol was monitored '*in-situ*' as the $^{13}CO_2$ evolved from the treated areas using the closed-top continuous flow-through chambers connected to the mobile laboratory described in section 2.1.1.

Two chambers were placed, on rings, outside the treatment areas to measure the natural abundance of CO_2 from soil at the site. Black bags were placed over the chambers, to exclude light, thus stopping the CO_2 evolved from being diluted with photosynthetically produced $^{12}CO_2$. Air from all 14 chambers, at a flow rate of 200 cm^3 min^{-1}, was drawn through PTFE lines to the mobile isotopic ratio mass spectrometer (IRMS) for semi-continuous measurement of $^{13}CO_2$. In addition a line carrying ambient air was also monitored. Gas was sampled from all chambers for 24 hours, enabling both the ^{13}C value and the ppm CO_2 to be measured.

Plate 2 Photograph of the field site at Sourhope, showing the PTFE air sampling lines. Two chambers are shown lying on their sides, prior to being connected, as are the air intake pipes connected to two sampling chambers, prior to being covered with black bags. The plate is for demonstration purposes only and does not reflect the methodology in experiments where there was only one chamber per block.

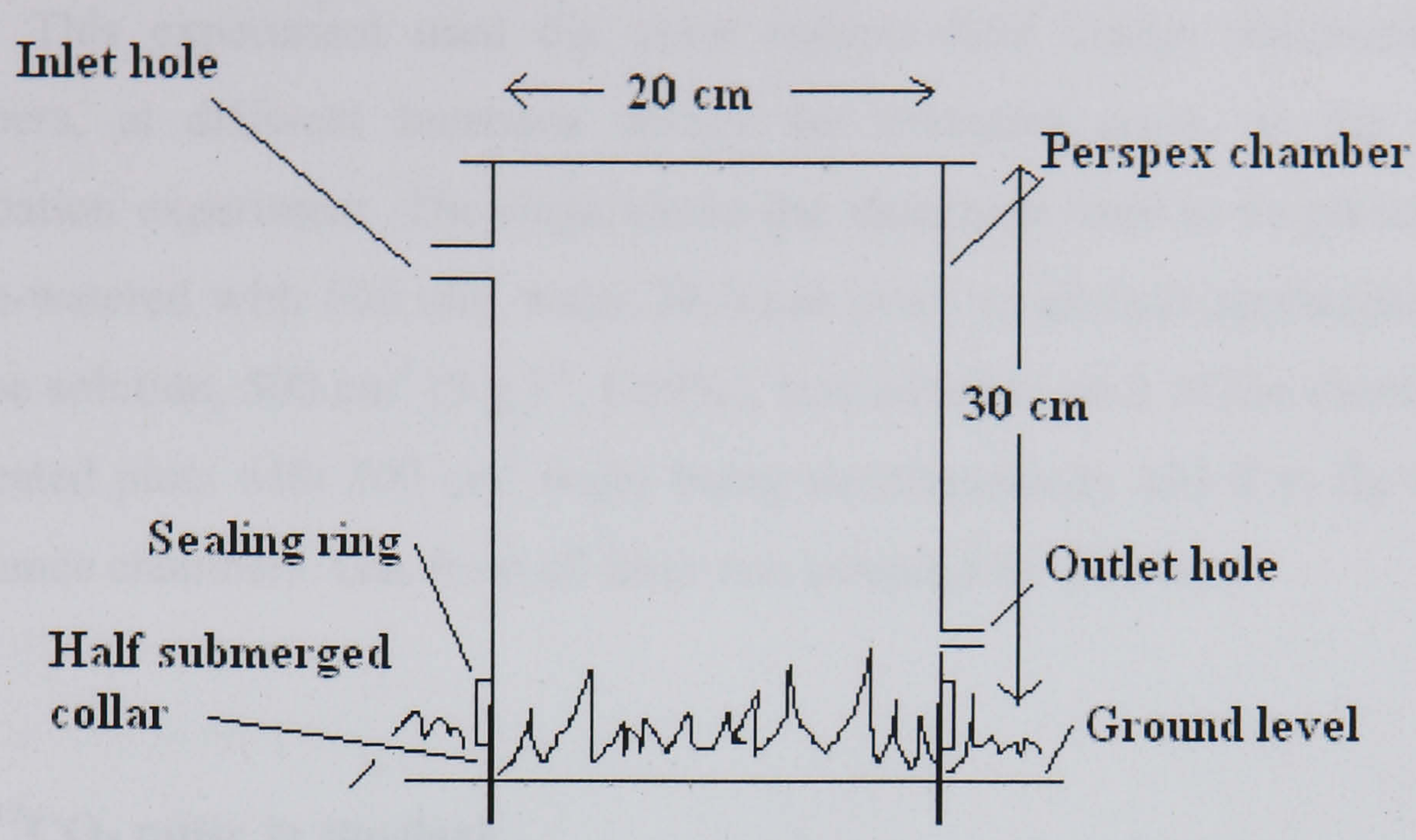

Figure 2.4 Diagram of a chamber, showing the location of the inlet and outlet tubes relative to each other and the ground.

2.2.3 *In situ* degradation of glucose monitored using $^{13}CO_2$

To establish the $^{13}CO_2$ flux from the addition of a substrate that does not possess antimicrobial properties, the experiment was repeated using glucose as a substrate Glucose is readily utilised as a carbon source by most soil organisms (Stotzky and Norman, 1961) and is involved in cellular respiration in both prokaryotes and eukaryotes. Killham (1994) reports that soil organic matter (SOM) exists in three main pools, the largest being inorganic carbon accounting for 90% of the total, followed by the carbon held in biomass, and less than 1% existing as soluble carbon. Soluble carbon comes primarily from, glucose, being produced by plants during photosynthesis and released into the soil through plant root exudates. Because glucose is metabolised so readily by soil organisms, it has a very high turnover rate in soil, with Killham (1994) stating turnover values of 1 day for glucose compared to 500 days for the more complex structure, lignin. Van Hees *et al.*, (2005) also found a rapid flux through the relatively low

concentrations of low molecular weight compounds, reporting a mean residence time in the soil of 1 – 10 hours and attributed it to microbial removal.

This experiment used the same experimental design, treatments and chambers, at different locations within the treatment areas, as the phenol degradation experiment. The rings where the chambers were to be placed were all pre-watered with 500 cm^3 water 24 hours prior to glucose application. $^{13}C_6$ glucose solution, 500 cm^3 (5 g l^{-1}, 1.69%), was added to each of the chambers in the treated plots with 500 cm^3 water being simultaneously added to the natural abundance chambers. Gas from all lines was sampled for 24 hours.

2.2.4 $^{13}CO_2$ pulse in the dark

To establish whether any differences in the $^{13}CO_2$ released from the L and control treatments were the result of biological or purely chemical differences (e.g. absorbance at different pHs) a $^{13}CO_2$ pulse experiment in the dark was conducted to eliminate photosynthetic uptake and compare simple physical phenomenon.

Six chambers, identical to those used in the phenol and glucose degradation experiments, were used to measure the $^{13}CO_2$ release from lime and control plots, three replicates of each. The six chambers were pulsed, in the dark, with 350 ppm $^{13}CO_2$ (Spectra Gas) for 30 minutes at 100 cm^3 min^{-1}. An additional chamber was used to measure natural abundance, which received no $^{13}CO_2$ but was also darkened. The outlet lines were then connected to the mobile mass spec with a flow rate of 250 cm^3 min^{-1} in order to remove and residual $^{13}CO_2$ from the lines. The chambers were opened and the head space allowed to 'breathe' before the chambers were replaced and the second cycle of sampling commenced.

2.2.5 Statistical analysis

The statistical analyses were performed using SPSS v.14.0 (2005 SPSS.inc). ANOVA with repeated measures was used to analysis the δ and flux measurements, with *a posterori t* tests. One-way ANOVA was used to compare the final cumulative ^{13}C fluxes between the four treatments, followed by a post hoc Duncan's test.

2.3 Results

2.3.1 *In situ* degradation of phenol monitored using $^{13}CO_2$

Phenol solution was added to the plots at 17:15 on 09/09/03. Fig. 2.5 indicates that the lime treatment had an effect on the rate of phenol degradation in the field. The control, N and B treatments all responded to the phenol addition in a similar way with an immediate sharp rise in the $^{13}CO_2$ evolved, reaching a peak six hours after phenol application. The L treatment showed a slower initial rise in the δ $^{13}CO_2$ value, with a less steep gradient, reaching a peak after 12 hours. ANOVA, with repeated measures, showed no significant differences in the $^{13}CO_2$ values between treatments prior to the addition of phenol. Similarly, there were no significant differences between the control, N and B treatments after the addition of phenol. However, when comparing the control and L treatments, the control treatment mineralised phenol significantly faster in the first eight analysis cycles following application of the labelled substrate, i.e. for the first 7 hours ($p=0.034$). After 7 hours any apparent differences between the control and L treatments are not significantly different. A *t* test on the $^{13}CO_2$ values in the first 7 hours of the experiment showed significant differences within the first 7 hours between 2 and 4 hours after phenol addition.

A graph of the phenol derived CO_2 flux, presented in Fig. 2.6, supports the data from the $^{13}CO_2$ graphs, negating the possibility that the δ values were masked by a higher overall rate of CO_2 evolution in the L treatment. ANOVA with repeated measures showed no significant differences in the phenol derived flux values between treatments prior to the addition of phenol. Again, there were

no significant differences between the control, N and B treatments after the addition of phenol, but in comparisons of the control and the L treatments, the control treatment showed a significantly higher flux in the first eight analysis cycles following application of the labelled substrate, i.e. for the first 7 hours ($p=0.044$). After this point there were no significant differences between the control and L treatments. A *t* test on the first 7 hours of the phenol derived CO_2 flux showed the significant differences within the first 7 hours were between 2 and 4 hours after phenol addition.

An ANOVA on the cumulative phenol derived CO_2 flux, Fig. 2.7, revealed that by the end of the experiment, there was no significant difference in the total ^{13}C flux between any of the treatments.

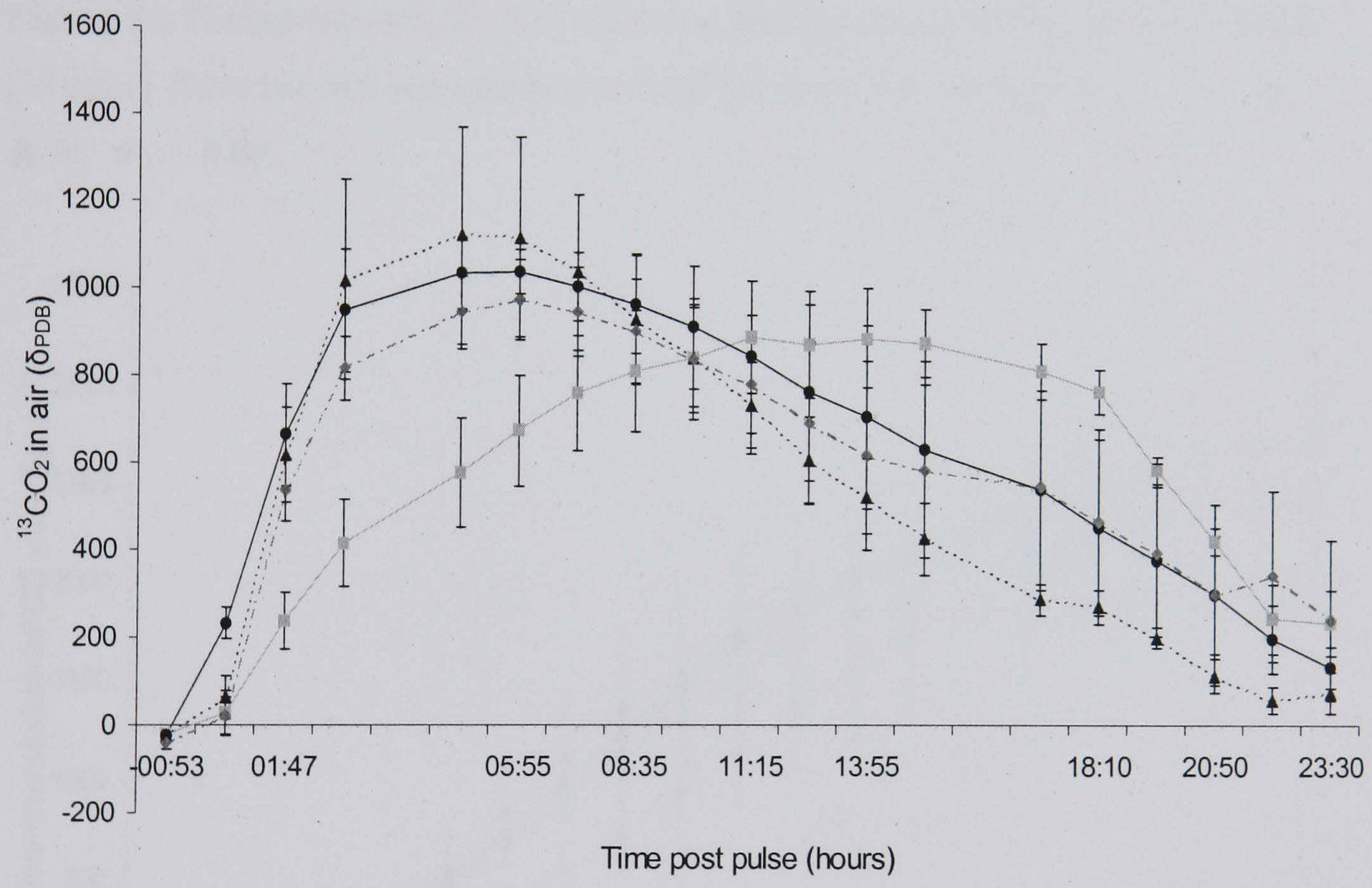

Figure 2.5 δ $^{13}CO_2$ in air following the application of 300 cm^3 $^{13}C_6$ phenol [50 ppm]. Error bars are one standard error of the mean. (●—● control, ■---■ L, ▲- - - ▲ N, ♦- - - ♦B) .

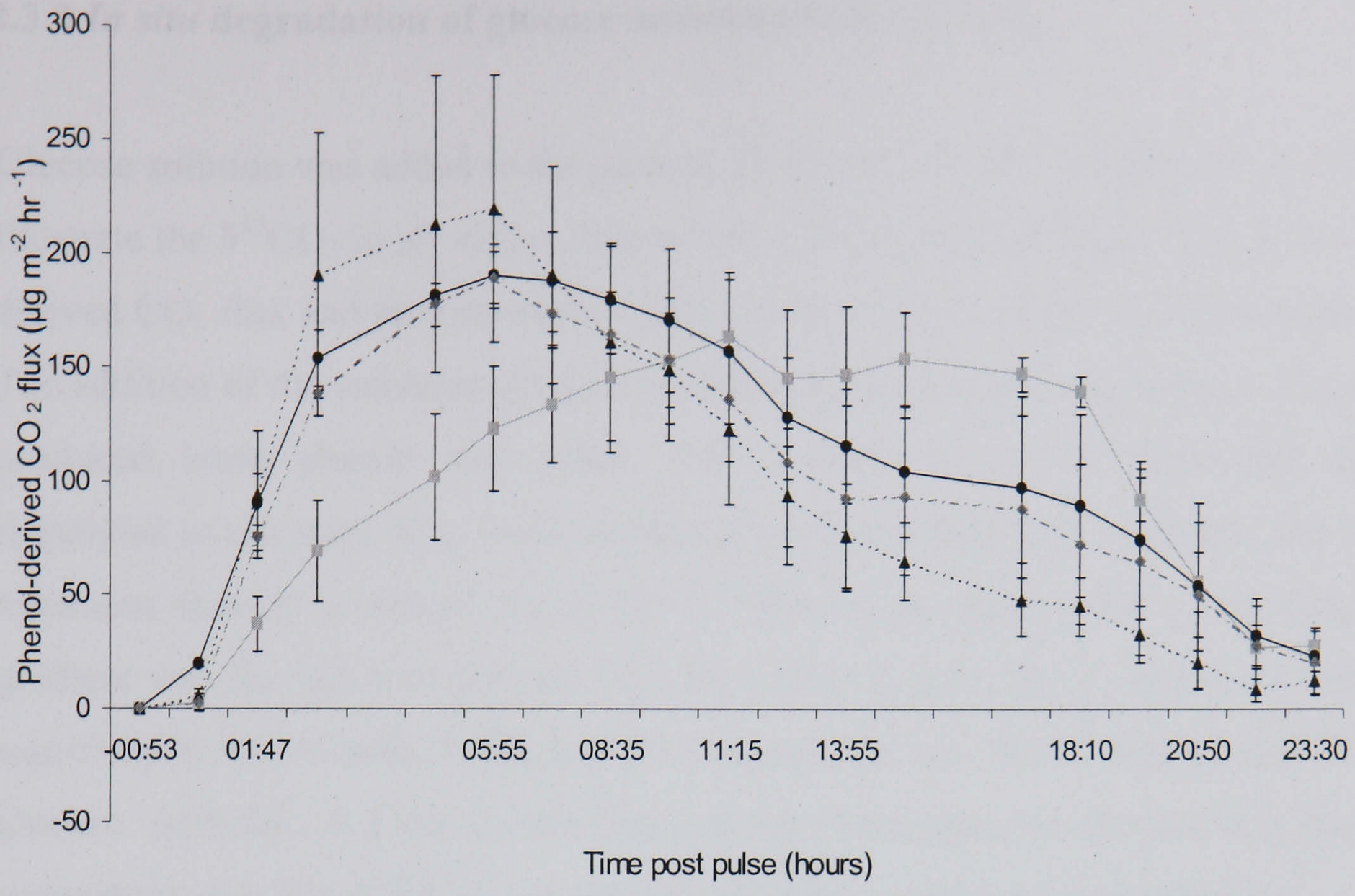

Figure 2.6 Phenol-derived CO_2 flux following the application of 300 cm^3 $^{13}C_6$ phenol [50 ppm]. Error bars are one standard error of the mean. (●—● control, ■—■ L, ▲- - - ▲ N, ♦- - - ♦B).

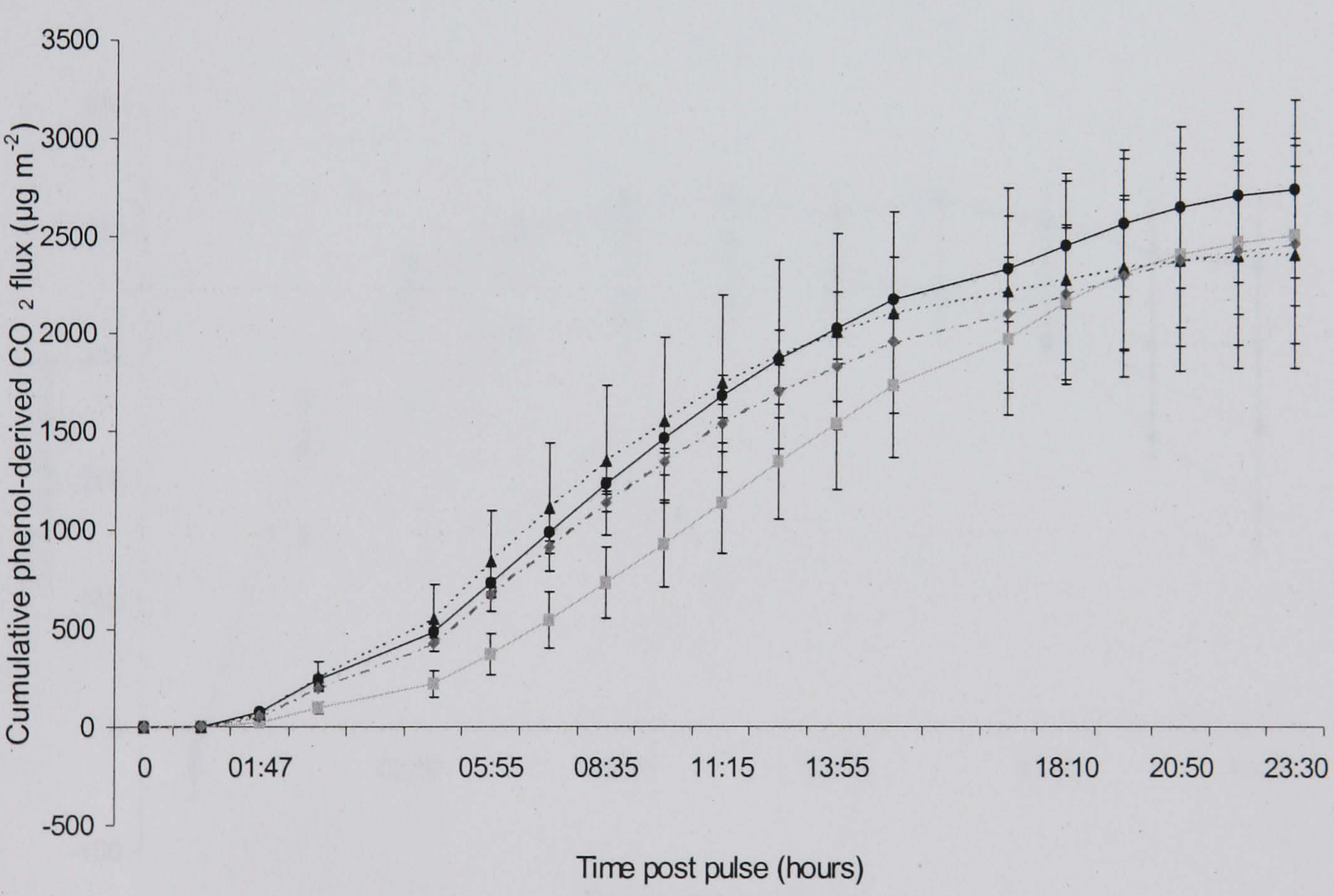

Figure 2.7 Cumulative phenol-derived CO_2 flux following the application of 300 cm^3 $^{13}C_6$ phenol [50 ppm]. Error bars are one standard error of the mean. (●—● control, ■—■ L, ▲- - - ▲ N, ♦- - - ♦B).

2.3.2 *In situ* degradation of glucose monitored using $^{13}CO_2$

Glucose solution was added to the plots at 18:15 on 10/09/03. Figures 2.8 – 2.10 illustrate the $\delta^{13}CO_2$ in air values derived from the glucose addition, the glucose-derived CO_2 flux and the cumulative glucose-derived CO_2 evolved, respectively. The addition of the substrate glucose caused similar treatment responses to those produced when phenol was added. The control, N and B treatments all responded in the same way, with an immediate rise in the $^{13}CO_2$ evolved. The L treatment showed a slower rise in the δ $^{13}CO_2$ in air value, with a less steep gradient and the glucose-derived CO_2 flux (Fig. 2.9) in the L treatment was significantly lower than in the control treatment in the first 7 hours after ^{13}C glucose ($p=0.04$). A *t* test on the first 7 hours of the glucose derived CO_2 flux showed the significant difference was around 4 hours after glucose addition.

An ANOVA on the final cumulative ^{13}C glucose-derived CO_2 flux shown in Fig. 2.10 again revealed that, by the end of the experiment, there was no significant difference in the total ^{13}C flux produced under any of the treatments.

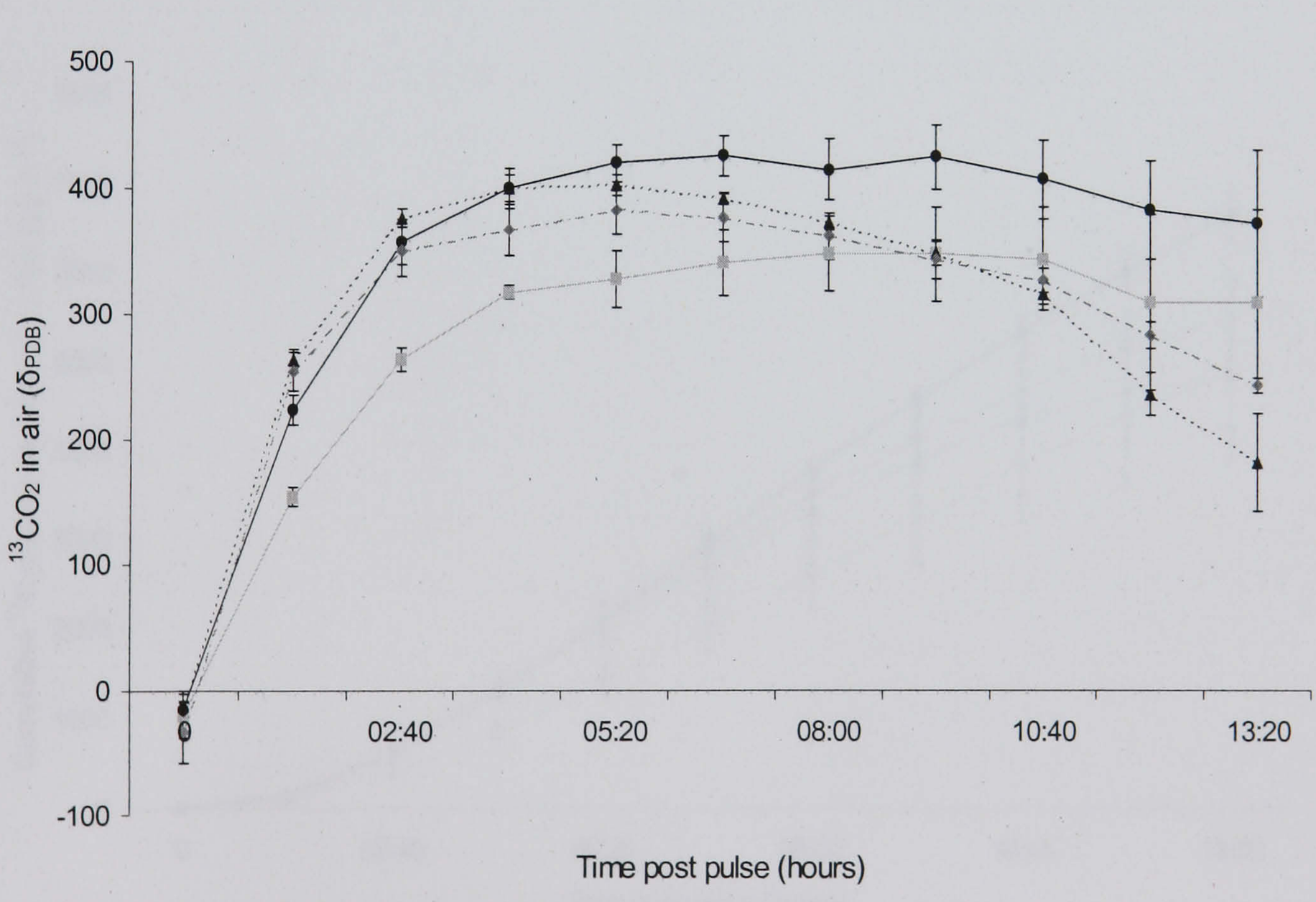

Figure 2.8 δ $^{13}CO_2$ in air following the application of 500 cm^3 $^{13}C_6$ glucose (5 g l^{-1}, 1.69%). Error bars are one standard error of the mean (●—● control, ■—■ L, ▲- - - ▲ N, ♦- - - ♦B).

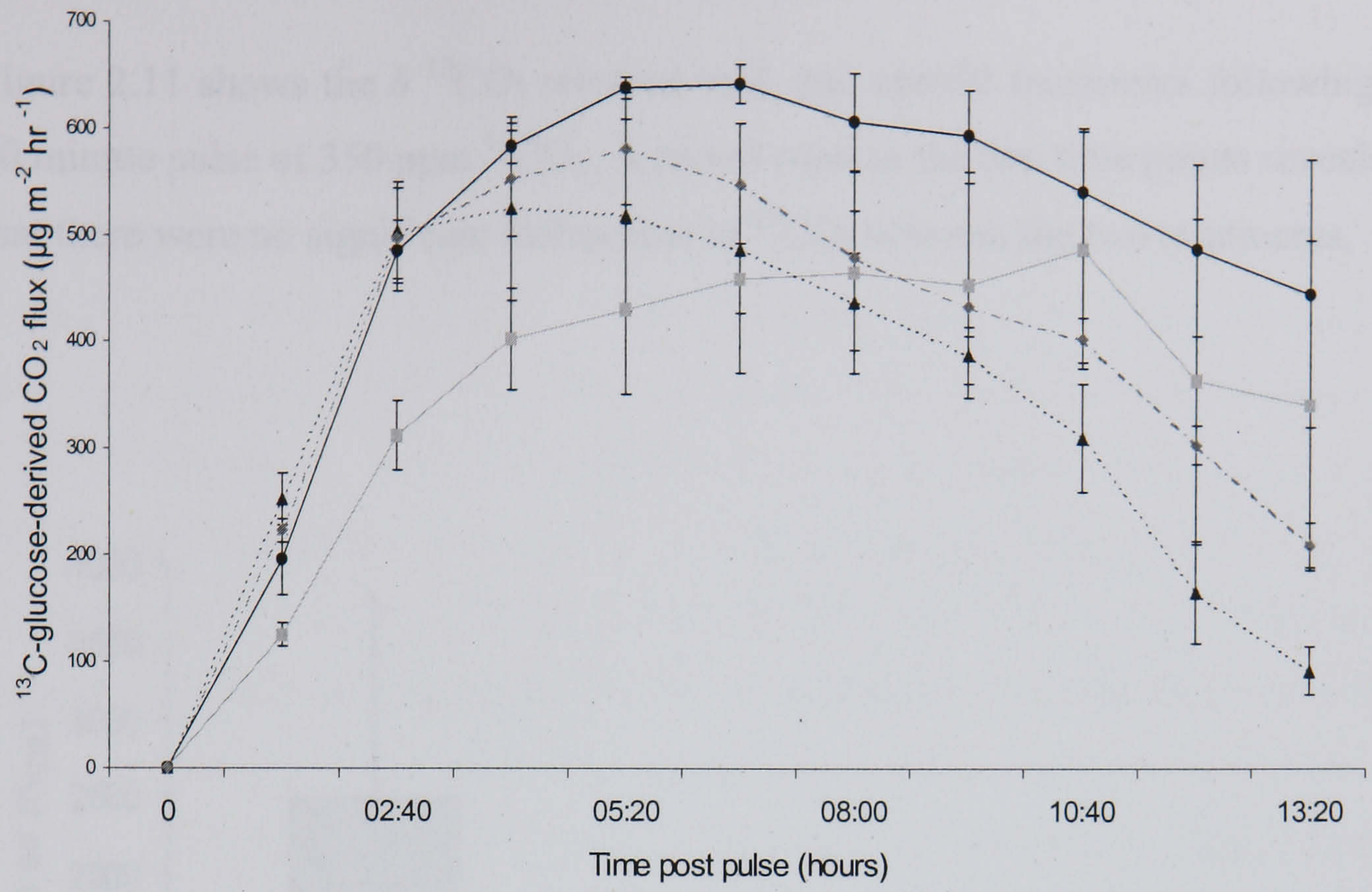

Figure 2.9 $^{13}CO_2$ flux values following the application of 300 cm^3 $^{13}C_6$ glucose (5 g l^{-1}, 1.69%). Error bars are one standard error of the mean (●—● control, ■---■ L, ▲- - - ▲ N, ♦- - - ♦B).

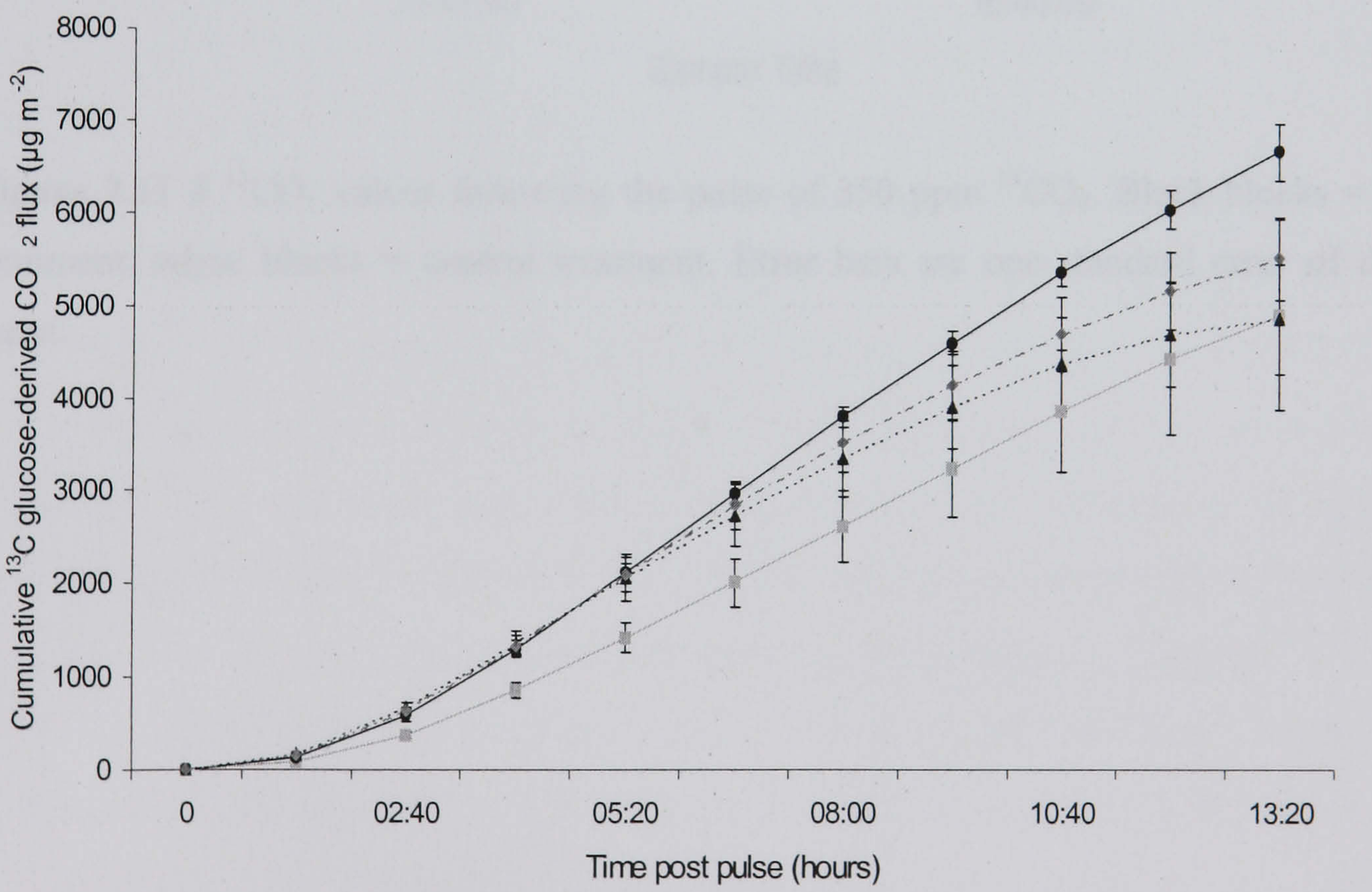

Figure 2.10 Cumulative flux $^{13}CO_2$ values following the application of 500 cm^3 $^{13}C_6$ glucose (5 g l^{-1}, 1.69%). Error bars are one standard error of the mean. (●—● control, ■---■ L, ▲- - - ▲ N, ♦- - - ♦B).

2.3.3 $^{13}CO_2$ pulse in the dark

Figure 2.11 shows the δ $^{13}CO_2$ released by L and control treatments following a 30 minute pulse of 350 ppm $^{13}CO_2$. A paired *t*-test at the two time points revealed that there were no significant differences in $^{13}CO_2$ between the two treatments.

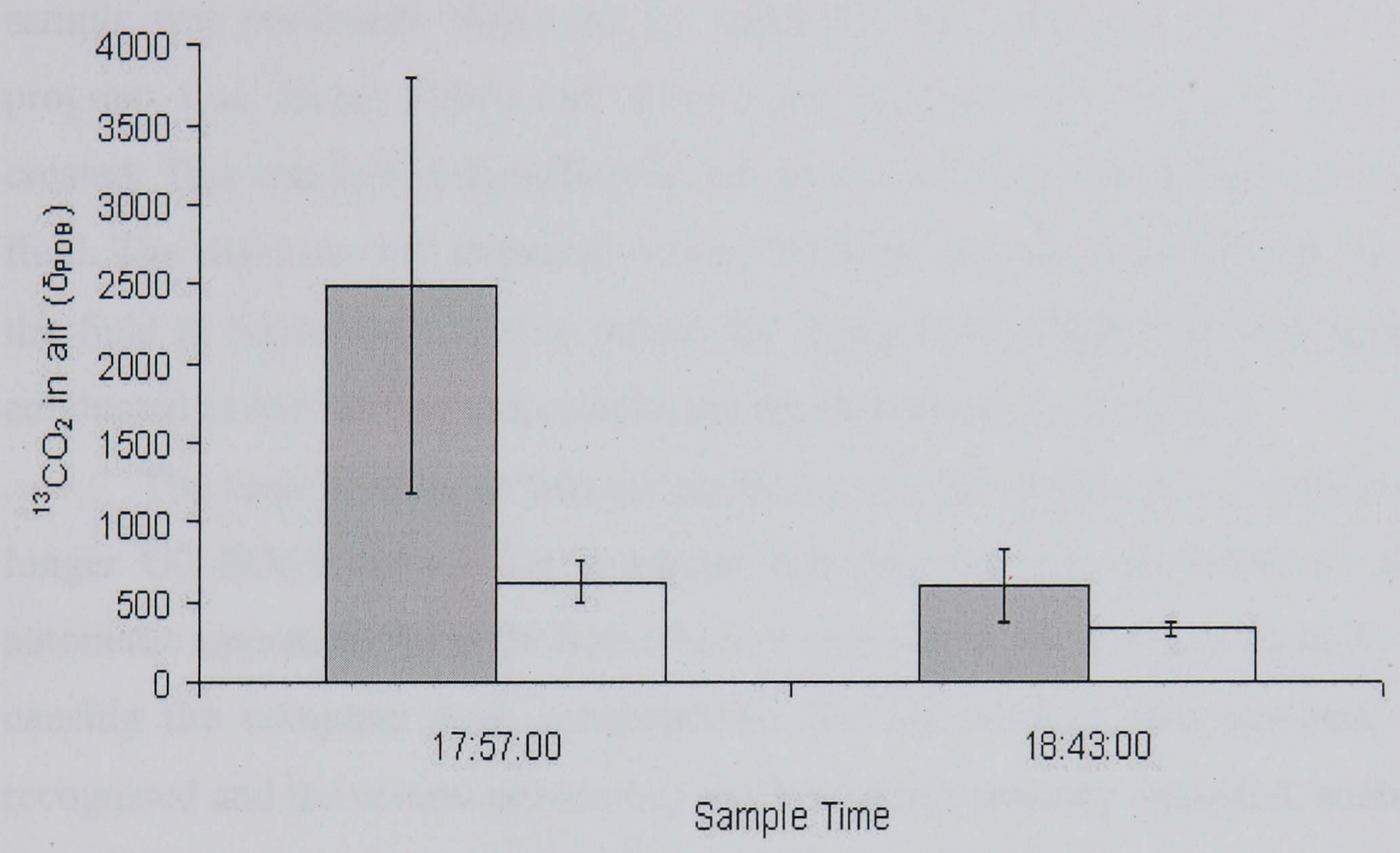

Figure 2.11 δ $^{13}CO_2$ values following the pulse of 350 ppm $^{13}CO_2$. Black blocks = L treatment, white blocks = control treatment. Error bars are one standard error of the mean.

2.4 Discussion

The initial deployment of the mobile GC-IRMS system highlighted that further developmental work was needed. The work described in Chapter 2 was conducted during a field campaign, in conjunction with other institutes (see above) in July 2003. The computer software both controlling and processing the data from the GC-IRMS was custom designed and produced, and consistent traces of the runs in real time were generated on the computer screen as each sample was processed. However, on returning from the field, an error in the program was found which had overwritten each data set as a new one was created. This resulted in the effective loss of all the data from the first run in the field. The software was altered to correct this error and a return trip was made to the field in September 2003 to repeat the experiment, which had been initially conducted in July of that year, producing the data shown in Chapter 2.

The large amount of data generated by the GC-IRMS created problem on longer GC-IRMS runs as the computer memory was only sufficient to allow automatic operation for eight hours before exceeding the memory capacity and causing the computer and, consequently, the GC to fail. This problem was recognised and the computer memory and hard drive capacity upgraded, enabling the millions of raw data points from a typical run to be stored.

The generator manufacturers strongly recommended an oil change every 48 hours when run continuously. Obviously, this meant that the generator had to be switched off during oil changes and stopping electricity supply to the laboratory resulted in a loss of unsaved data together with the loss of system vacuum, This potential problem was overcome by installing a UPS (uninterruptible power supply) in the mobile laboratory, providing up to ten minutes of power when the mains supply from the generator was stopped.

In 2004, when the samples for the PLFA analyses shown in Chapter 4 were obtained, the aim had been to measure the $^{13}CO_2$ in sample gas flow lines at the same time. The generator was parked, as previously mentioned, in a field adjoining the site, with the power cable running through a fence and to the laboratory. The field containing the generator was grazed by a large number of cashmere goats and, during the first night of the fieldwork in 2004, it later became apparent that the livestock had pulled out the cable carrying electricity

from the generator to the laboratory. This resulted in the laboratory losing all power, together with unsaved data, and immediate loss of mass spectrometer vacuum, blowing the source filament. Field repairs were performed immediately on realisation of the problem and the filament replaced, but by the time the GC-IRMS had regained sufficient vacuum, the $^{13}CO_2$ from the pulse had passed. It was therefore necessary to return to the field in 2005 to repeat the work lost in 2004. Subsequently, a fence was installed round the generator for all field studies at the site, protecting it from livestock, allowing safe passage for the cable to the experimental site.

The mobile mass spectrometer was able to successfully detect $^{13}CO_2$ enriched air following the application of 300 cm^3 $^{13}C_6$ phenol (99%, 50 ppm) and $^{13}C_6$ glucose solution, 500 cm^3 (5 g l^{-1}, 1.69%) to the soil surface. The concentration of phenol used in all the experiments throughout this thesis, 50 ppm, was chosen following the work of Padmanabhan *et al.* (2003) who found at those concentrations both the CO_2 evolved and the incorporation into the nucleic material was detectable. During further discussions with the authors regarding the choice of concentration they knew that such concentrations commonly occur in soil as a result of either pollution events or naturally occurring root exudation, and thus it was the most suitable concentration, being well beneath the published laboratory inhibitory concentrations (e.g. ca. 500 ppm, Kumar *et al.,* 2005).

The detection of ^{13}C enriched air after the addition of a liquid substrate to soil has been demonstrated by Högberg and Ekblad (1996) who used the natural isotopic difference between a C_3-plant ecosystem and C_4-sucrose to study substrate-induced respiration in an *in situ* forest soil, with minimal disturbance to the ecosystem. Högberg and Ekblad (1996) had initially proved this approach in the laboratory and then replicated the procedure in the field, where they produced consistent results, with the addition of sucrose causing a rise in substrate induced respiration ca. 1.5 to 2.5 times the basal respiration rate. Since then a variety of ^{13}C labelled substrates have been applied to soils at varying concentrations, ranging from pulsing with $^{13}CO_2$ in the laboratory (Ostle *et al.*, 2000; Butler *et al.*, 2003; Yu *et al.*, 2004; Gavito and Olsson, 2003), and in the field, (Treonis *et al.*, 2004) through simple compounds such as glucose (Padmanahban *et al.*, 2003), methane (Boschker *et al.,* 1998; Bull *et al.,* 2000; Hinsrichs *et al.,* 1999; Radajewski *et al.*, 2000; Crossman *et al.*, 2005; Crossman *et al.*, 2006) and

acetate (Boschker *et al.,* 1998; Pombo *et al.*, 2005) to more complex substrates such as, phenol, (Padmanahban *et al.*, 2003), toluene (Hanson *et al.,* 1999), naphthelene, (Padmanahban *et al.*, 2003) and caffeine (Padmanahban *et al.*, 2003).

Padmanahban *et al.* (2003) applied solutions of phenol, glucose, naphthalene and caffeine to soil at concentrations of 50, 50, 2 and 50 ppm, respectively. All the solutions were labelled to 99 atm% ^{13}C and resulted in the detection of mineralization of the glucose, phenol and naphthalene to CO_2 within 24 hours. Glucose was the fastest to be metabolised, with almost 7% of the total ^{13}C added returned as $^{13}CO_2$ within 2 hours, whilst 9% of the ^{13}C added as phenol in this study was returned after 8 hours; they were unable to detect any $^{13}CO_2$ from the addition of caffeine. The low solubility of naphthalene led to high variability in the results, whilst the ^{13}C produced following the addition of caffeine was not significantly higher than the background flux. The other isotope of C, radioactive ^{14}C, has also been used extensively to study substrate induced respiration with Topp *et al.* (2006) using ^{14}C labelled caffeine additions to soil to detect the mineralization of caffeine in the laboratory, measuring the production of $^{14}CO_2$. They found the mineralization of this substrate was strongly affected by soil temperature and moisture.

Similarly, at the Sourhope experiment, the addition of phenol and glucose had an effect on C release, evident in the consequent flux of $^{13}CO_2$. Whilst glucose is well known as a C source for microbes, phenol is more widely recognised for it's antibacterial properties and it is perhaps surprising that these two substrates produced similar responses in respired CO_2 fluxes. The overall time course for phenol degradation at Sourhope was consistent with the results of Padmanabhan *et al.* (2003), who found that nearly all the $^{13}CO_2$ derived from a ^{13}C phenol addition to soil had occurred within 24 hours of application, peaking at around eight hours.

In the Sourhope experiment two of the treatments, N and B, did not have a significant effect on the $^{13}CO_2$ flux, when compared to the control treatment or on the cumulative amount of $^{13}CO_2$ produced by either the phenol or glucose addition experiment. The addition of N to plots at Sourhope had a slight but significant effect on the pH of the upper section of the soil profile, raising it from a mean value of pH 4.7 in 1998 to pH 4.8 in 2002, whilst the application of the

biocide had no significant impact on soil pH. The amount of above-ground biomass, measured in 2002, was significantly higher in the N treatments than the control, whilst the biocide had no significant effect on the above-ground biomass (Burt-Smith, 2003).

Lime was the only treatment to have a significant effect at Sourhope on the $\delta^{13}CO_2$ signal in respired CO_2 and the $^{13}CO_2$ flux dynamics for both the phenol and glucose addition experiments. The $^{13}CO_2$ pulse in the dark negated the possibility that the differences observed between the control and lime treatments was due to an abiotic factor, such as differences in pH affecting the solubility and subsequent re-release of CO_2. Rather, these results suggest that differences in the fluxes resulting from substrate addition experiments between the L and control treatments were the result of biological differences. These differences may be the result of changes in the microbial community pH, with Grayston *et al.* (2001) reporting that, in a similar soil, a raised pH (from pH 4.1 to pH 6.0) resulted in an increase in both soil microbial biomass and soil microbial activity. Fuentes *et al.* (2006) reported that the addition of lime to no-till soil had the effect of raising the pH of the soil whilst also increasing the amount of soil nitrate, indicating that lime application favoured N-mineralisation and nitrification. These authors also attributed greater respiration rates and microbial biomass C to the increase in pH caused by the liming and also found that, when compared to unlimed soil, limed soil had faster C turnover rates and increased mineralization of organic matter. However, Treonis *et al.* (2004) pulsed lime and control treatments at the Sourhope field site with photosythetically assimilated $^{13}CO_2$ and, from the ^{13}C-enrichment of the PLFAs, concluded that liming did not affect the turnover rates of ^{13}C labelled carbon, or which organisms were utilising the recent photoassimilate.

The addition of lime to plots at Sourhope significantly affected the pH of the upper section of the soil profile, raising it from a mean value of pH 4.6 in 1998 to pH 6.7 in 2002 and there was a strong negative correlation between soil moisture content and soil pH, with the more acidic plots showing higher soil moisture content, (Burt-Smith, 2003). The rise in the upper soil profile pH at Sourhope was also strongly positively correlated with biomass productivity (Burt-Smith, 2003). The results of a point analysis survey in 2002 found differences in vegetation between the lime plots and the control, with *Festuca*

rubra and *Poa pratensis*, two species commonly associated with improved pastures, accounting for 30% of the hits in the lime plots, but never accounting for more that 10% in the controls. Conversely, *Festuca ovina* and *Anthoxanthum odoratum*, two species commonly associated with unimproved pastures, were more abundant in the control plots, accounting for up to 30% of hits, while only accounting for 16% of hits in the limed plots (Burt-Smith, 2003).

When phenol was added to the treatments at Sourhope, the L plots responded more slowly to the addition of the substrate with a lower initial rate of substrate-induced respiration (SIR); the SIR continued to rise even after the control treatment had reached a peak and was in decline. A very similar different treatment response was seen after the glucose addition. This may simply be that the control plot has metabolised the substrate to a degree where it is now substrate limited.

The underlying question remains as to which changes in the L plots were responsible for the clear and significant differences in the processing of added substrates. It could be the change in vegetation composition, and/or the associated changes in the microbial community that are responsible for the differing activities of the microbial populations under the different treatments; alternatively, a direct treatment-induced shift in the community (not connected with vegetation changes) may be at the root of these observations. In order to differentiate between these underlying causes, ideally plots would be created which were vegetation free, to test whether vegetation needs to be present for the observed changes in substrate utilisation to occur.

Chapter 3. Investigating the effect of vegetation on the degradation of phenol in soils *in situ* using stable isotopes

3.1 Introduction

The results from Chapter 2 indicated that, out of the three treatments, lime (L), nitrogen (N) and biocide (B) applied at Sourhope, the L addition was the only treatment that appeared to have a significant effect, relative to the control, on the flux of $^{13}CO_2$ from both ^{13}C phenol addition and ^{13}C glucose additions. The $^{13}CO_2$ flux from the L plots (Fig. 2.4) peaked approximately 11 hours after the addition of phenol, occurring around 5 hours after the peak responses in the control, N and B treatments. As discussed in Chapter 2, the addition of lime to the soil at Sourhope had both direct chemical effects and indirect biological effects (e.g. vegetation change) on the treated areas. The addition of lime directly affected the soil chemistry, raising the pH of the upper section of the soil profile from pH 4.6 in 1998 to pH 6.7 in 2002, and also led to a lowering of the water content of the soil, probably through a vegetation change (Burt-Smith, 2003).

Other indirect effects on soil may have been exerted via the changes in vegetation, with the flora in the L plots having a greater proportion of *Festuca rubra* and *Poa pratensis* with less *Festuca ovina* and *Anthoxanthum odoratum* than in the control, typical of the vegetation changes associated with improved grasslands (Burt-Smith, 2003). So, from Chapter 2, it is still unclear whether it was a direct or indirect effect of the lime addition which caused the observed difference in respired $^{13}CO_2$ seen after substrate addition. To distinguish between the two possible mechanisms, experiments were performed at the Sourhope field site designed to compare two new treatments, namely, with and without vegetation. Hence, the work described here repeated the experiments described in Chapter 2 but included additional long-term treatments where vegetation had been removed in order to examine the link between plant cover and microbial substrate processing. The unvegetated or 'bare' treatments were achieved by the manual removal of all vegetation, with subsequent prevention of vegetation re-growth over a two year period prior to the second labelled substrate addition experiment described here. The time length for monitoring $^{13}CO_2$ release from

these field addition experiments in Chapter 3 was also increased from 24 hours to 48 hours, based upon the results from the first field experiment.

3.2 Methods

3.2.1 Site description and treatment preparation

The experiment was performed at the Sourhope field site, but was restricted to the L and control plots. Within each of these plots, areas were rendered vegetation free two years prior to the actual substrate addition experiment being performed. Vegetation was manually removed from one meter square plots, which were then covered with a double layer of black porous fabric (Weed Control Fabric, B&Q), to prevent any regeneration of the vegetation. This procedure avoided the addition of any herbicides to the vegetation in the plots, whilst the choice of porous fabric enabled full ingress of precipitation. Galvanized steel sheets were inserted into the ground to fully isolate these plots, preventing any roots from surrounding vegetation from colonising the vegetation-free areas. The steel sheets were galvanized to prevent corrosion and the plots were checked regularly during the two years for any signs of plant re-growth.

3.2.2 *In situ* degradation of phenol monitored using $^{13}CO_2$

The experimental approach repeated that described for Chapter 2, with slight modifications. To measure the degradation of phenol in the field, $^{13}C_6$ phenol (Cambridge Isotope Laboratories, UK) 300 cm^3 $^{13}C_6$ (99%, 50 ppm), was applied to the soil surface (314 cm^2) in each of the 12 treated plots in the four different treatments, with three replicates of each treatment. An equal volume of water was added to provide two "natural abundance" chambers which were monitored to provide the background ^{13}C ratio of soil respiration. The treatments were; control with vegetation (CV), control with vegetation removed, i.e. 'bare' plots (CB), lime with vegetation intact (LV) and lime with the vegetation removed (LB). The data from the 2003 pulse suggested that it would be preferable to

monitor the addition experiment for slightly longer to allow for the elevated $^{13}CO_2$ signal from the limed plots to decrease further towards natural abundance levels; therefore, the CO_2 flux was measured for 48 hours in these experiments.

3.2.3 Statistical analysis

All statistical analyses were performed using SPSS (v.14.0 2005 SPSS.inc). ANOVA with repeated measures was used to analysis the δ and flux measurements, with appropriate *a posterori t* testing, where significance differences were established.. Conventional one-way ANOVA was used to compare the final cumulative single ^{13}C fluxes between the four treatments, followed by a *post hoc* Duncan's test. All treatments were included and compared in the analyses but, for clarity of presentation, the treatments are frequently shown as pair-wise comparisons for graphical purposes.

Plate 3 Photograph of the field site at Sourhope, showing a vegetation free plot in block 1, with the plastic collar inserted into the ground and two chambers connected to the air intake and PTFE pipes prior to being covered with black bags. This plate is for illustrative purposes only, since all the addition experiments used only one chamber per block.

3.3 Results

Phenol, 300 cm^3 $^{13}C_6$ (99%, 50 ppm) was added at 17:45 GMT on the 24/10/05 to the treatments. For clarity, Figs. 3.1 to 3.4 show the comparisons between individual pairs of treatments since, when all treatments are displayed on a single graph, the overlapping error bars create confusion.

When comparing the LV and CV treatments (Fig. 3.1), similar to the experiments performed in Chapter 2, the CV treatment showed a faster and greater response than the LV treatment; the δ $^{13}CO_2$ air and phenol-derived CO_2 fluxes peaked ca. 6 and ca. 8 hours after phenol addition in the CV and LV treatments, respectively. The LV treatment peaked shortly after the CV treatment and then remained lower than for the CV treatment over the remaining ca. 40 hours. However, ANOVA with repeated measures revealed no significant differences for the δ $^{13}CO_2$ in air, or for the phenol-derived CO_2 flux between these two treatments.

Comparing the CB and LB treatments (Fig. 3.2), again the CB treatment responded more rapidly to the addition than for the LB, peaking at ca. 6 hours and 7 hours in the δ $^{13}CO_2$ and phenol-derived CO_2 flux, respectively. Indeed, somewhat surprisingly, there was no definite peak in the LB treatment and ANOVA with repeated measures, showed the CB δ $^{13}CO_2$ in air to be significantly higher than the LB treatment in the first ca. 6 hours after phenol addition ($p=0.045$); *a posterori t* tests revealed the significant differences within the first 6 hours were between 2 and 6 hours after the phenol addition. The phenol-derived CO_2 flux in the CB treatment was also significantly higher than the LB treatment between ca. 2 hours and 11 hours after phenol addition ($p=0.033$); on this occasion *a posterori t* tests showed the significant differences within this time were at 2 hours and between 8 and 10 hours after phenol addition.

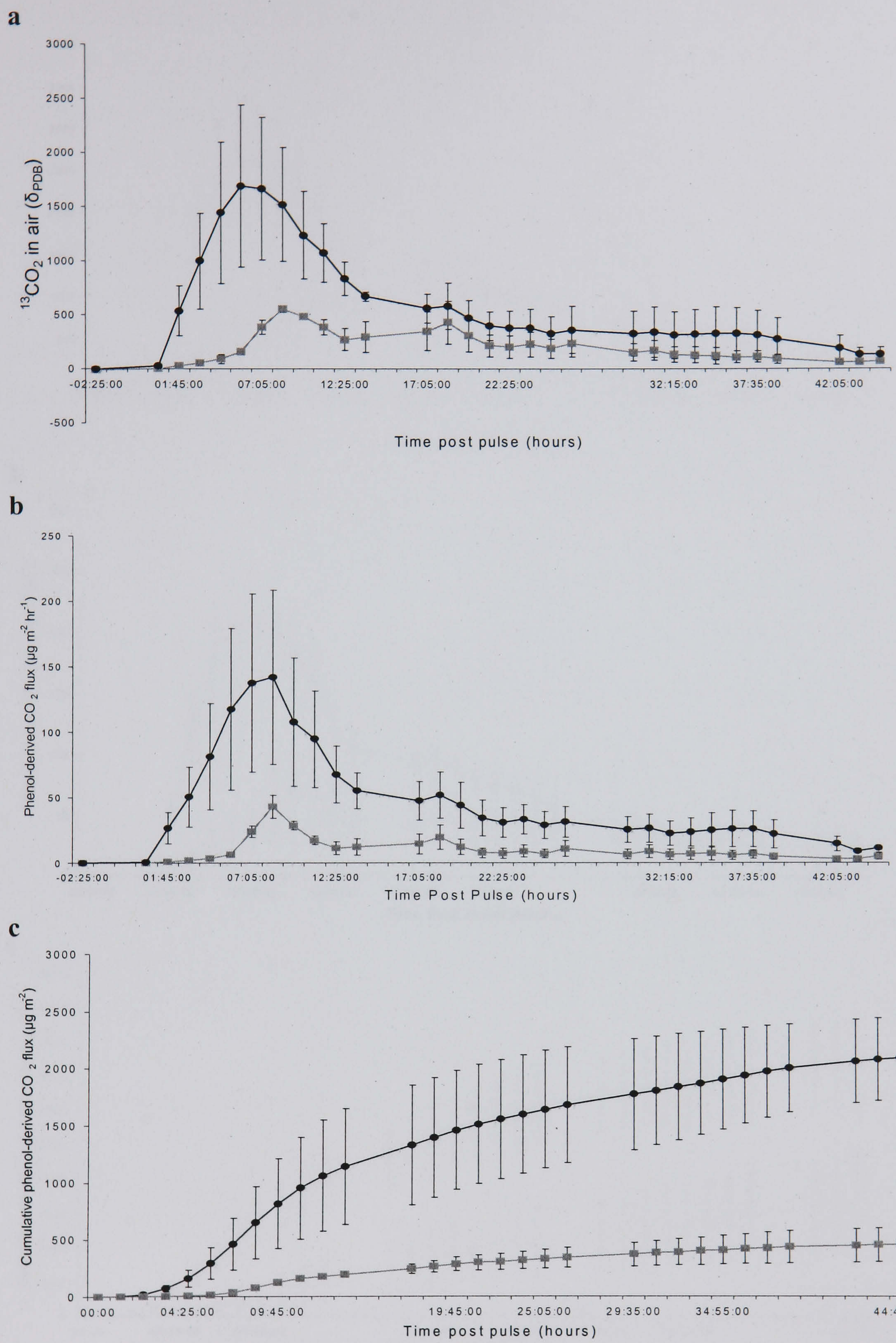

Figure 3.1 a, b, c δ $^{13}CO_2$ air values, phenol-derived CO_2 flux values and cumulative phenol-derived CO_2 values following the application of 300 cm^3 $^{13}C_6$ phenol [50 ppm] to the control (●—● CV), and limed (■—■ LV) vegetated plots. Error bars are one standard error of the mean.

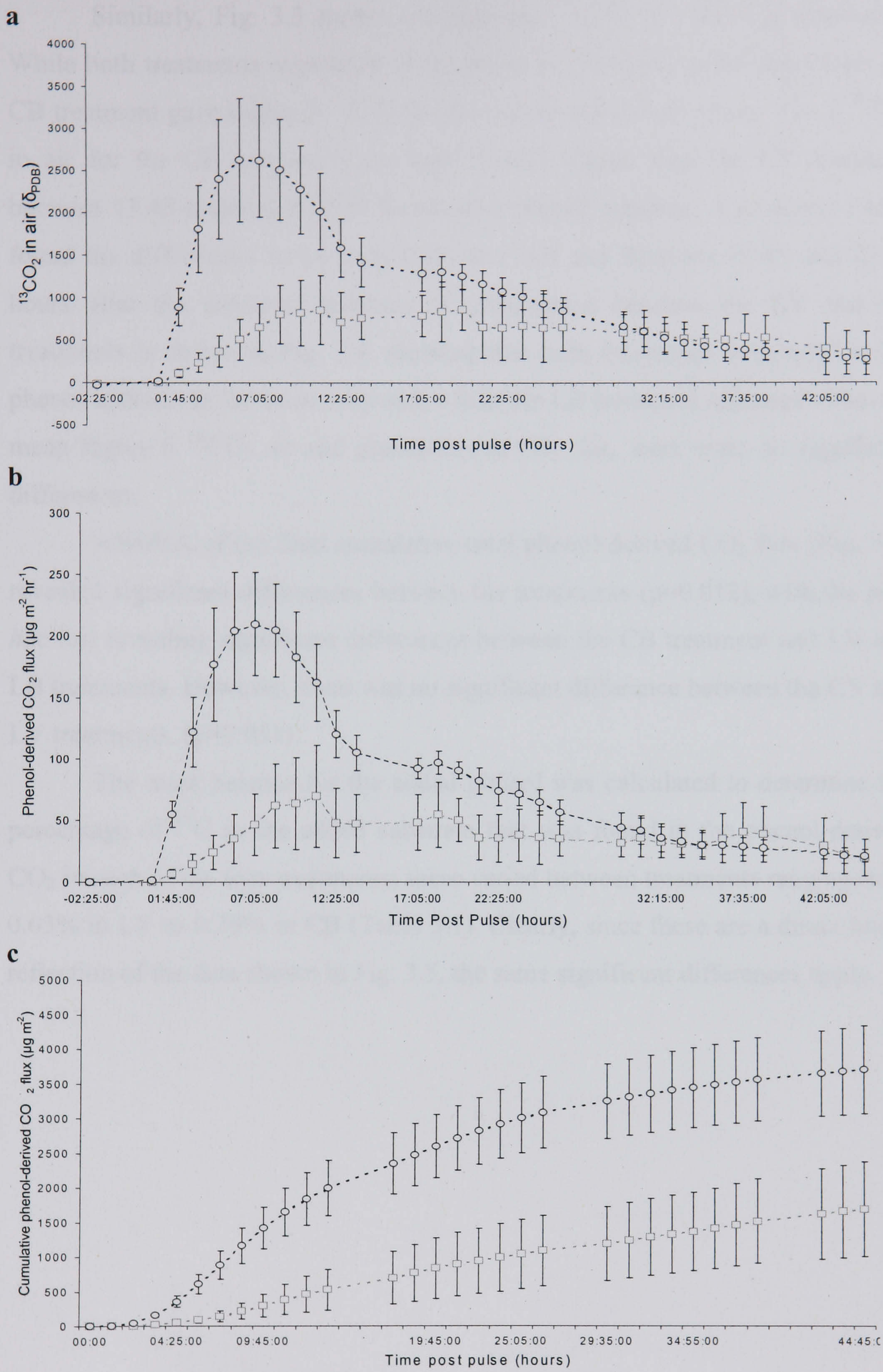

Figure 3.2 a, b, c δ $^{13}CO_2$ air values, phenol-derived CO_2 flux values and cumulative phenol-derived CO_2 values following the application of 300 cm^3 $^{13}C_6$ phenol [50 ppm] to the control (○- -○ CB), and limed (□- -□ LB) bare plots. Error bars are one standard error of the mean.

Similarly, Fig. 3.3 shows a comparison of the CV and CB treatments. While both treatments responded to the addition of phenol in the same way, the CB treatment gave higher $\delta\ ^{13}CO_2$ air and phenol-derived CO_2 fluxes. The $\delta\ ^{13}CO_2$ in air for the CB treatment was significantly higher than the CV treatment between 13:45 hours and 26:25 hours after phenol addition. *A posterori t* tests found the differences to be significant at 17:05 and between 19:45 and 22:25 hours after the substrate addition. A comparison between the LV and LB treatments is shown in Fig. 3.4, showing that both treatments responded to the phenol addition in the same way and, whilst the LB treatment appeared to have a mean higher $\delta\ ^{13}CO_2$ air and phenol-derived CO_2 flux, there were no significant differences.

ANOVA of the final cumulative total phenol-derived CO_2 flux (Fig. 3.5) revealed significant differences between the treatments ($p=0.012$), with the *post hoc* test revealing significant differences between the CB treatment and LV and LB treatments. However, there was no significant difference between the CV and LV treatments, ($p=0.051$).

The mass balance for the added phenol was calculated to determine the percentage of ^{13}C in the added substrate that was found in the phenol-derived CO_2 in each of the four treatments; these varied between treatments ranging from 0.03% in LV to 0.29% in CB (Table 3.1). Clearly, since these are a direct linear reflection of the data shown in Fig. 3.5, the same significant differences apply.

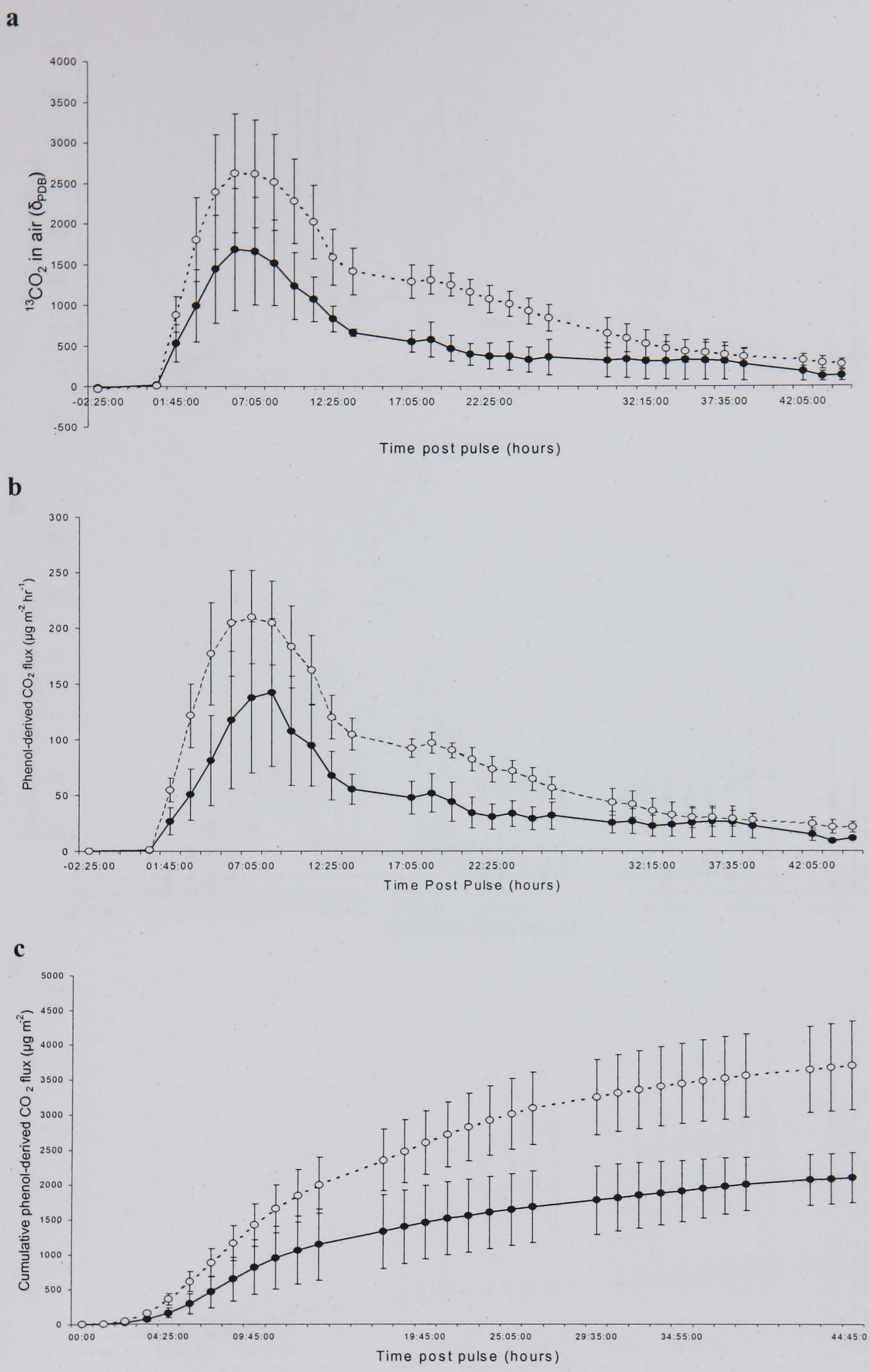

Figure 3.3 a, b, c δ $^{13}CO_2$ air values, phenol-derived CO_2 flux values and cumulative phenol-derived CO_2 values following the application of 300 cm^3 $^{13}C_6$ phenol [50 ppm] to the vegetated (●—● CV), and bare (○- -○ CB) control plots. Error bars are one standard error of the mean.

a

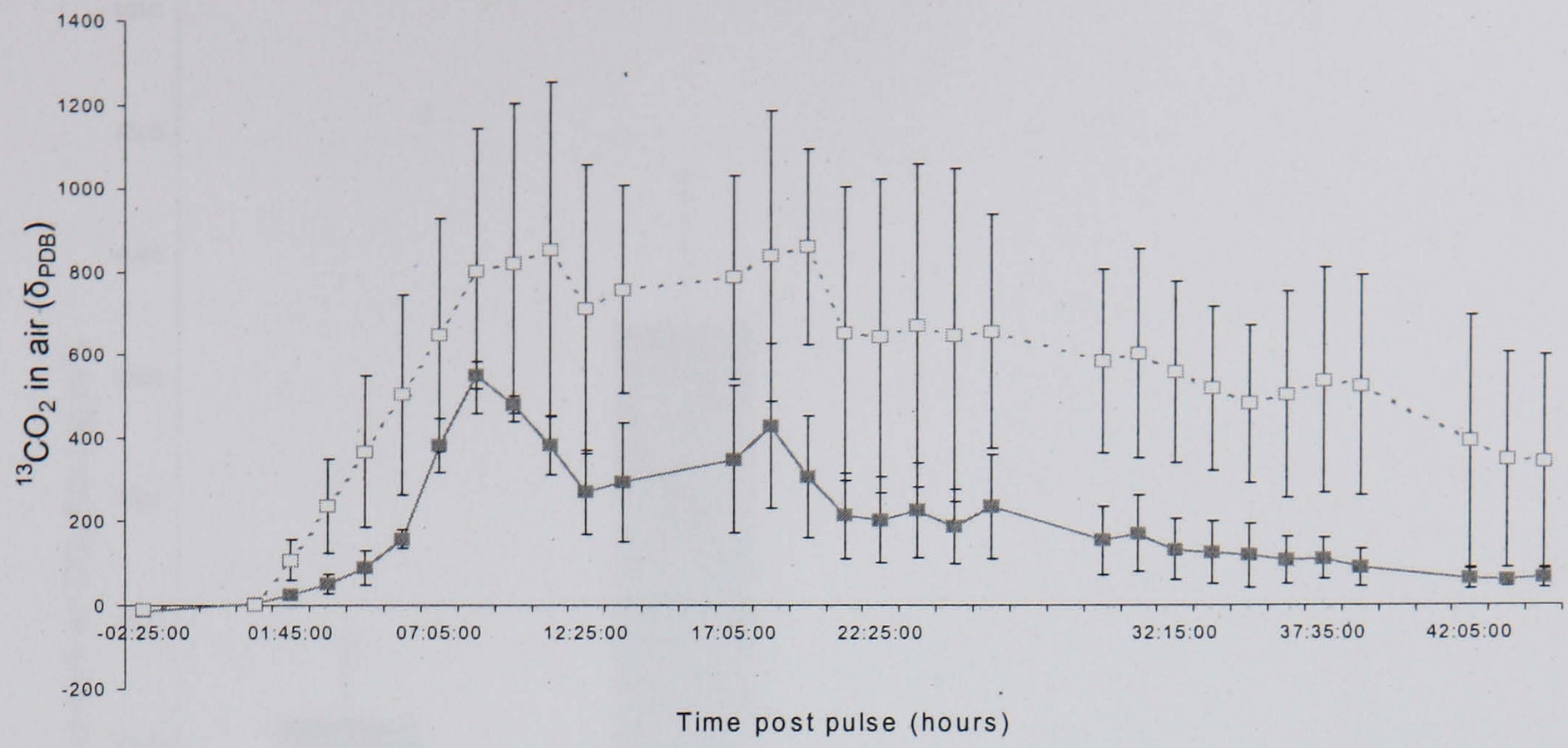

b

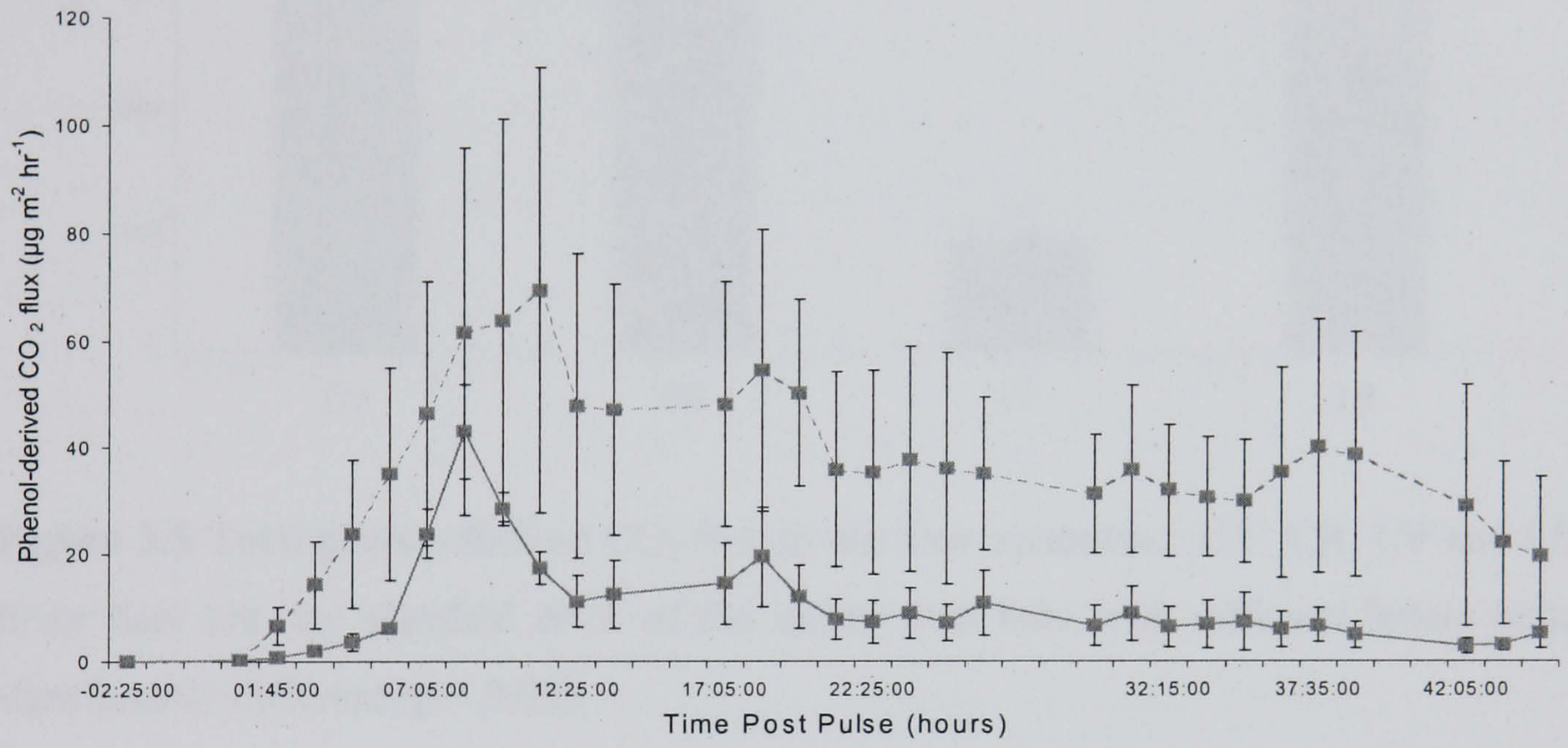

c

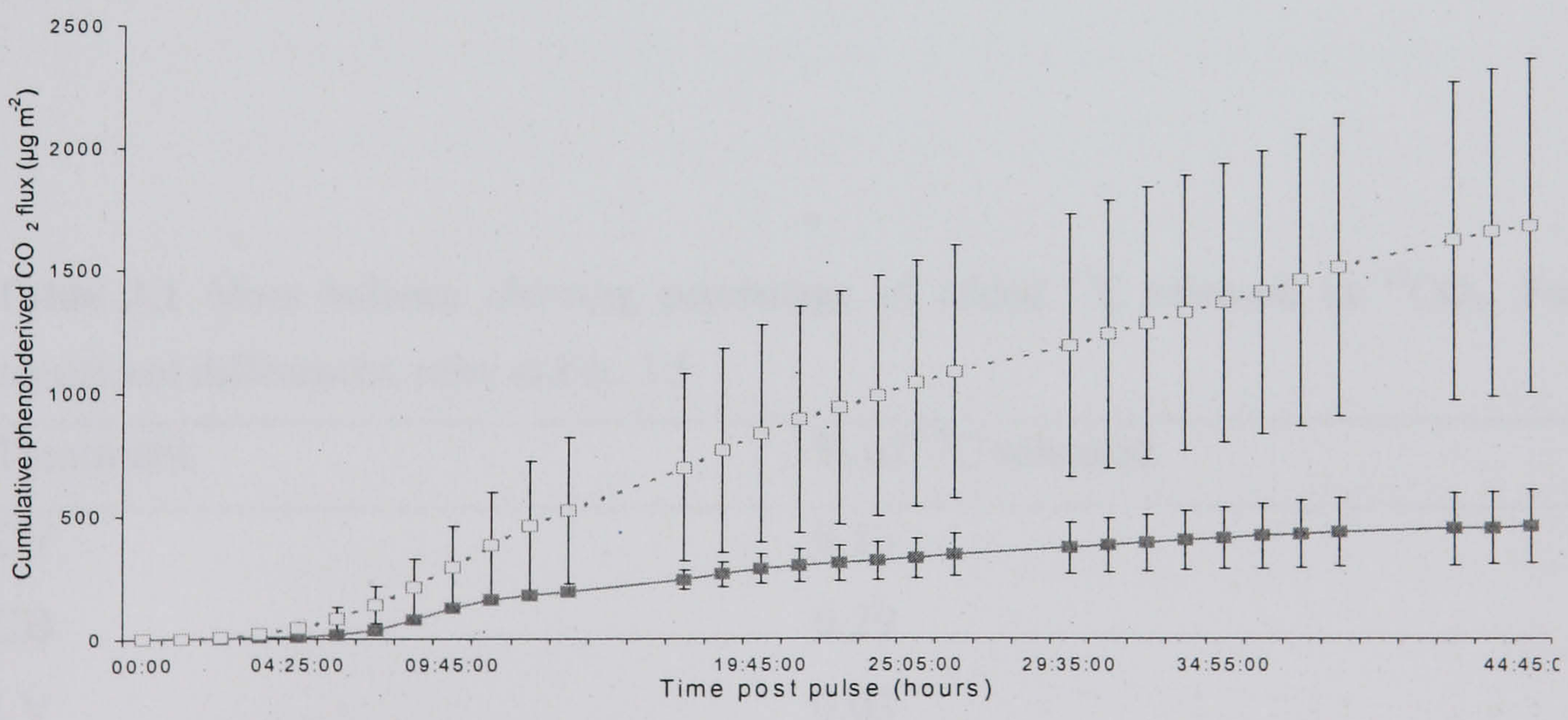

Figure 3.4 a, b, c δ $^{13}CO_2$ air values, phenol-derived CO_2 flux values and cumulative phenol-derived CO_2 values following the application of 300 cm^3 $^{13}C_6$ phenol [50 ppm] to the vegetated (■—■ LV), and bare (□- -□ LB) limed plots. Error bars are one standard error of the mean.

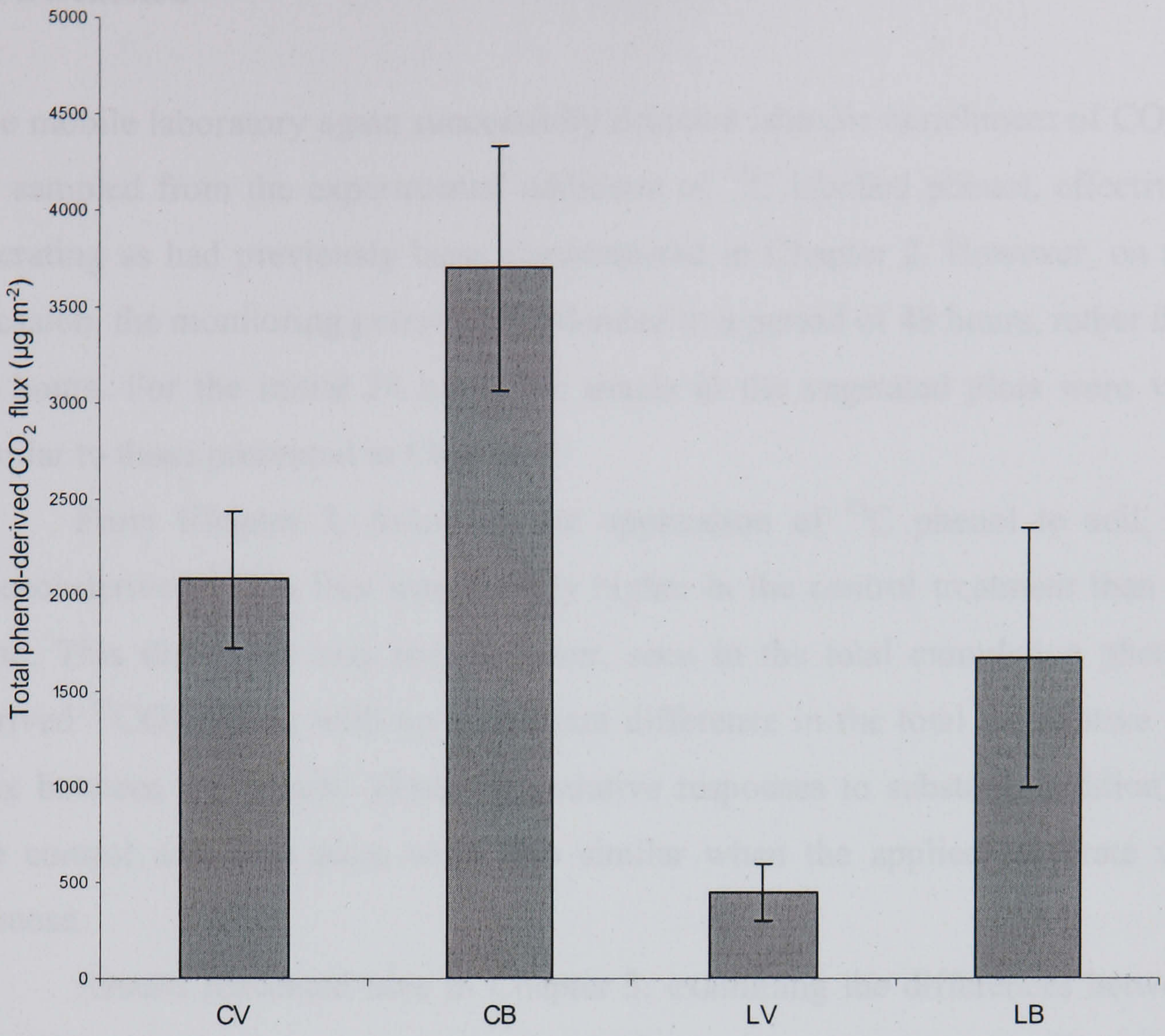

Figure 3.5 Total phenol-derived CO_2 flux in the four treatments: CV, CB, LV and LB, Error bars are one standard error of the mean, with bars with different letters being significantly different ($p < 0.05$).

Table 3.1 Mass balance showing percentage of added ^{13}C released as $^{13}CO_2$. For significant differences, refer to Fig. 3.5.

Treatment	% of ^{13}C released
CV	0.16
CB	0.29
LV	0.03
LB	0.13

3.4 Discussion

The mobile laboratory again successfully detected isotopic enrichment of CO_2 in air sampled from the experimental additions of ^{13}C labelled phenol, effectively operating as had previously been demonstrated in Chapter 2. However, on this occasion, the monitoring period was extended to a period of 48 hours, rather than 24 hours. For the initial 24 hours the trends in the vegetated plots were very similar to those presented in Chapter 2.

From Chapter 2, following the application of ^{13}C phenol to soil, the phenol-derived $^{13}CO_2$ flux was initially higher in the control treatment than the lime. This difference was not, however, seen in the total cumulative phenol-derived $^{13}CO_2$ fluxes, with no significant difference in the total cumulative ^{13}C flux between treatments. These comparative responses to substrate addition by the control and lime plots were also similar when the applied substrate was glucose.

Results presented here in Chapter 3, examining the differences between the CV and LV treatments were much the same as reported in Chapter 2. Although the monitoring was extended to twice the previous length of time, this did not result in a significant difference between the total cumulative phenol-derived $^{13}CO_2$ fluxes between the treatments, although the CV treatment consistently responded faster to the addition of the phenol than the LV treatment.

The differences between the responses of the control and lime treatments to phenol additions appeared robust across the two experiments which probably reflect the long-term changes in soil pH and vegetation cover, already discussed in Chapter 2 (Burt-Smith, 2003). The increase in pH, as a result of liming, is known to increase microbial biomass and activity (Frostegard *et al.*, 1993; Stenberg *et al.*, 2000). Gray *et al.,* (2003) studied the effects of lime of the bacterial community structure and soil processes at Sourhope and also reported a significant increase in soil pH from 4.9 in the control to pH 7.1 in the lime treatment. Additionally, comparisons between treatments of the above-ground biomass, an indication of plant productivity, showed greater biomass in the lime treatment (also supported by Rangel-Castro *et al.,* 2004). Gray *et al.* (2003) also used temporal temperature gradient electrophoresis (TTGE) to examine to composition of the soil biota and lime was found to have a significant effect on

the composition of the bacterial community, saprotrophic fungi and enchytraeid worms. However these authors did not detect any differences in the basal respiration rate, concluding that the addition of lime had little effect on the overall metabolic activity of the soil biota, supported by Kuan *et al.* (2006). Staddon *et al.* (2003) reported, after pulsing lime and control treatments at Sourhope with $^{13}CO_2$ that the concentration of the soil respired $^{13}CO_2$ was significantly higher in the lime treatments, yet this difference disappeared after one day post labelling.

In the plots studied here, with long-term vegetation removal, the same effects of lime were found again, with the initial response to phenol addition responding more slowly in the limed treatment when compared to the control. However, the effect on the cumulative phenol-derived $^{13}CO_2$ flux appeared exaggerated for these plots, as the LB treatment was significantly lower than the CB treatment. This effect did not appear to be as a result of a reduction in the phenol mineralization rate in the L treatment after the removal of vegetation, but rather an increase in the rates in the control plots. The relative effect of liming in reducing the phenol-derived $^{13}CO_2$ flux appeared greater in the vegetated treatments, suggesting that there is an interaction between the lime treatment and the presence of vegetation.

The time trends for $^{13}CO_2$ release in the bare plots generally followed those in the vegetated plots, but at higher absolute enrichment values, typically around 50% higher in the control plots and 100% higher in the lime plots, when compared to the vegetated plot equivalents. This could be due to the fact that there were fewer available C substrates in the soil where live vegetation was excluded, since plants release C substrates from their roots, which are available as a substrate supply for the organisms in the soil. It is known that the population of microorganisms in the soil are normally C limited, (Raynard *et al.*, 2006; Yoshitake *et al.*, 2007) and it is hypothesised that the phenol was more rapidly utilised in the absence of other, alternative, C sources.

The percentage of ^{13}C released as $^{13}CO_2$ indicated that the greatest mineralization (0.29%) of the phenol added was seen in the CB treatment, but this still left over 99% of the original substrate unaccounted for. This again highlights the sensitivity gained from the use of stable isotopes in soil research, demonstrating the ability to detect very small amounts of substrate degradation

difficult to detect using unlabelled phenol. There are three possible explanations for the small percentage of label appearing in the respired $^{13}CO_2$; firstly, either the organisms degrading the phenol are largely assimilating the C into microbial tissue as well as mineralising some of the substrate to CO_2, secondly, the phenol is remaining largely undegraded in the soil, or thirdly, most of the phenol is volatilising into the atmosphere.

Clearly, the addition of lime to the soil at Sourhope results in detectable changes the microbial community (Treonis *et al.*, 2004; Grayston *et al.*, 2001; Fuentes *et al.*, 2006). Whilst there is no other information available on the effect of this microbial community shift on the ability to degrade added C sources, it is clear from the results reported here that the organisms degrading phenol in the lime plots reacted differently to those in the control plots, mineralising a smaller percentage of the added substrate in the short term. One possibility is that the organisms in the lime plots are degrading the labelled substrate more slowly that those in the control plots, another is that the organisms in the lime and control treatments are assimilating the label into tissues to differing extents. The monitoring of ^{13}C incorporation into microbial tissue could potentially resolve which of these processes is dominating with the analysis of ^{13}C incorporation into PLFAs also offering great potential in respect of identifying the actual organisms responsible for these differences between treatments (Treonis *et al.*, 2004).

Chapter 4. Nucleic acid and PLFA SIP; tools for identifying *in situ* phenol degraders in soils

4.1 Introduction

The $^{13}CO_2$ evolved from soils exposed to ^{13}C labeled phenol in Chapters 2 and 3 demonstrated that liming the soil at Sourhope had an effect on phenol degradation as did vegetation coverage on the amount of $^{13}CO_2$ returned 48 hours after an addition of highly labelled ^{13}C phenol. Unfortunately, this approach alone does not offer any reason as to why those differences were seen.

Stable isotope probing (Radajewski *et al.,* 2000) of nucleic acids can assist in functional identification of organisms, having the ability to identify a species carrying out a specific function. Nucleic acids in organisms that assimilate a substance of interest, for example in the degradation of labelled phenol, will have the label present in the phenol incorporated. Ultracentrifugation can be used to separate the enriched, heavy nucleic material from that containing isotopes at natural abundance levels. The technique, using DNA as a labelled biomarker, was first performed by Radajewski *et al.* (2000) and identified the organisms responsible for the assimilation of methanol as a carbon source in a temperate forest soil. Manefield *et al.* (2002b) have subsequently used RNA SIP to identify a non-culturable bacterial *Thauera* sp. important in phenol degradation in a bioreactor.

At the time of the experiment outlined in this Chapter there had only been one published account of the use of RNA-based SIP (Manefield *et al.*, 2002b) unlike DNA SIP which had been used by several workers (Radajewski *et al.*, 2000; Padmanabhan *et al.,* 2003; Manefield *et al.*, 2002a; Radajewski *et al.*, 2003). Although it was recognised that RNA-SIP presented a much more difficult challenge, the advantages of being able identify active organisms meant that work was concentrated on the RNA approach. The potential disadvantages of using RNA are in the far more stringent conditions necessary for successful application of RT-PCR, together with the avoidance of RNAase contamination.

As discussed in Chapter 1, the pathways of phenol degradation result in the formation of substrates, which may enter the Krebs cycle and are therefore available for incorporation into cellular structures, including nucleotides and, subsequently, nucleic acids.

Stable isotope probing of PLFAs also offers general identification of active organisms, though only to the group level, rather than the species as with DNA or RNA SIP. There are advantages of using PLFAs as a functional biomarker, above nucleic acids, namely the robustness of the technique, and the reliability of the results produced. DNA and, especially, RNA SIP is still very much an emerging technology, and while results using these apparatus are impressive, they pose a technical challenge in terms of optimising conditions and the reproducibility of results. In contrast, SIP using PLFAs has been used for several years now, being first pioneered by Boschker (1998), and has become widely used because of reliability, simplicity and low costs, when compared with DNA or RNA SIP.

Both SIP techniques, lipid or nucleic acid, offer an insight into the changes in the microbial community that are responsible for the differences in phenol degradation as seen in chapters 2 and 3.

4. 2 Methods

4.2.1 RNA Extraction

Root and soil samples from a C labelling experiment at Sourhope were used to optimise and perfect the processes of RNA extraction, separation and subsequent RT-PCR, prior to using any experimental samples.

4.2.1.1 Soil RNA Extraction

Soil, 0.3 g dry weight, was placed in an Eppendorf tube, together with CTAB buffer (5% CTAB/ phosphate buffer (120 mM pH 8) mix 50/50 (10% CTAB in 0.7M

NaCl) and (240 mM potassium phosphate buffer pH 8), 0.5 ml, and P:C:I (phenol: chloroform: isoamyl alcohol, pH 8 25:24:1), 0.5 ml. Two 1 mm glass beads were placed in the Eppendorf, which was sealed and vortexed for 30 seconds at high speed to lyse the cells. The tubes were incubated on ice before being centrifuged at 18,000 G (14,000 rpm) at 4°C, for 10 minutes. The top layer was removed and placed into a new Eppendorf tube containing an equal volume of chloroform: isoamyl alcohol (24:1). This was vortexed for 30 seconds to form an emulsion, followed by centrifugation at 18,000 G for 10 minutes at room temperature. The top layer was removed and nucleic acids precipitated by adding 2 volumes of PEG solution and vortexing for 30 seconds. The tubes were then left at room temperature overnight. Samples were subsequently centrifuged at 18,000 G for 10 minutes at room temperature, the supernatant was removed and the pellet washed with 70% ethanol, 500 µl. The ethanol was removed and the pellet of nucleic acids was left to air dry for 20 minutes before being resuspended in TE buffer, 30 µl. This nucleic extract was run on a gel, 1% agarose (Sigma, UK) in TBE buffer, to check extraction was successful. DNA was removed by digestion with a DNAse kit, (Promega) leaving only RNA. Samples were then re-run on a 1% agarose gel, in TBE buffer, to check for the presence of RNA.

4.2.1.2 Root RNA Extraction

Root, length 2 cm, was placed in a glass pestle and ground in liquid nitrogen. CTAB buffer, 500 µl, was added and the root ground again as the CTAB thawed. The sample was transferred to an Eppendorf tube and CTAB, 300 µl, was added to the pestle, to maximise sample recovery. This was then added to the Eppendorf, which was then incubated at 65°C for 60 minutes, and extracted with an equal volume of phenol:$CHCl_3$:isopropanol(25:24:1). The sample was centrifuged at 18,000 G for 5 minutes at room temperature and extracted again with an equal volume of $CHCl_3$, and further centrifuged at 18,000 G for 5 minutes at room temperature. The nucleic acids were precipitated using isopropanol, 1.5 volumes and incubated on ice for 10 minutes, prior to being centrifuged at 14,000 rpm for 15 minutes. The isopropanol

was removed and the pellet washed with 70% ethanol, and this was centrifuged at 14,000 rpm for 5 minutes, the ethanol removed and the pellet allowed to air dry before being resuspended in deionised H_2O, 100 µl. The nucleic extract was run on an electrophoresis gel, 1% agarose in TBE buffer, to check that extraction was successful. The nucleic acids were purified using a kit for the purification of PCR products (Qiagen, UK) and the DNA was removed by digestion with a DNAse kit, (Promega), leaving RNA. Samples were then re-run on an electrophoresis gel, 1% agarose in TBE buffer, to check for the presence of RNA.

4.2.1.3 Separation of ^{12}C and ^{13}C

A spectrophotometer, λ=260 nm, was used to quantify the amount of RNA present in 6 samples, 3 from soil extracts, 3 from root extracts. Deionised water, 50 µl, was placed into a 50 µl cuvette and the spectrophotometer set to zero absorbance. The calibration was tested with another cuvette containing 50 µl of deionised water before the RNA samples were measured. Soil RNA sample, 2 µl, was added to deionised water, 78 µl, to give a 1 in 40 dilution. Each soil dilution, 50 µl was then placed in the cuvette and the absorbance measured. This was repeated for each of the root samples but, as their nucleic acid yield appeared to be less than the soil, based on the eletrophoresis gel (Plate 4), 4 µl of root RNA sample was added to 76 µl of deionised water to give a 1 in 20 dilution. The amount of RNA digest required to load into centrifuge tubes was 0.45 µg (based on Gornall, 2000) and was calculated using the following equation.

Volume to load (mls) = 0.45 x (1 / µg RNA / ml)

Caesium trifluoracetate (CsTFA) was added to 6 13 cm^3 Quick Seal centrifuge tubes ultraclear 15 x 76 mm, (Beckman Coulter, Switzerland), until they were approximately ¾ full. The tubes had been sterilised, and any nucleic acids on them degraded, prior to use by irradiation with UV light. The RNA sample was

added to the tube and more CsTFA was added until the level reached almost the top of the tube. Each sample was then weighed and more CsTFA was added drop wise, until all 6 tubes were within 0.1 g of each other and tapping the side of the tube gently removed any air bubbles in the CsTFA. The tubes were then heat-sealed using a Beckman tube sealer, the CsTFA above the RNA sample protecting it from the brief period of heat, and placed into a Beckman fixed angle, 70.1 T1 rotor with the closest in weight being opposite pairs. The rotor with samples was sealed and placed into a Beckman L8-70M ultracentrifuge and spun at 43,000 rpm (320,000 G) at 4°C for 36 hours with no brake applied. Once spun the tubes were carefully removed and secured upright between two bosses on a clamp stand. (Fig. 4.1)

A template, made from the side of a tube identical to the one with the sample in with 23 small holes vertical holes 2 mm apart, was stuck to the side of the tube with double-sided tape, having been irradiated prior to use with UV light. (Fig 4.1)

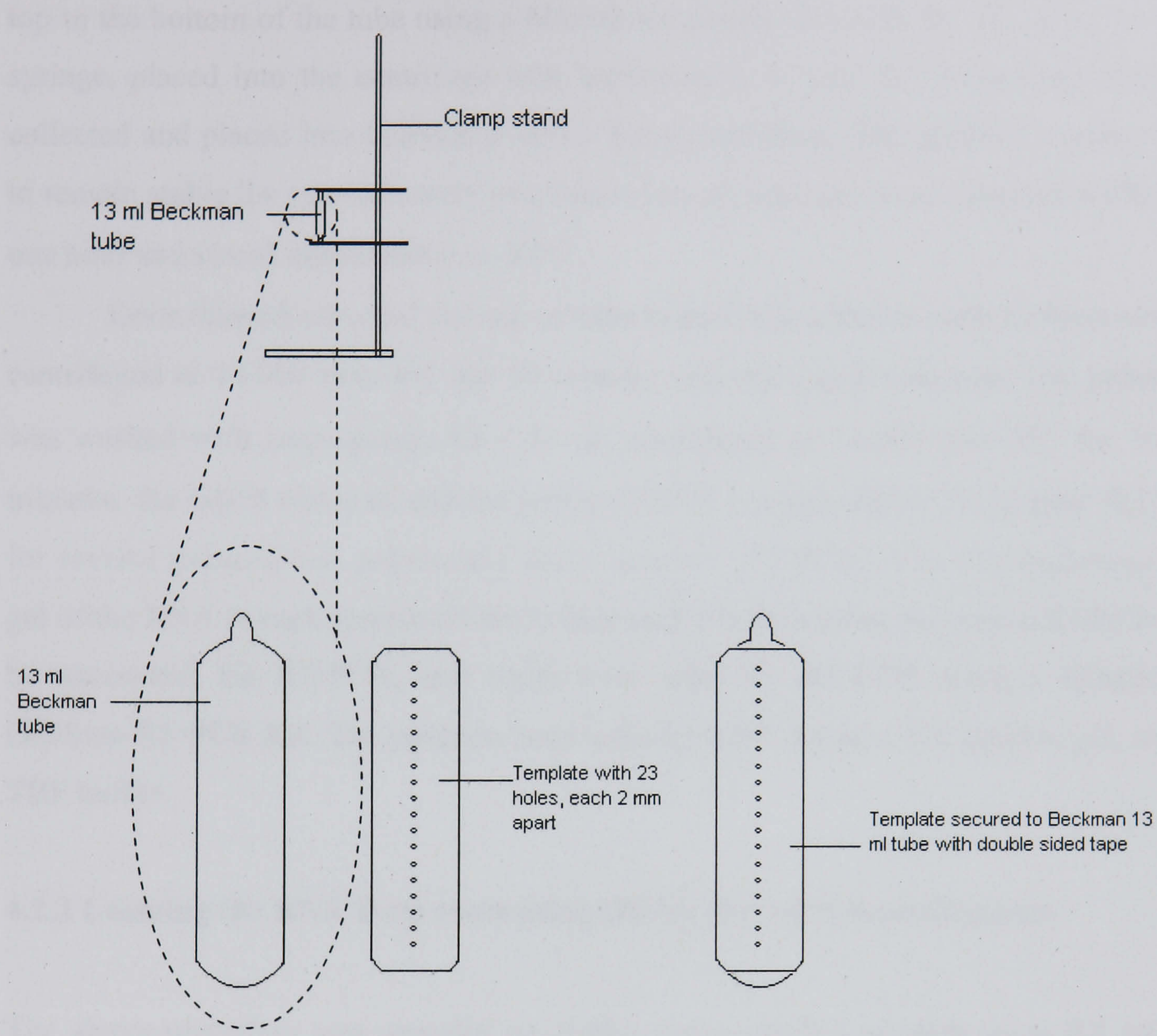

Fig 4.1 Visualisation of the arrangement of the ultracentrifuge tube in the clamp stage for fractionation and the template used to deliver fractions after ultracentrifugation.

After a needle had been inserted into the top of the tube to prevent a vacuum forming, fractions were collected though each 2 mm hole in the template from the top to the bottom of the tube using a Microlance needle, 0.5 x 25 Nr. 18, and 2 cm^3 syringe, placed into the centrifuge tube horizontally, A total of 24 fractions were collected and placed into individual sterile Eppendorf tubes. The gradient is known to remain stable for approximately two hours, and all fractions were collected within one hour and stored immediately at -80°C.

Once thawed, an equal volume of isopropanol was added to each fraction and centrifuged at 14,000 rpm 4°C for 30 minutes and the liquid removed. The pellet was washed with isopropanol, 40 – 50 µl, centrifuged at 14,000 rpm 4°C for 10 minutes, the liquid removed and the pellet of RNA resuspended in 20 µl pure H_2O for reverse transcription polymerase chain reaction (RT-PCR). The electrophoresis gel of the RNA in each sample (Plate 5) indicated which samples were most likely to be successful for RT-PCR, and these were used for RT-PCR using a Qiagen OneStep RT-PCR Kit. The products were subsequently run on a 1% agarose gel, in TBE buffer.

4.2.2 Locating the RNA from roots using IRMS after ultracentrifugation

The above procedure was repeated on further pulse labelled samples using 0.6 µg RNA and included some highly labelled *Ranunculus* roots. The fractions were extracted using the same methods as previously described and, after ultracentrifugation, a sub sample, 25 µg of each fraction was taken for analysis using an isotope ratio mass spectrometer (IRMS). IRMS is a powerful tool to detect isotopic label, as it can detect enrichments of only a few per mil, and so presented an opportunity to identify the position with any ^{13}C enriched RNA within the tube. A tube containing only CsTFA was subject to all the above treatments and analysed to act as a control.

4.2.3 Locating the RNA from *E. coli* using IRMS after ultracentrifugation

There was no detectable label present, in either roots or soil, from the pulse described in Section 4.2.1. In order to isolate the more likely reason for the inability to detect the label it was decided to establish that the application of the basic molecular methodology was not the reason. In order to test this it was decided to produce labelled standard laboratory material with all nucleic acids unambiguously and heavily labelled with ^{13}C. By growing *E. coli*, a readily culturable bacterium, on a medium with 99% $^{13}C_6$ glucose as the sole C source, all resulting cellular components, including RNA, would be highly enriched; an approach analogous to the classical conservative and semi-conservative ^{15}N studies performed by Meselson and Stahl (1958).

In order to determine the optimum amount of RNA to load onto the CsTFA gradient and to check that the ^{12}C and ^{13}C labelled RNA samples separated on the CsTFA gradient, *E. coli* was cultured on LB broth containing either ^{12}C or 99% ^{13}C glucose as the carbon source, thus producing unlabelled and highly enriched nucleic acid material. RNA from the *E. coli* was extracted using a Qiagen RNeasy Kit and DNase Option with four different total amounts of RNA: 0.3 μg, 0.6 μg, 1.2 μg and 2.4 μg, (50% ^{12}C 50% ^{13}C), being loaded onto CsTFA tubes for ultracentrifugation. The fractions were collected in the same manner as in sections 4.2.1 and 4.2.2 and were analysed using the IRMS to look for enrichment, as in section 4.2.2.

4.2.4 Sourhope 2004 soil sampling for PLFA work

To measure the degradation of phenol in the field $^{13}C_6$ phenol (Cambridge Isotope Laboratories, UK) 600 cm^3 $^{13}C_6$ (99%, 50 ppm), was applied to soil (628 cm^2) in each of the 12 treated plots, across four different treatments, with three replicates of each treatment. Water, 300 cm^3, was added to two "natural abundance" rings (314 cm^2) and the treatment plots were; control with vegetation (CV), control without vegetation or 'bare' (CB), lime with vegetation (LV), and lime without vegetation (LB).

Soil samples, 6 cm diameter, 4 cm depth were taken for PLFA analysis at 3, 6, 9, 12, 18, 24, 36, and 48hours after application. Samples were also taken from the natural abundance plots. The treated areas were then covered over with black plastic sheeting. This served two purposes; it reduced the photosynthetic ^{12}C input into the system and prevented any precipitation from washing the phenol from the system. Once the samples were taken they were immediately frozen in liquid N_2 to halt any microbial activity.

4.2.5 PLFA Extraction

PLFAs were extracted using a modified Bligh-Dyer extraction (White *et al.*, 1979). The samples, stored at -80°C, were freeze-dried, with roots and small stones being removed by hand. The resulting samples were ground using a pestle and mortar to ensure the full PLFAs recovery and maximise yield. Each sample, 2 g, was then added to a Pyrex screw top tube, 35 cm^3, and the same volume of DCM/MeOH/citrate buffer (5:10:4 v/v/v; citrate buffer 0.15M adjusted to pH 4 using NaOH pellets), was added to each sample. A screw cap sealed the tube and the sample was mixed and placed in an ultrasonic bath, 15 minutes, and then centrifuged at 1000 rpm for 3 minutes. The supernatant was transferred to another Pyrex screw top tube, 35 cm^3 and the soil extracted with fresh solvent twice more. Citrate buffer, 2 cm^3 and DCM, 2 cm^3 were added to the supernatant, to break the organic and aqueous phases of the combined solvent extracts, then mixed and centrifuged at 1000 rpm for 3 minutes, and the organic layer removed. The aqueous was layer washed with DCM, 2 cm^3, 3 times and the combined extracts were then placed on a heated block at 40°C and blown down with OFN until dry.

An aminopropyl solid phase extraction cartridge (Bond Elut NH_2, Varian, Surry UK) was used to separate the PLFAs from the other lipids. The column was conditioned with DCM:IP, 2:1, 6 cm^3 , and the dry sample added to the column re-suspended in DCM:IP, 2:1 3 x 1 ml. DCM:IP, 2:1, 6 cm^3 was then added to the column to elute neutral lipids, followed by 2% glacial acetic acid in diethyl ether, 8 cm^3, to elute the acidic lipids. Methanol, 8 cm^3, was then added to he column and the

eluted polar lipids, including PLFAs, were collected in a Pyrex culture tube. The sample was then placed on a heated block at 50°C and blown down with OFN until dry.

A known concentration of internal standard, Nonadecane, was added to the samples to enable the quantity of PLFAs to be calculated. The samples were then saponified by the addition of 0.5M NaOH in methanol, 2 cm^3, and a few drops of DCM-extracted water and susequently sealed, mixed and placed on a heated block at 70°C for 90 minutes. Samples were then acidified to pH 1 – 2 with 0.5M HCl (analytical grade), and the lipids were extracted using 3 x 2 cm^3 DCM and blown down on a heated block at 40°C with OFN until dry. Fatty acids were derivatised to produce fatty acid methyl esters (FAMEs) using BF_3-MeOH, 8 drops, and sealed samples placed on a heated block at 70°C for 10 minutes. DCM-extracted water, 6 drops, quenched the reaction and the FAMEs were extracted using 3 x 1 cm^3 hexane. The samples were then placed on a hot block at 40°C, blown down with OFN until dry, sealed and stored in a fridge until analysis, at which stage they were redissolved in an appropriate amount (depending on the amount of PLFA in the sample, calculated by analysing first on a GC) of hexane for analysis by gas chromatography (GC) and gas chromatography-mass spectrometry (GC-MS).

4.2.6 PLFA Profiles

The conventional way to designate PLFAs is by the number of C atoms, then a colon, followed by the number of double bonds and the position of the first double bond from the methyl end of the molecule. A prefix of 'i' or 'a' designates branched chain PLFAs, representing iso and anteiso branching respectively, whilst a prefix 'cy' denotes a cyclopropane fatty acid and Br and Me denote a branch at an unknown location and a methyl group respectively. For example 18:2(n-6) is a PLFA with 18 carbon atoms and 2 double bonds, the first of which is 6 carbon atoms away from the methyl end of the molecule. The PLFAs were assigned to groups as per the identifications reported by Phillips *et al*. (2002).

4.2.7 Statistical analysis

ANOVA with repeated measures was also used to analyse all the grouped PLFA data with the data being logged if necessary to normalise it, using SPSS (v.14.0 2005 SPSS. Inc). A post hoc Tukey was then applied.

SAS (V8 2000 SAS Institute Inc) was used to perform ANOVAs on each of the individual PLFAs for the compositions, $\delta^{13}C$ and ng. It is recognised that doing high numbers of ANOVA increased the likelihood of Type II statistical errors. Principal components analysis (PCA) was then performed on the compositions, $\delta^{13}C$ and ng, also using SAS.

4.3 Results

4.3.1 RNA Extraction and separation of ^{12}C and ^{13}C

Plate 4 shows successful nucleic extraction from all samples. More nucleic material was obtained from the soil samples than the roots, indicated by the amount of fluorescence. Traces of possible RNA were seen on the electrophoresis gel in 3 soil samples, so these were selected for RT-PCR.

The fractions collected after ultra centrifugation from each of the 3 samples selected all failed to yield any detectable nucleic material after RT-PCR.

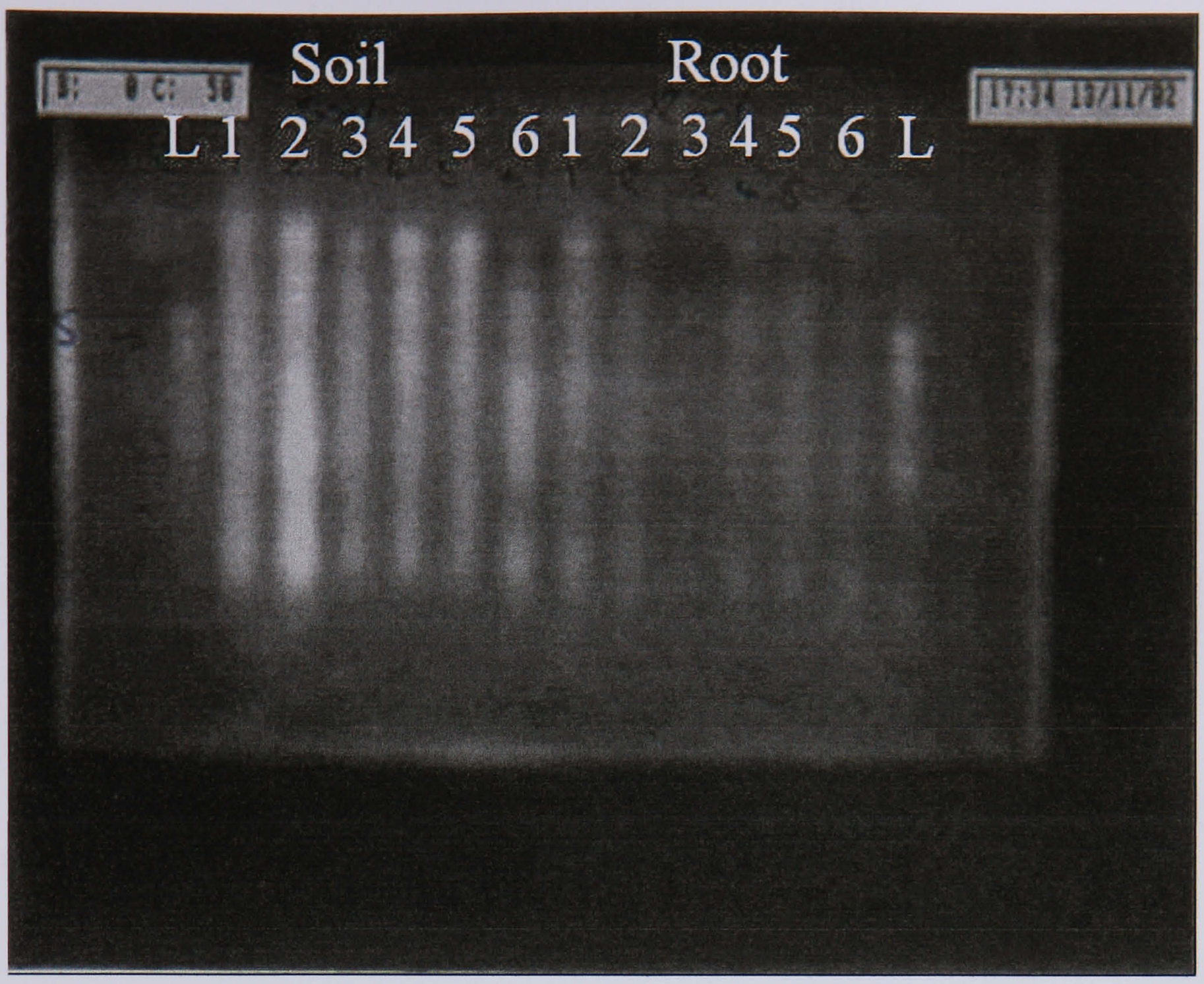

Plate 4 Total nucleic extraction from all samples. L represents a nucleic ladder at each end.

4.3.2 Locating the RNA from roots using IRMS after ultracentrifugation

Figure 4.2 demonstrates that the IRMS detected an isotope gradient within the CsTFA after ultracentrifugation. The IRMS did not detect any enriched RNA in any of the samples.

RT-PCR on the fractions also failed to produce any nucleic material.

4.3.3 Locating the RNA from *E. coli* using IRMS after ultracentrifugation

Figure 4.3 indicates that the IRMS detected an isotope gradient within the CsTFA after ultracentrifugation. The IRMS did detect apparent enrichment in some fractions, although this was not consistent throughout the series, which would have been expected. RT-PCR on the fractions failed to produce any nucleic material.

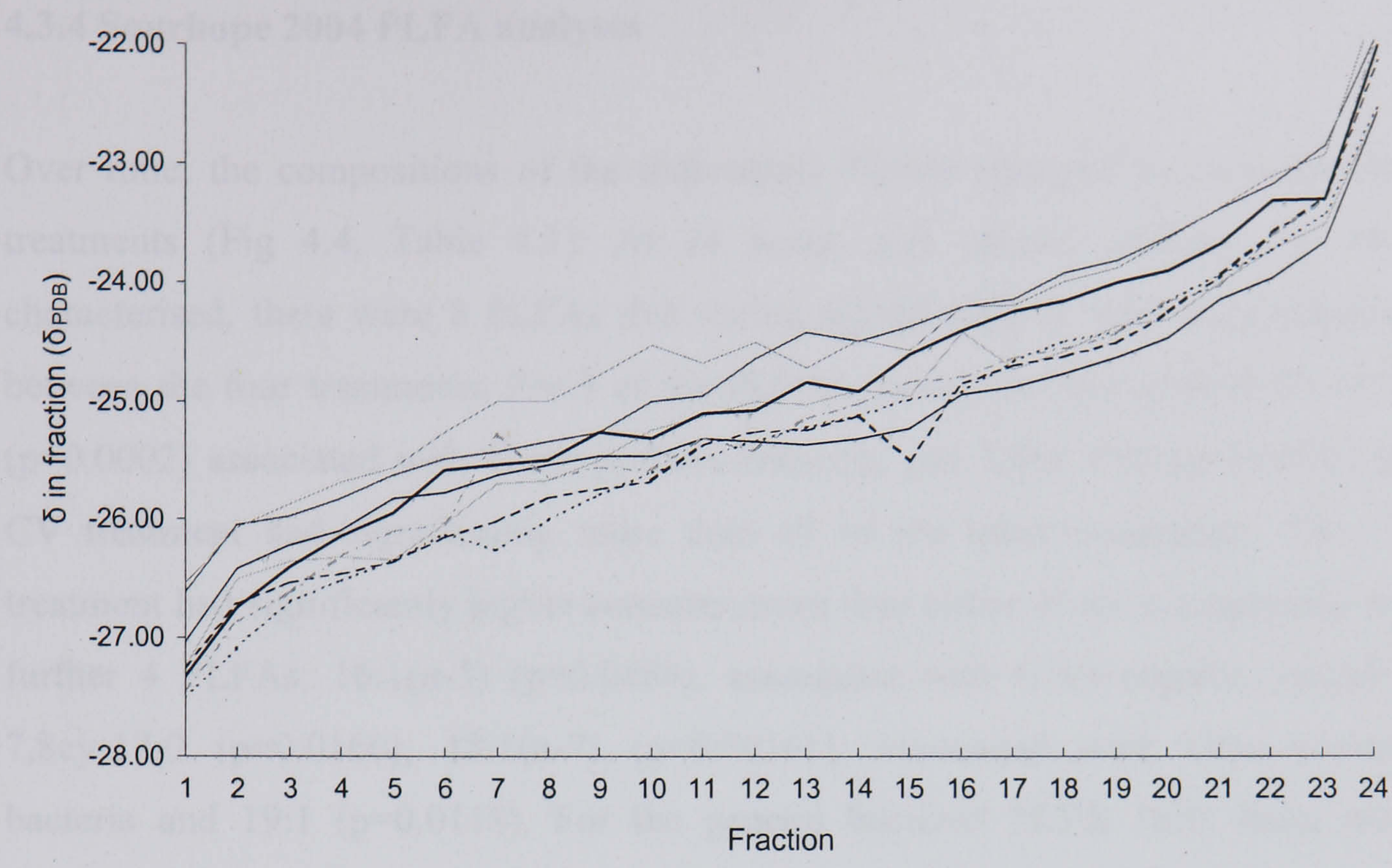

Figure 4.2 δ ^{13}C values for the fractions after ultra-centrifugation, fraction 1 was at the top of the tube, fraction 24, at the bottom.

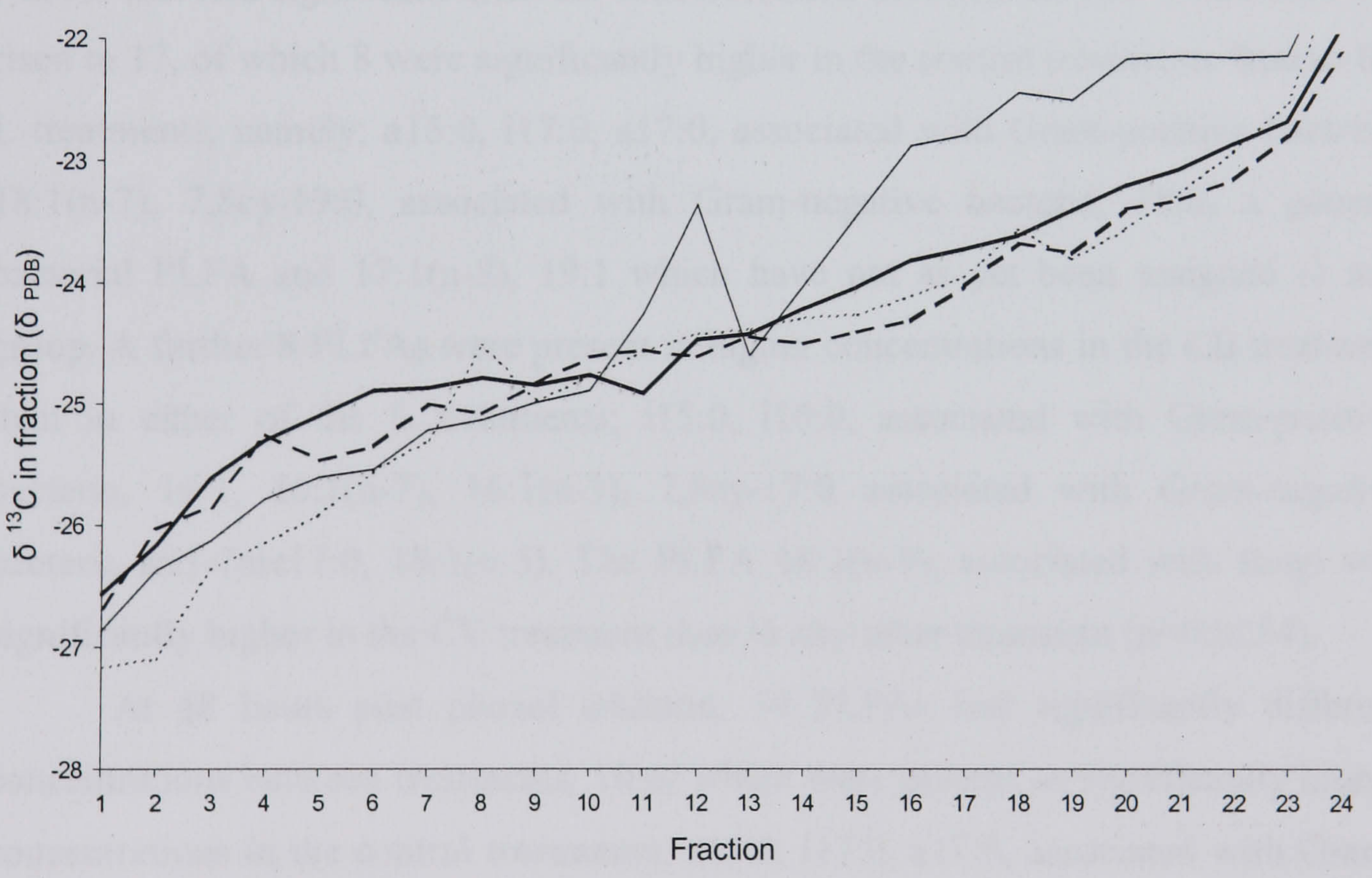

Figure 4.3 δ ^{13}C values for the fractions after ultra-centrifugation, fraction 1 was at the top of the tube, fraction 24, at the bottom. - - - 0.3 µg RNA, —— 0.6 µg RNA, ▫ ▫ ▫ ▫ 1.2 µg RNA, ——2.4 µg RNA.

4.3.4 Sourhope 2004 PLFA analyses

Over time, the compositions of the individuals PLFAs changed between the four treatments (Fig 4.4, Table 4.1). At 24 hours post phenol addition, of those characterised, there were 8 PLFAs that varied significantly in their concentrations between the four treatments. For 3 of the PLFAs, namely br17:0 ($p=0.0276$), i17:0 ($p=0.0002$) associated with Gram-positive bacteria, and 7,8cy-19:0 ($p=0.0001$) the CV treatment had significantly more than all of the other treatments. The CV treatment had significantly higher concentrations than either of the L treatments in a further 4 PLFAs; 16:1(n-5) ($p=0.0484$), associated with Gram-negative bacteria, 7,8cy-17:0 ($p=0.0166$), 18:1(n-7) ($p=0.00161$), associated with Gram-positive bacteria and 19:1 ($p=0.0118$). For the general bacterial PLFA 18:0, there were significantly more in the control treatments than the L treatments ($p=0.0035$)

After a further 12 hours, at 36 hours post phenol addition, the number of PLFAs that had significant different concentrations between the four treatments had risen to 17, of which 8 were significantly higher in the control treatments than in the L treatments, namely; a15:0, i17:0, a17:0, associated with Gram-positive bacteria, 18:1(n-7), 7,8cy-19:0, associated with Gram-negative bacteria, 18:0, a general bacterial PLFA and 17:1(n-8), 19:1 which have not as yet been assigned to any group. A further 8 PLFAs were present in higher concentrations in the CB treatment than in either of the L treatments; i15:0, i16:0, associated with Gram-positive bacteria, 16:1, 16:1(n-7), 16:1(n-5), 7,8cy-17:0 associated with Gram-negative bacteria and 7me17:0, 18:1(n-5). The PLFA 18:1(n-9), associated with fungi was significantly higher in the CV treatment than in any other treatment ($p=0.0254$).

At 48 hours post phenol addition, 14 PLFAs had significantly different concentrations between treatments, 10 of which were present as significantly higher concentrations in the control treatments; a15:0, i17:0, a17:0, associated with Gram-positive bacteria, 16:1, 7,8cy-17:0, 18:1(n-7), 7,8cy-19:0, associated with Gram-negative bacteria, general bacterial PLFA 18:0 and non specific 17:1(n-8), 18:1(n-5). Whilst different PLFAs either became or stopped being significantly different between treatments, the interaction between the treatment and time resulted in

significance for only 2 PLFAs; 14:0 (p=0.0481) and the Gram-positive bacterial PLFA i17:0 (p=0.0349). It can therefore be concluded that phenol had an effect on these 2 PLFA.

a

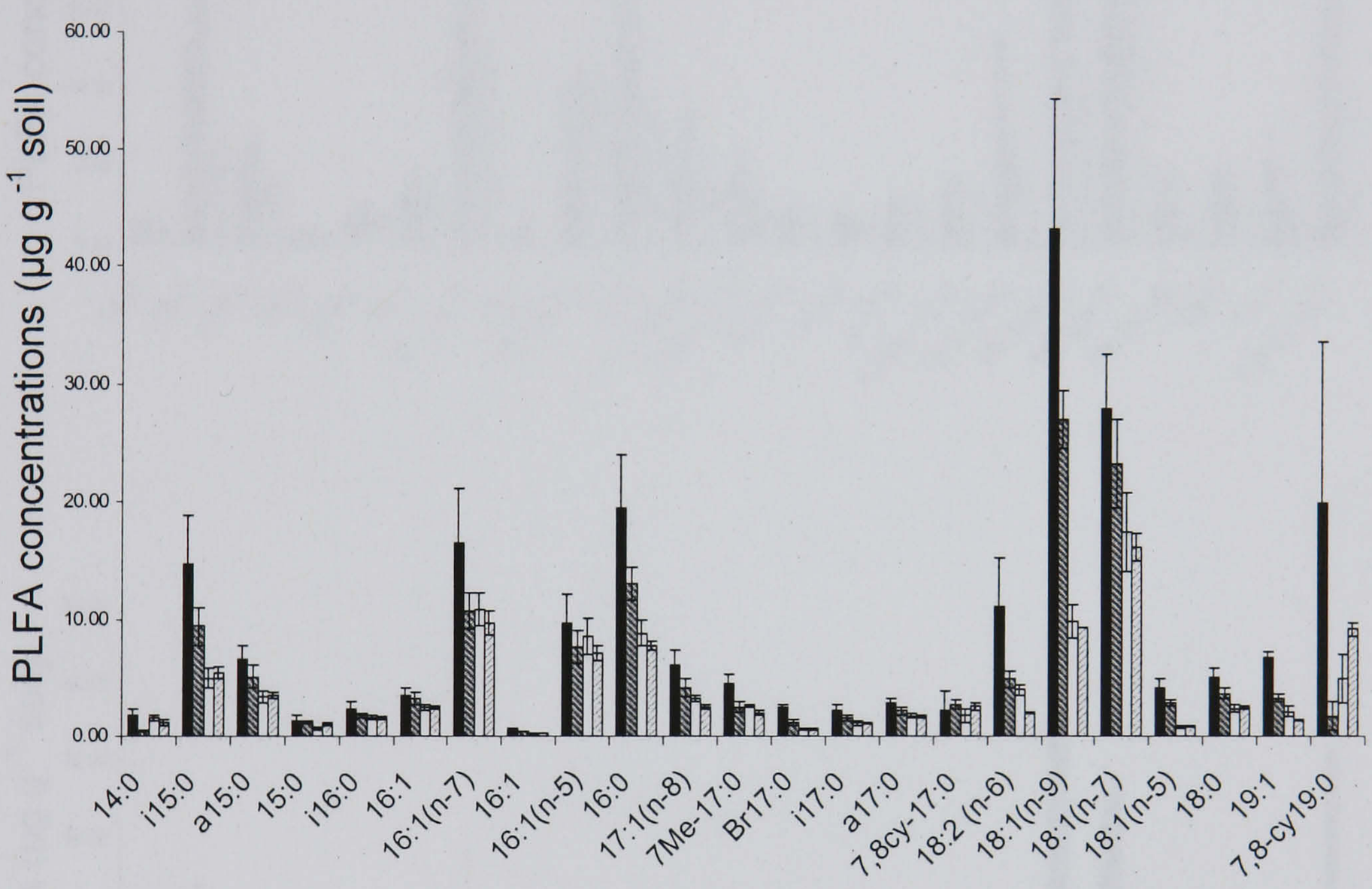

b

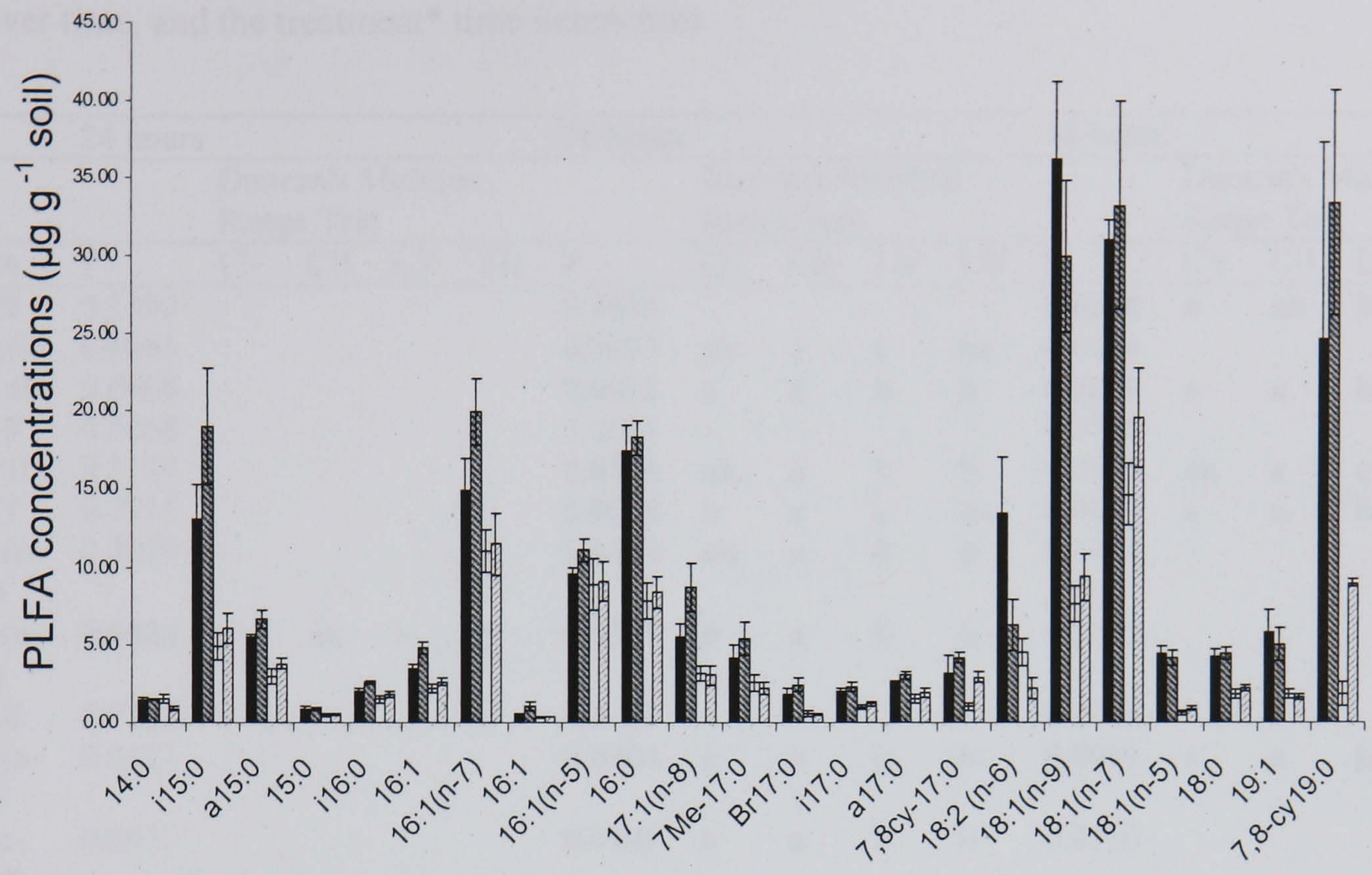

c

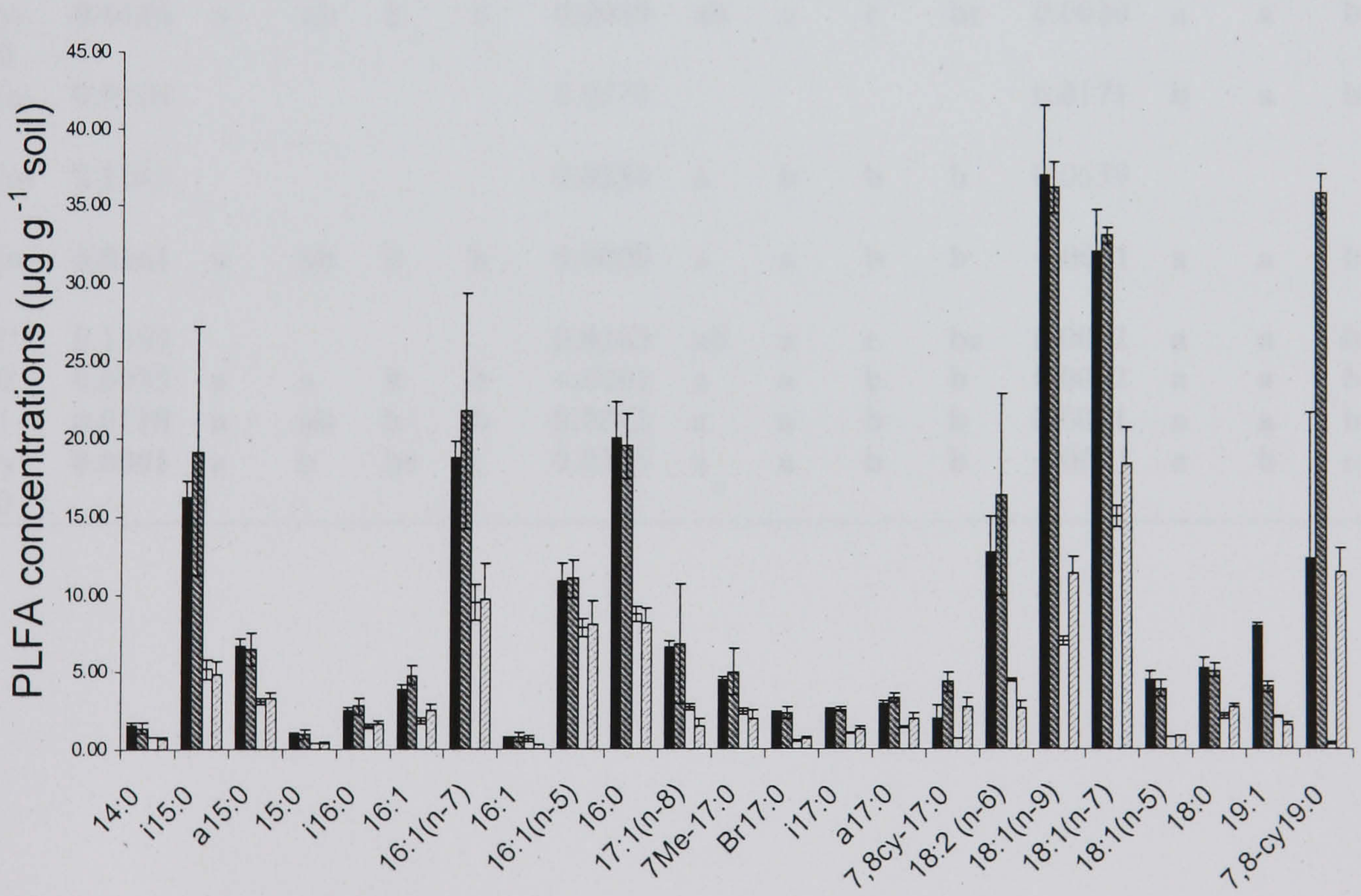

Figure 4.4 a,b,c. PLFA composition in the four treatments at times (**a**) 24 (**b**) 36 and (**c**) 48 hours post phenol addition. Error bars are one standard error of the mean. (■ CV, ■ CB, □ LV, ■ LB)

Table 4.1 ANOVA and post hoc Duncan's of PLFA compositions in the four treatments over time, and the treatment* time interaction.

	24 hours					36 hours					48 hours					Interaction
		Duncan's Multiple Range Test					Duncan's Multiple Range Test					Duncan's Multiple Range Test				
PLFA	P	CV	CB	LV	LB	P	CV	CB	LV	LB	P	CV	CB	LV	LB	
14:0	0.1392					0.2014					**0.0268**	**a**	**ab**	**bc**	**c**	**0.0481**
i15:0	0.0681					**0.0077**	**ab**	**a**	**c**	**bc**	0.0754					0.6823
a15:0	0.0608					**0.0012**	**a**	**a**	**b**	**b**	**0.0051**	**a**	**a**	**b**	**b**	0.5602
15:0	0.5668					0.0661					0.0726					0.9278
i16:0	0.3747					**0.0204**	**ab**	**a**	**b**	**b**	**0.0390**	**ab**	**a**	**c**	**bc**	0.5155
16:1	0.2711					**0.0015**	**b**	**a**	**c**	**bc**	**0.0027**	**a**	**a**	**b**	**b**	0.3055
16:1(n-7)	0.3329					**0.0364**	**ab**	**a**	**b**	**b**	0.1414					0.5383
16:1(n-5)	**0.0484**	**a**	**ab**	**b**	**b**	**0.0397**	**b**	**a**	**b**	**b**	0.3720					0.2768
16:0	0.7168					0.5281					0.1778					0.7885
17:1(n-8)	0.0521					**0.0004**	**a**	**a**	**b**	**b**	**0.0009**	**a**	**a**	**b**	**b**	0.6276
7me-17:0	0.0637					**0.0101**	**b**	**a**	**b**	**b**	0.2100					0.6506
br17:0	**0.0276**	**a**	**b**	**b**	**b**	0.0551					0.0764					0.4366
i17:0	**0.0002**	**a**	**b**	**b**	**b**	**0.0036**	**a**	**a**	**b**	**b**	**0.0002**	**a**	**a**	**b**	**b**	**0.0349**
a17:0	0.0552					**0.0031**	**a**	**a**	**b**	**b**	**<.0001**	**a**	**a**	**b**	**b**	0.3212
7,8cy-17:0	**0.0166**	**a**	**ab**	**b**	**b**	**0.0089**	**ab**	**a**	**c**	**bc**	**0.0020**	**a**	**a**	**b**	**b**	0.1592
18:2(n-6)	0.9104					0.0573					**0.0171**	**b**	**a**	**b**	**ab**	0.7421
18:1(n-9)	0.1043					**0.0254**	**a**	**b**	**b**	**b**	0.0639					0.3577
18:1(n-7)	**0.0161**	**a**	**ab**	**b**	**b**	**0.0009**	**a**	**a**	**b**	**b**	**<.0001**	**a**	**a**	**b**	**b**	0.7094
18:1'	0.1369					**0.0263**	**ab**	**a**	**c**	**bc**	**0.0002**	**a**	**a**	**b**	**b**	0.7239
18:0	**0.0035**	**a**	**a**	**b**	**b**	**<.0001**	**a**	**a**	**b**	**b**	**0.0002**	**a**	**a**	**b**	**b**	0.9218
19:1	**0.0118**	**a**	**ab**	**b**	**b**	**0.0012**	**a**	**a**	**b**	**b**	**0.0011**	**a**	**a**	**b**	**b**	0.5340
'7,8cy-19:0	**0.0001**	**a**	**b**	**bc**	**c**	**0.0255**	**a**	**a**	**b**	**b**	**<.0001**	**a**	**b**	**c**	**c**	0.2486

Liming resulted in a significant decrease in the total amount of PLFAs present per gram DW soil compared to the control treatment (Fig 4.5, Table 4.2) ($p=0.0001$), the presence or absence of vegetation made no significant difference.

Within the total PLFA concentration liming caused a significant decrease in the fungal PLFA concentration (Fig. 4.6, Table 4.3) ($p<0.000$) and the bacterial PLFA concentration (Fig. 4.7, Table 4.4) ($p=0.0001$). Post hoc Tukey revealed the decrease in the bacterial PLFA concentration in the lime treatments was significant in both the LV ($p=0.002$) and LB ($p=0.005$) treatments. The fungal PLFA concentration was also significantly affected by the removal of vegetation ($p=0.038$) Over time the fungal PLFA concentration increased ($p=0.01$) with the concentration at 48 hours after the addition of phenol significantly higher than at 24 hours. This increase was significant when comparing the vegetated and bare treatments over time, ($p=0.04$) post hoc Tukey revealed the same trend in the bare treatments as seen in the total fungal PLFA concentrations over time approaching significance ($p=0.057$).

The bacterial / fungal ratio (Fig. 4.8, Table 4.5) was significantly lower in the vegetated treatments than the bare ones ($p=0.002$), with the post hoc Tukey showing the bacterial / fungal ratio in the LB treatment was significantly higher than all other treatments. The ratio also varied significantly over time ($p=0.04$) with the ratio at 36 hours after phenol addition being significantly higher than at 48 hours, but not at 24 hours. This was still significant when comparing the vegetated to bare treatments over time in the bare treatments having a significantly higher bacterial / fungal ratio at 36 hours after phenol addition than at 48 hours.

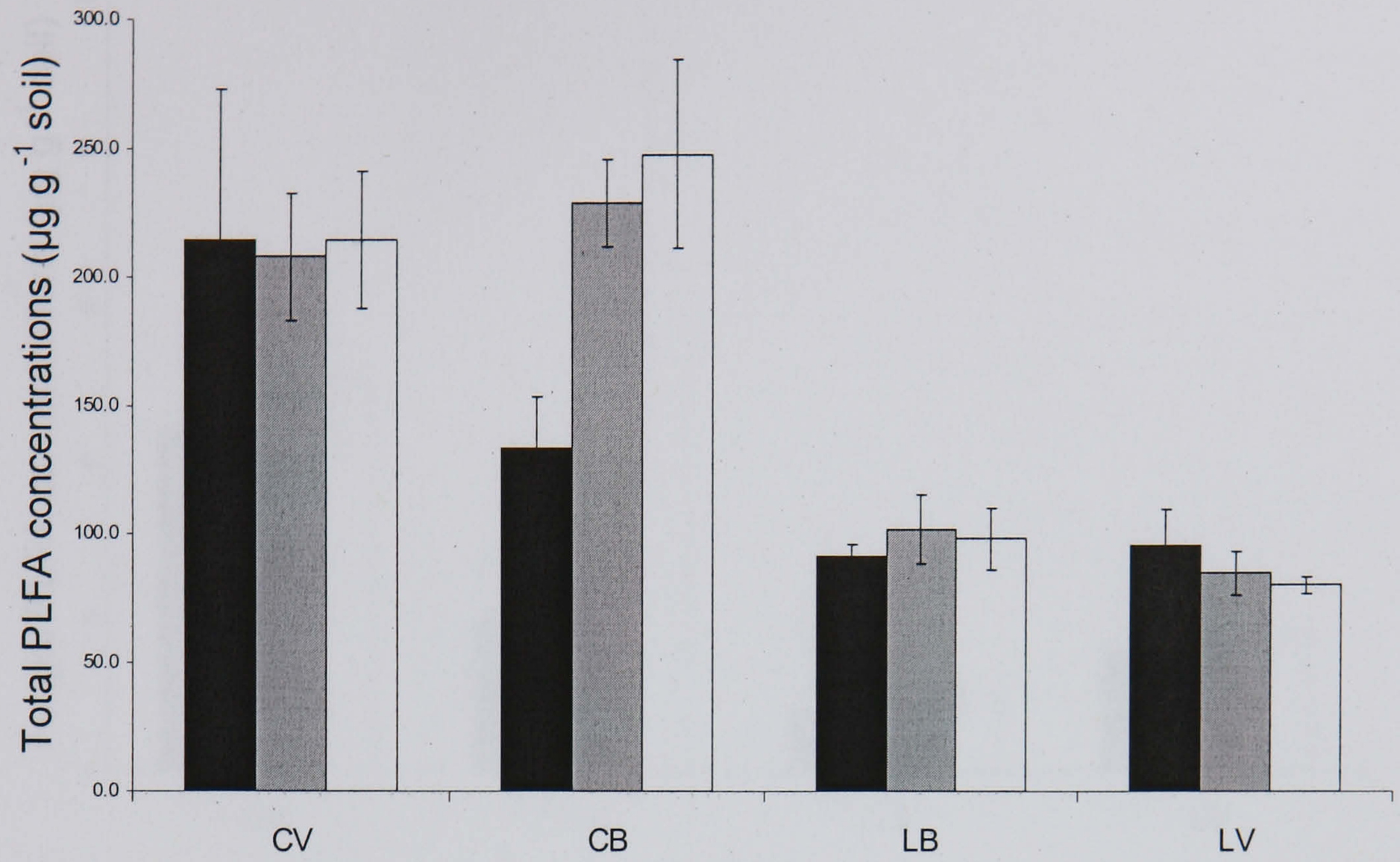

Figure 4.5 Total PLFA concentrations in the four treatments at 24 hours ■, 36 hours ■, 48 hours □, CB = control bare, CV = control with vegetation, LV = lime with vegetation, LB = lime bare). Error bars are one standard error of the mean.

Table 4.2 Results of the ANOVA of total PLFA concentrations comparing the four treatments over time.

Source	Type III Sum of Squares	df	Mean Square	F	Sig.
Intercept	**738764.4**	**1**	**738764.4**	**397.7623**	**0.000000**
Vegetation	191.3	1	191.3	0.1030	0.757615
Lime	**115119.3**	**1**	**115119.3**	**61.9820**	**0.000101**
Vegetation*Lime	236.8	1	236.8	0.1275	0.731555
Error	13001.1	7	1857.3		
TIME	5699.7	2	2849.9	1.4833	0.260445
TIME*Vegetation	9285.8	2	4642.9	2.4166	0.125435
TIME*Lime	6915.8	2	3457.9	1.7998	0.201543
TIME*Vegetation *Lime	4606.0	2	2303.0	1.1987	0.330725
Error	26897.4	14	1921.2		

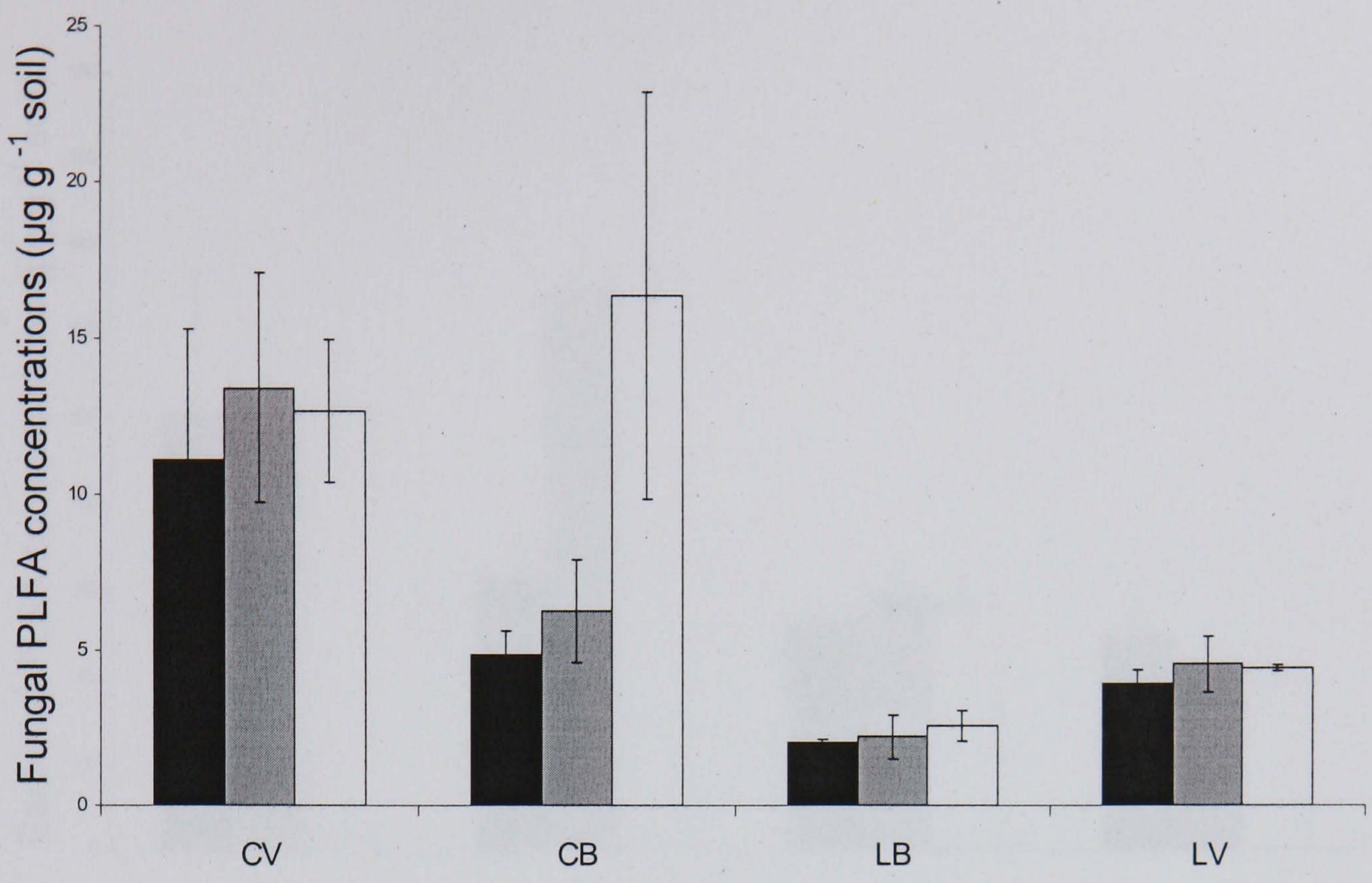

Figure 4.6 Fungal PLFA concentrations in the four treatments at 24 hours ■, 36 hours ■, 48 hours□, CB = control bare, CV = control with vegetation, LV = lime with vegetation, LB = lime bare). Error bars are one standard error of the mean.

Table 4.3 Results of the ANOVA of fungal PLFA concentrations comparing the four treatments over time.

Source	Type III Sum of Squares	df	Mean Square	F	Sig.
Intercept	**19.38163**	**1**	**19.38163**	**448.7399**	**0.000000**
Vegetation	**0.27779**	**1**	**0.27779**	**6.4316**	**0.038887**
Lime	**1.63404**	**1**	**1.63404**	**37.8326**	**0.000467**
Vegetation*Lime	0.02633	1	0.02633	0.6095	0.460557
Error	0.30234	7	0.04319		
TIME	**0.27645**	**2**	**0.13823**	**6.5113**	**0.010019**
TIME*Vegetation	**0.17248**	**2**	**0.08624**	**4.0625**	**0.040618**
TIME*Lime	0.14826	2	0.07413	3.4919	0.058845
TIME*Vegetation* Lime	0.11964	2	0.05982	2.8179	0.093661
Error	0.29720	14	0.02123		

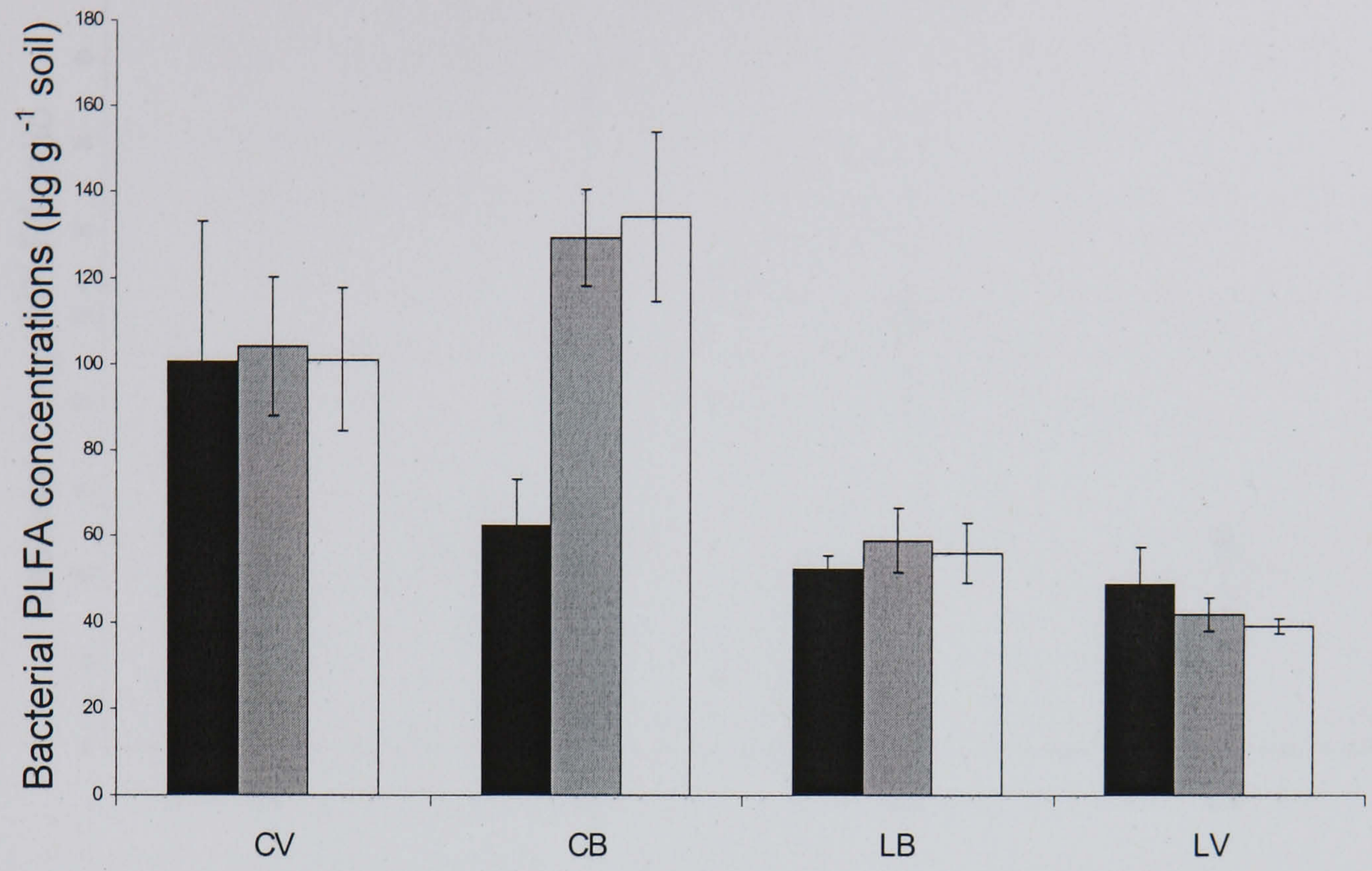

Figure 4.7 Bacterial PLFA concentrations in the four treatments at 24 hours ■, 36 hours ■, 48 hours□, CB = control bare, CV = control with vegetation, LV = lime with vegetation, LB = lime bare). Error bars are one standard error of the mean.

Table 4.4 Results of the ANOVA of bacterial PLFA concentrations comparing the four treatments over time.

Source	Type III Sum of Squares	df	Mean Square	F	Sig.
Intercept	**197274.2**	**1**	**197274.2**	**463.8320**	**0.000000**
Vegetation	1100.5	1	1100.5	2.5876	0.151739
Lime	**26689.7**	**1**	**26689.7**	**62.7529**	**0.000097**
Vegetation*Lime	7.1	1	7.1	0.0167	0.900808
Error	2977.2	7	425.3		
TIME	2457.9	2	1228.9	1.6485	0.227567
TIME*Vegetation	3472.6	2	1736.3	2.3290	0.133917
TIME*Lime	2966.3	2	1483.2	1.9895	0.173597
TIME*Vegetation*Lime	1642.8	2	821.4	1.1018	0.359430
Error	10437.0	14	745.5		

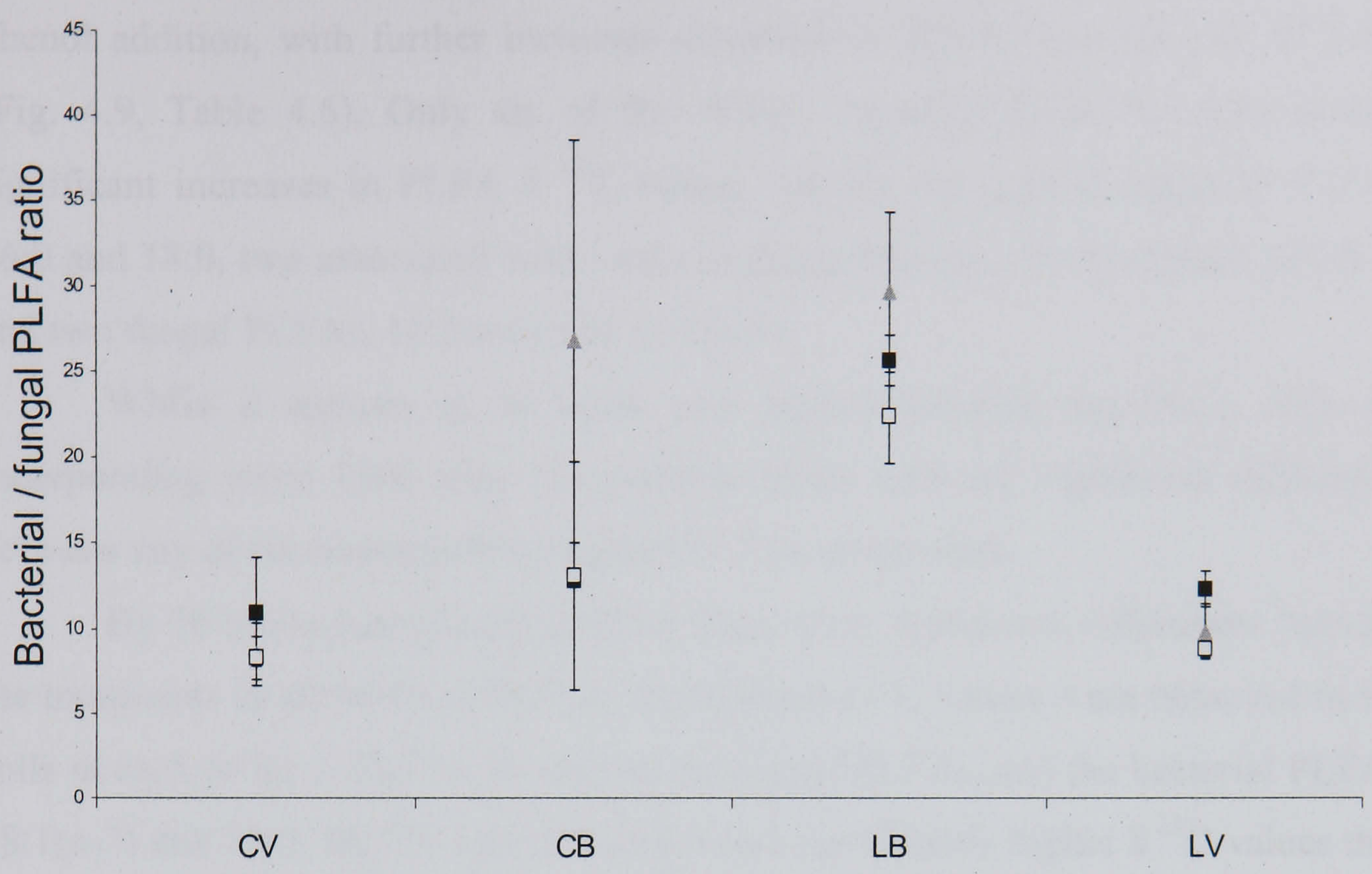

Figure 4.8 Bacterial / fungal PLFA ratios in the four treatments at 24 hours ■, 36 hours ▲, 48 hours□, CB = control bare, CV = control with vegetation, LV = lime with vegetation, LB = lime bare). Error bars are one standard error of the mean.

Table 4.5 Results of the ANOVA for bacterial / fungal PLFA ratios in the four treatments over time.

Source	Type III Sum of Squares	df	Mean Square	F	Sig.
Intercept	**7833.474**	**1**	**7833.474**	**166.6685**	**0.000004**
Vegetation	**1099.028**	**1**	**1099.028**	**23.3834**	**0.001887**
Lime	198.673	1	198.673	4.2271	0.078831
Vegetation*Lime	121.358	1	121.358	2.5821	0.152116
Error	329.002	7	47.000		
TIME	**383.268**	**2**	**191.634**	**4.1644**	**0.038092**
TIME*Vegetation	**398.544**	**2**	**199.272**	**4.3304**	**0.034354**
TIME*Lime	120.905	2	60.453	1.3137	0.300004
TIME*Vegetation*Lime	134.912	2	67.456	1.4659	0.264228
Error	644.241	14	46.017		

Increases in the δ ^{13}C values of some PLFAs were observed 24 hours after phenol addition, with further increases observed in PLFAs after 36 and 48 hours (Fig. 4.9, Table 4.6). Only six of the PLFAs extracted from the soils showed significant increases in PLFA δ ^{13}C values, namely the general bacterial PLFAs, 16:0 and 18:0, two associated with Gram-negative bacteria, 16:1(n-7) and 18:1(n-7) and two fungal PLFAs, 18:2(n-6) and 18:1(n-9).

Whilst it appears at 24 hours post phenol addition that the L soils are incorporating more label than the controls, there were no significant differences between any of the treatments for these 6 PLFAs at that time.

By 36 hours post phenol addition there were significant differences between the treatments in all of the 6 PLFAs. The highest δ ^{13}C values were observed in LV soils in each of the 6 PLFAs. In both of the fungal PLFAs, and the bacterial PLFAs, 18:1(n-7) and 16:0, the LV soil had resulted in significantly higher δ ^{13}C values than in any other treatments, and whilst the LB treatment exhibited lower PLFA δ ^{13}C values than LV, PLFA δ ^{13}C values in this treatment were significantly higher than either of the control treatments. The δ ^{13}C values in 16:1(n-7) were significantly higher in the L treatments than the control. Incorporation of the ^{13}C label into the 18:0 PLFA was significantly higher in the LV treatment than in either of the bare treatments, whilst not being significantly higher than the CV soil.

After 48 hours post phenol addition four of the six PLFAs that had shown incorporation of the ^{13}C label were significantly different between treatments. Surprisingly, the differences were no longer dominated by the LV soil. In all of the PLFAs showing significant differences, 16:1(n-7), 16:0, 18:2(n-6) and 18:1(n-7), the LB soil had resulted in significantly higher δ ^{13}C values than any other treatments.

a

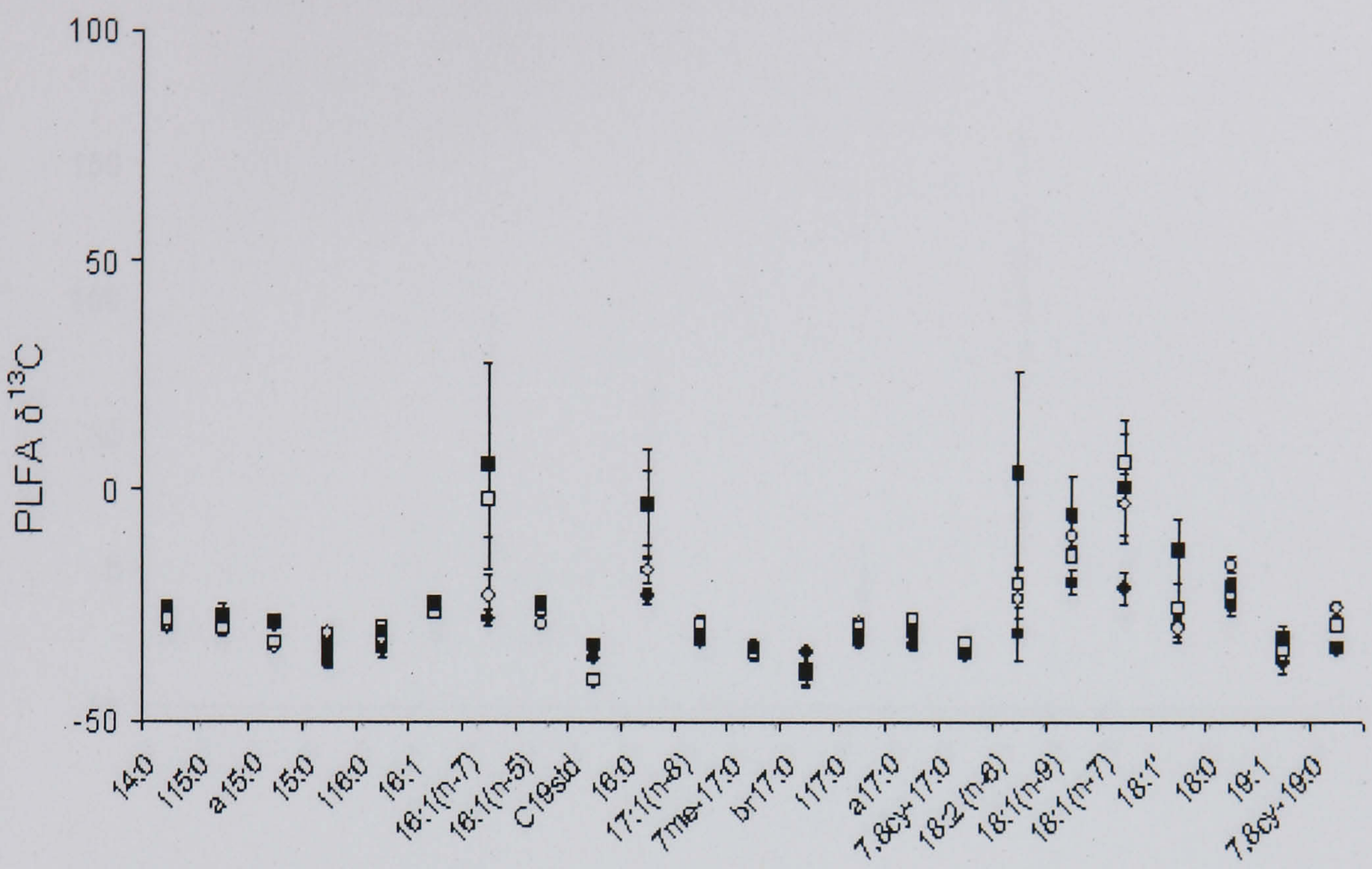
100
50
0
-50
PLFA δ13C
14:0
i15:0
a15:0
15:0
i16:0
16:1
18:1(n-7)
18:1(n-5)
C19sdd
18:0
17:1(n-8)
7me-17:0
br17:0
i17:0
a17:0
7,8cy-17:0
18:2 (n-6)
18:1(n-9)
18:1(n-7)
18:1'
18:0
19:1
7,8cy-19:0

b

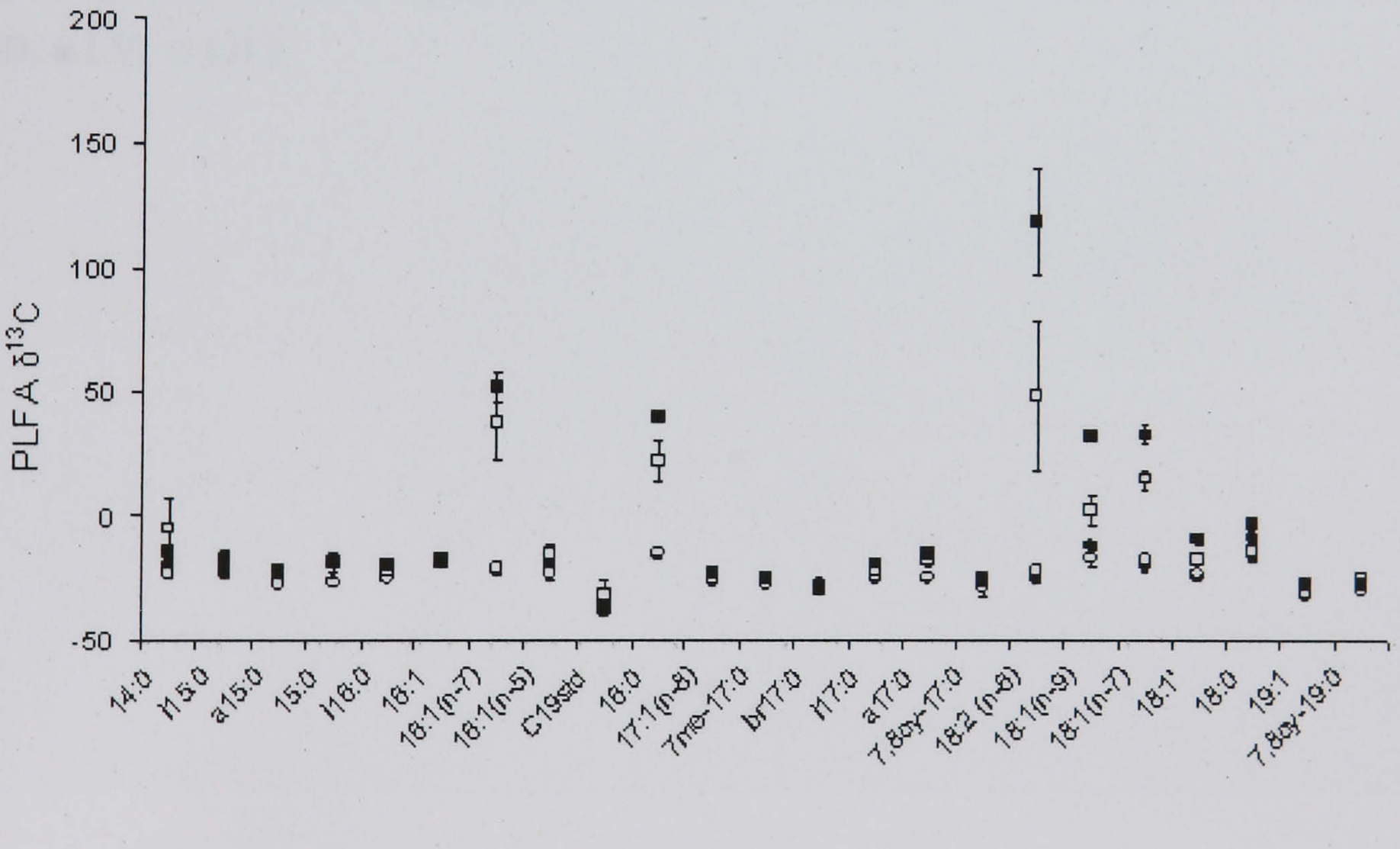
200
150
100
50
0
-50
PLFA δ13C
14:0
i15:0
a15:0
15:0
i16:0
16:1
18:1(n-7)
18:1(n-5)
C19sdd
18:0
17:1(n-8)
7me-17:0
br17:0
i17:0
a17:0
7,8cy-17:0
18:2 (n-6)
18:1(n-9)
18:1(n-7)
18:1'
18:0
19:1
7,8cy-19:0

c

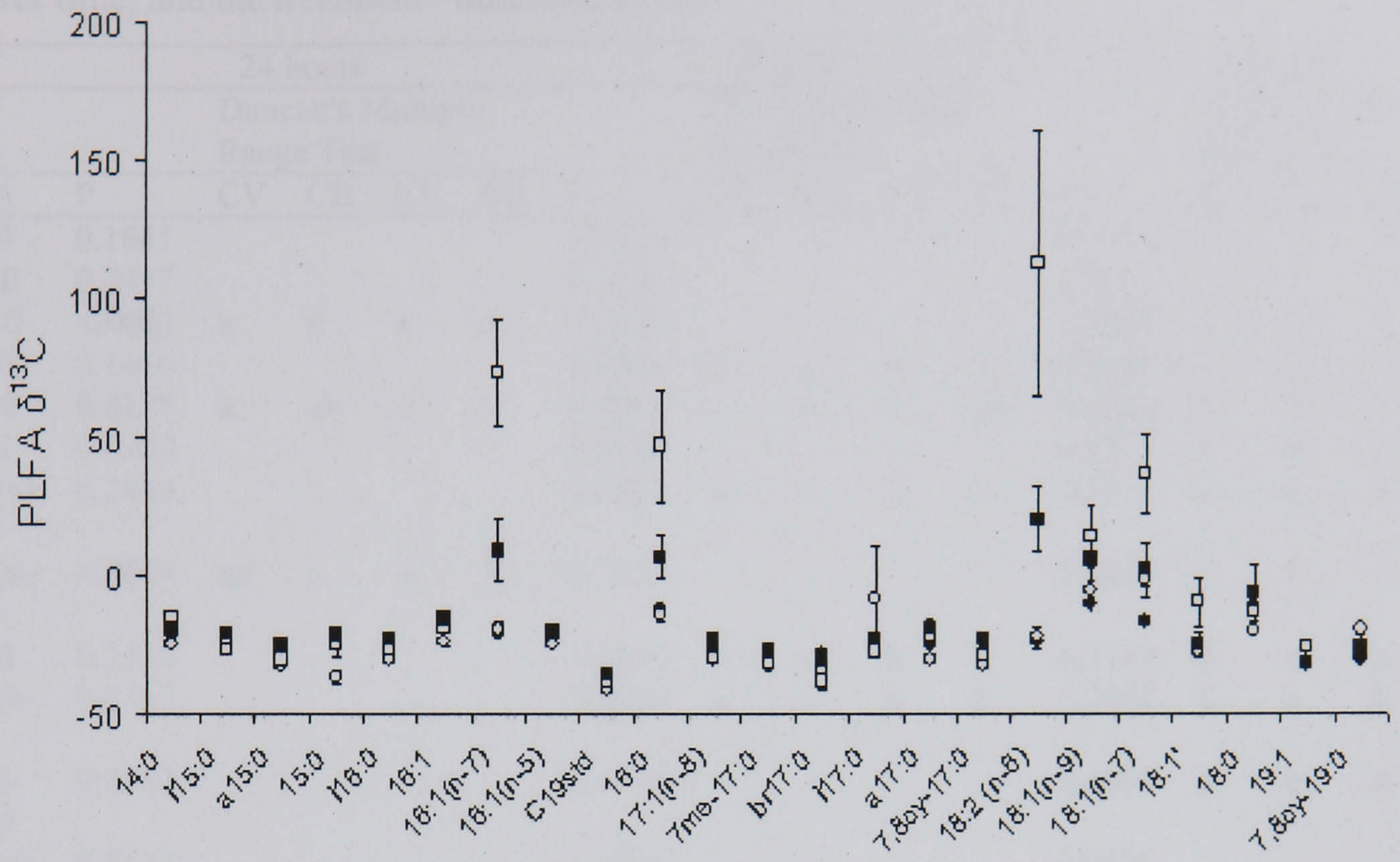

Figure 4.9 a,b,c. PLFA δ ^{13}C values across the four treatments at times (**a**) 24 (**b**) 36 and (**c**) 48 hours post phenol addition. Error bars are one standard error of the mean. (● CV, ○ CB, ■ LV, □ LB).

Table 4.6 ANOVA and post hoc Duncan's of PLFA δ ^{13}C values across the four treatments over time, and the treatment* time interaction.

	24 hours					36 hours					48 hours					Int
		Duncan's Multiple Range Test					Duncan's Multiple Range Test					Duncan's Multiple Range Test				
PLFA	P	CV	CB	LV	LB	P	CV	CB	LV	LB	P	CV	CB	LV	LB	
14:0	0.1641					0.2335					**0.0122**	**ab**	**a**	**bc**	**c**	0.4265
i15:0	0.7417					0.3522					0.2213					0.2234
a15:0	**<.0001**	**a**	**b**	**a**	**b**	0.0550					**<.0001**	**a**	**b**	**c**	**d**	**0.0003**
15:0	0.1686					**0.0361**	**a**	**a**	**b**	**b**	**0.0147**	**a**	**b**	**a**	**a**	**0.0043**
i16:0	**0.0177**	**a**	**ab**	**b**	**b**	**0.0152**	**a**	**a**	**b**	**ab**	**0.0009**	**a**	**b**	**c**	**a**	**0.0037**
16:1	0.4240					**0.7758**					**0.0375**	**a**	**b**	**a**	**ab**	**0.0079**
16:1(n-7)	0.2456					**0.0002**	**a**	**a**	**b**	**b**	**0.0010**	**a**	**a**	**a**	**b**	**0.0052**
16:1(n-5)	**<.0001**	**ab**	**c**	**a**	**b**	0.2482					**0.0007**	**a**	**b**	**c**	**c**	0.5094
16:0	0.2320					**<.0001**	**a**	**a**	**b**	**c**	**0.0144**	**a**	**a**	**a**	**b**	**0.0120**
17:1(n-8)	0.2157					**0.0024**	**a**	**a**	**b**	**b**	**<.0001**	**a**	**c**	**b**	**c**	**<.0001**
7me-17:0	0.8252					0.0710					**0.0009**	**a**	**b**	**a**	**b**	**0.0054**
br17:0	0.5822					0.4980					0.0626					0.1371
i17:0	**0.0255**	**a**	**b**	**ab**	**b**	**0.0055**	**a**	**ab**	**c**	**bc**	0.5267					0.5332
a17:0	**0.0457**	**a**	**ab**	**ab**	**b**	**0.0074**	**a**	**a**	**b**	**b**	**0.0262**	**ab**	**a**	**b**	**b**	0.1864
7,8cy-17:0	**0.0258**	**a**	**ab**	**a**	**b**	0.4993					0.0588					0.0866
18:2(n-6)	0.2305					**0.0017**	**a**	**a**	**b**	**c**	**0.0137**	**a**	**a**	**a**	**b**	**0.0014**
18:1(n-9)	0.2326					**<.0001**	**a**	**a**	**b**	**c**	0.1441					**0.0058**
18:1(n-7)	0.1861					**<.0001**	**a**	**a**	**b**	**c**	**0.0124**	**a**	**a**	**a**	**b**	**0.0097**
18:1'	0.1073					**0.0003**	**a**	**a**	**b**	**c**	0.1205					
18:0	0.1977					**0.0214**	**ab**	**a**	**b**	**a**	0.4821					0.2485
19:1	0.3754					0.0571					**0.0005**	**a**	**a**	**a**	**b**	0.1308
'7,8cy-19:0	**0.0019**	**a**	**b**	**a**	**c**	0.0756					**0.0455**	**a**	**b**	**ab**	**ab**	**0.0043**

The amount of ^{13}C incorporated into individual PLFAs (Fig 4.10, Table 4.7) was significantly higher in those PLFAs which had significantly higher $\delta\,^{13}C$ values, with the exception of 18:0, with a maximum value of 12 ng g^{-1} soil seen in the LB treatment 48 hours after phenol addition.

Within those 5 PLFAs, 4 showed significant differences between treatments 36 hours post phenol addition. 16:0 and 18:1(n-7) were significantly higher in the lime soils than the controls, whilst 16:1(n-7) revealed a significantly higher amount of ^{13}C in the LB soil relative to all other treatments. The fungal PLFA 18:2(n-6) had a greater amount of incorporation in the LV treatment with ca. 7 ng ^{13}C g^{-1} dw soil.

a

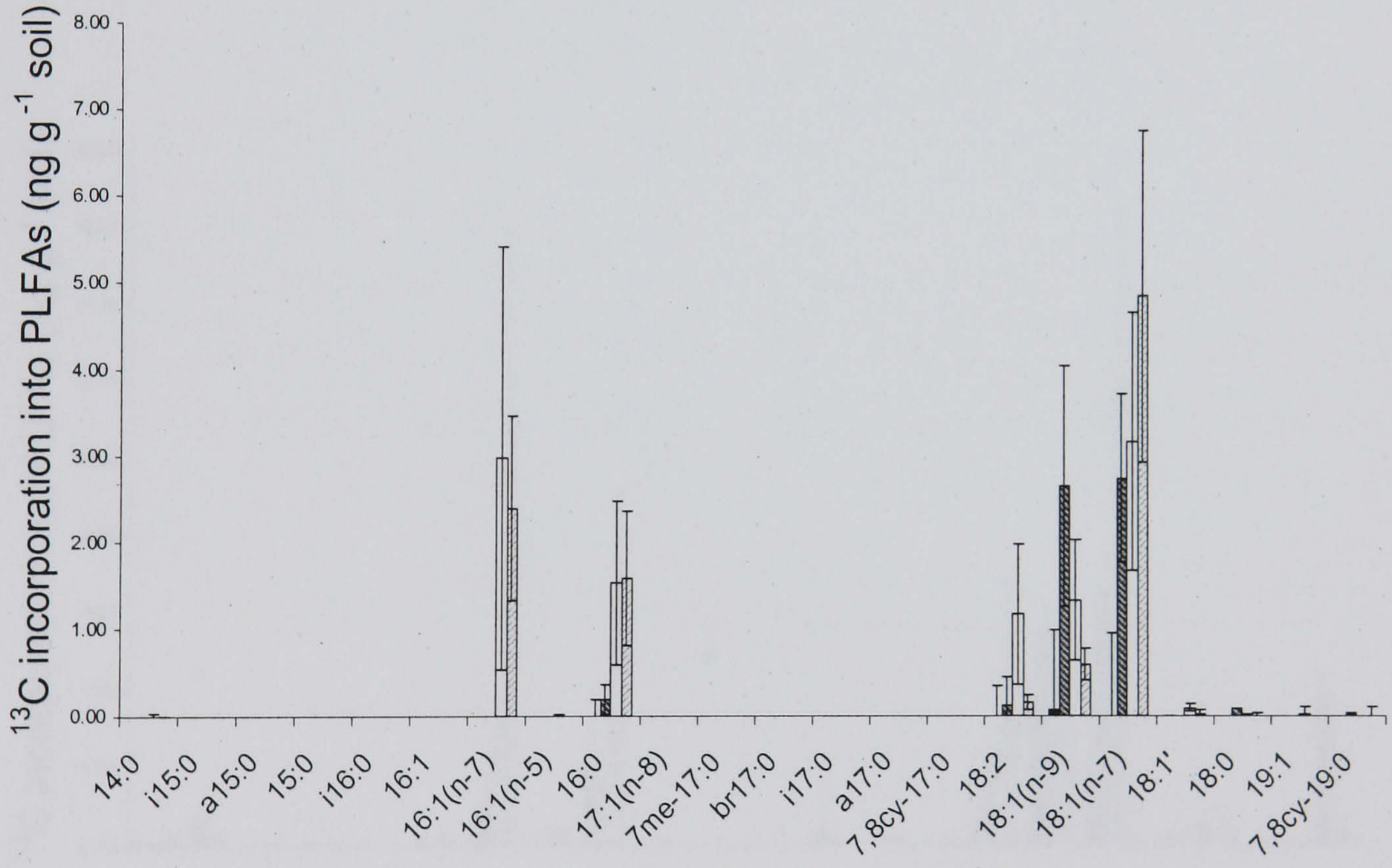

b

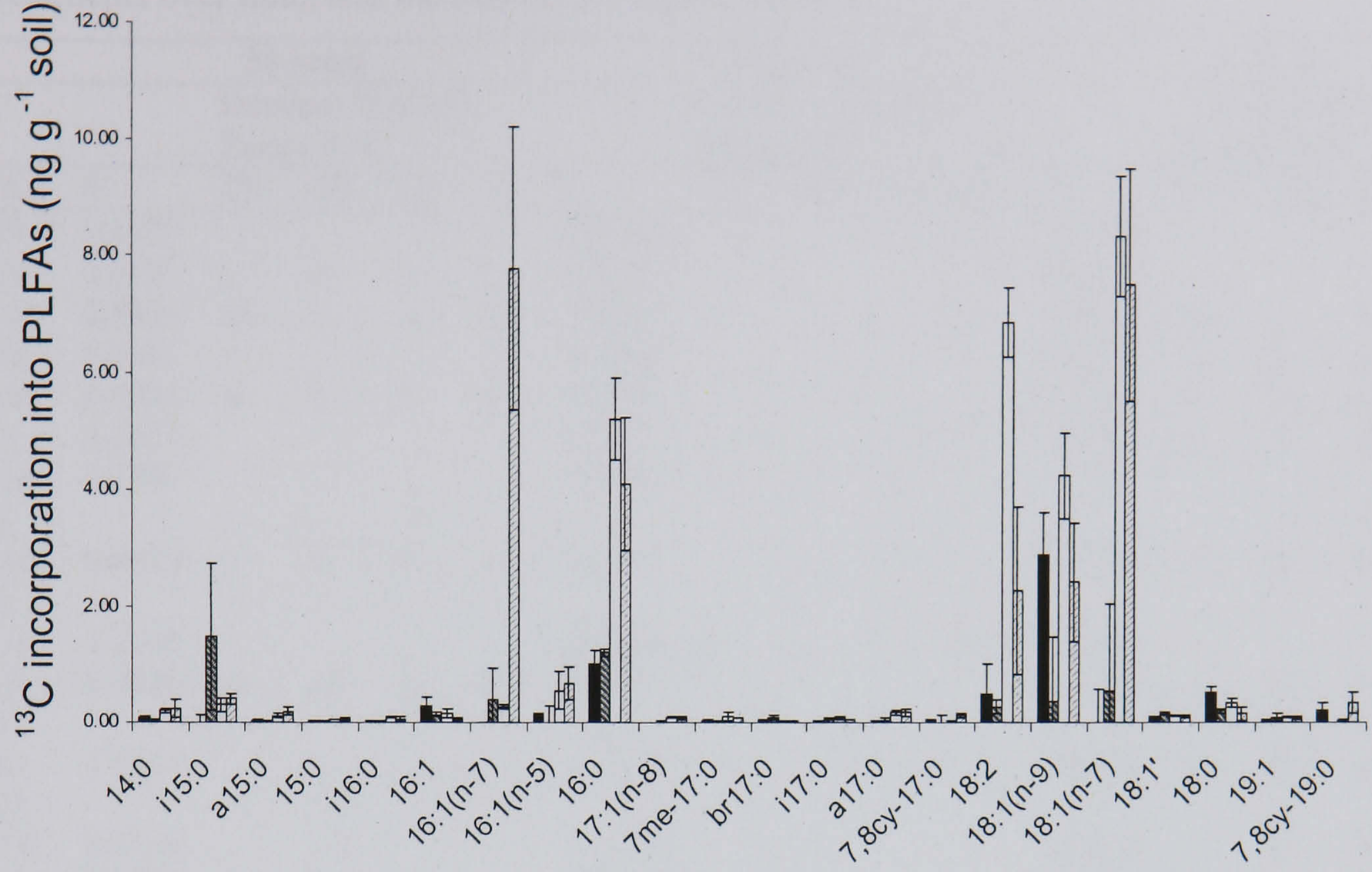

c

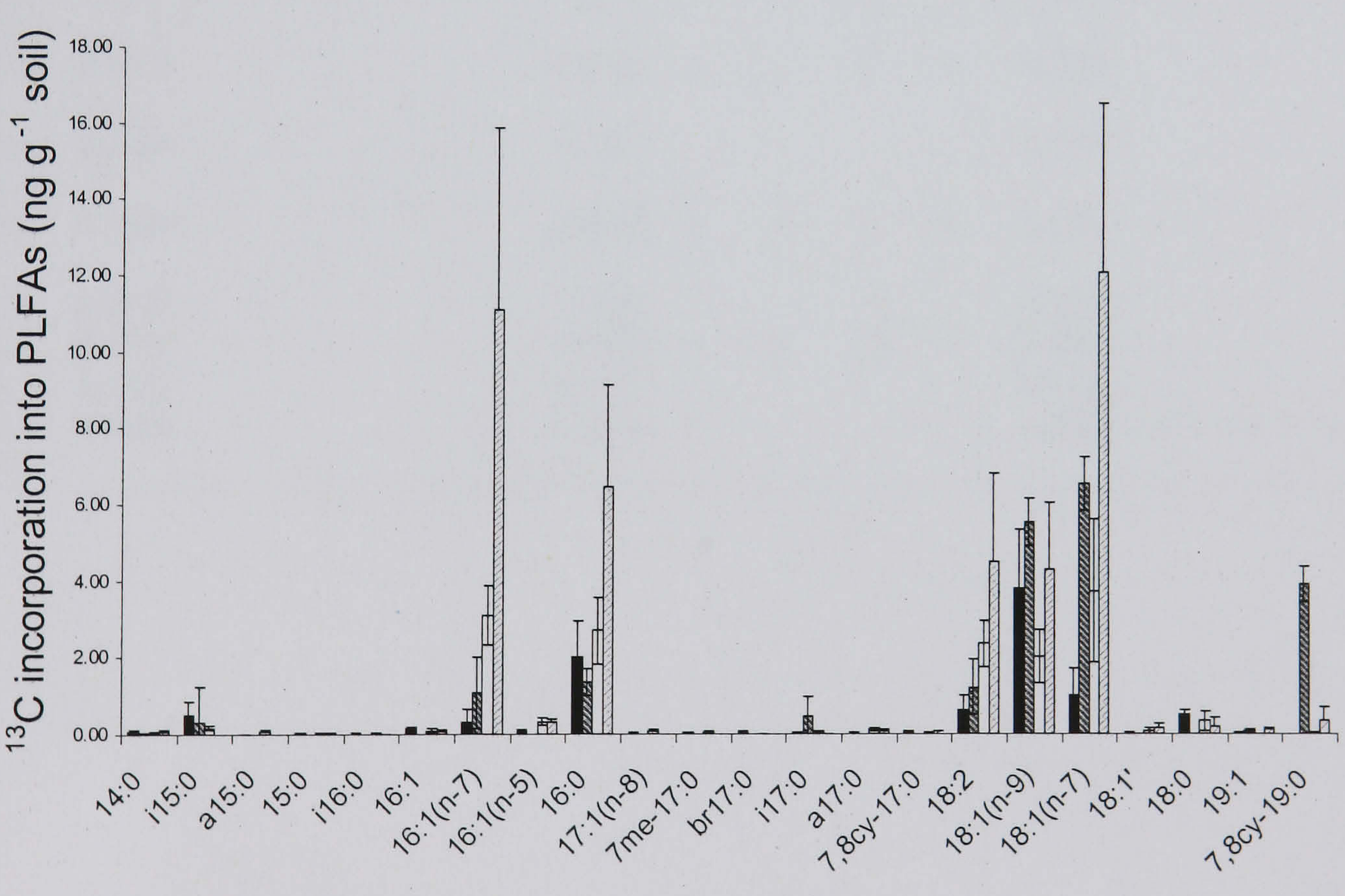

Figure 4.10 a,b,c. ^{13}C incorporation into PLFAs across the four treatments at times (**a**) 24 (**b**) 36 and (**c**) 48 hours post phenol addition. Error bars are one standard error of the mean. (■ CV, ■ CB, □ LV, ■ LB)

Table 4.7 ANOVA and post hoc Duncan's of ^{13}C incorporation into PLFAs across the four treatments over time, and the treatment* time interaction.

	24 hours					36 hours					48 hours					Int
		Duncan's Multiple Range Test					Duncan's Multiple Range Test					Duncan's Multiple Range Test				
PLFA	P	CV	CB	LV	LB	P	CV	CB	LV	LB	P	CV	CB	LV	LB	
14:0	0.1329					0.3186					0.2083					0.3781
i15:0	0.0087	a	a	b	b	0.4375					0.8268					0.5647
a15:0	**0.0016**	**ab**	**c**	**a**	**b**	0.0551					**0.0005**	**ab**	**c**	**a**	**b**	**0.0005**
15:0	0.2853					0.1064					**0.0019**	**a**	**b**	**a**	**a**	**0.0031**
i16:0	**0.0092**	**a**	**b**	**b**	**b**	0.0855					**0.0034**	**a**	**b**	**a**	**a**	**0.0008**
16:1	0.1672					0.3147					**0.0032**	**a**	**b**	**a**	**a**	**0.0233**
16:1(n-7)	0.2582					**0.0053**	**a**	**a**	**a**	**b**	0.0510					0.2028
16:1(n-5)	**0.0023**	**a**	**b**	**a**	**a**	0.2659					**0.0046**	**a**	**b**	**a**	**a**	0.4985
16:0	0.2588					**0.0049**	**a**	**a**	**b**	**b**	0.1508					0.2085
17:1(n-8)	**0.0200**	**a**	**ab**	**b**	**b**	0.0591					**0.0315**	**a**	**b**	**a**	**ab**	**0.0051**
7me-17:0	0.0573					0.2825					**0.0072**	**a**	**b**	**a**	**a**	**0.0015**
br17:0	0.0770					0.0738					**0.0267**	**a**	**b**	**ab**	**b**	**0.0010**
i17:0	**0.0092**	**a**	**b**	**b**	**b**	0.4434					0.5259					0.7020
a17:0	**0.0129**	**a**	**b**	**b**	**b**	**0.0434**	**a**	**ab**	**b**	**b**	**0.0028**	**a**	**b**	**a**	**a**	**0.0170**
7,8cy-17:0	0.9181					0.5418					**0.0222**	**a**	**b**	**a**	**a**	0.6403
18:2(n-6)	0.3634					**0.0016**	**a**	**a**	**b**	**a**	0.2304					**0.0141**
18:1(n-9)	0.2484					0.0873					0.3290					**0.0387**
18:1(n-7)	0.1992					**0.0042**	**a**	**a**	**b**	**b**	0.0623					0.1011
18:1'	0.0949					0.1602					0.2464					0.0745
18:0	0.2010					**0.0488**	**a**	**b**	**ab**	**b**	0.2923					0.0857
19:1	0.1427					0.6871					0.0610					0.1143
'7,8cy-19:0	0.3048					0.0886					**<.0001**	**a**	**b**	**a**	**a**	**<.0001**

$\delta^{13}C$ values were combined with PLFA concentrations to estimate the total amount of phenol-derived ^{13}C present in the PLFAs (Fig. 4.11; Table 4.8). The total amount of ^{13}C in the PLFAs was not affected by the presence or absence of vegetation, but was significantly higher in the L treatments compared to the controls ($p=0.033$). The removal of vegetation has the same effect in both the L and control treatments, resulting in an increase in the amount of ^{13}C in the PLFAs. Unsurprisingly, the amount of the ^{13}C label increases significantly over time ($p=0.018$). However, interestingly, comparing L treatments, the amount of ^{13}C in the PLFAs increases throughout the experiment in the LB soil, while peaking in the LV treatment at 36 hours post phenol addition.

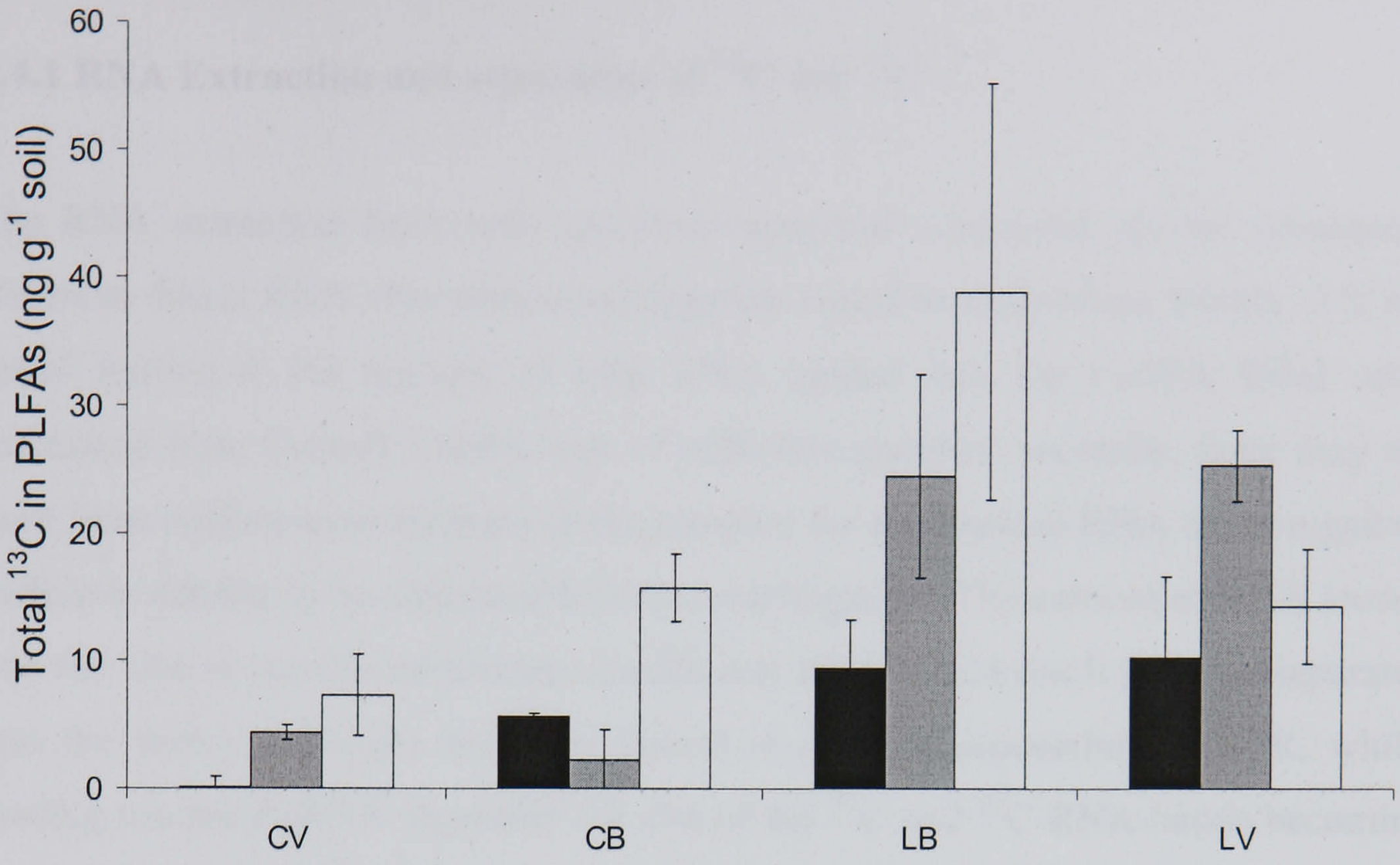

Figure 4.11 Total amount of ^{13}C PLFA across the four treatments over time. Error bars are one standard error of the mean. (CB = control bare, CV = control with vegetation, LV = lime with vegetation, LB = lime bare)

Table 4.8 Results of the ANOVA of total amount of ^{13}C PLFA comparing the four treatments over time.

Source	Type III Sum of Squares	df	Mean Square	F	Sig.
Intercept	**5960.306**	**1**	**5960.306**	**27.27667**	**0.001222**
Soil	**1518.317**	**1**	**1518.317**	**6.94841**	**0.033619**
Plant	230.095	1	230.095	1.05300	0.338964
Soil*Plant	41.534	1	41.534	0.19008	0.675982
Error	1529.591	7	218.513		
TIME	**826.638**	**2**	**413.319**	**5.41795**	**0.018086**
TIME*Soil	263.011	2	131.505	1.72382	0.214160
TIME*Plant	414.935	2	207.467	2.71956	0.100498
TIME*Soil*Plant	195.662	2	97.831	1.28241	0.308027
Error	1068.018	14	76.287		

4.4 Discussion

4.4.1 RNA Extraction and separation of ^{12}C and ^{13}C

The RNA extraction from soils and roots appeared successful yet the subsequent failure to detect RNA after ultra-centrifugation raised two questions. Firstly, it is not really known if the amount of total RNA loaded into the CsTFA filled tube, calculated from Gornall (2000), was of sufficient quantity; secondly, there may not have been sufficient enrichment in the samples for the labelled RNA to have gained sufficient density to be separated by ultracentrifugation. The amount of RNA loaded into the tube is considered precise; insufficient RNA would result in (once separated into the heavy and light bands) a failure to achieve successful RT-PCR, whilst loading too much RNA increases the risk of the ^{12}C and ^{13}C RNA bands becoming merged in the tube, failing to achieve clear separation during ultracentrifugation. If the labelling of the RNA was inadequate, then it would not be dense enough for clear separation from the unlabelled material during ultracentrifugation and confirmation of the extent of labelling was attempted using IRMS analysis of the separated bands. IRMS is very sensitive and precise and capable of detecting extremely small changes in the isotopic composition of C within a sample (normally to 0.1 per mil) and even if relatively small traces of ^{13}C were present in the isolated gradient fractions, which failed to yield and RNA using RT-PCR, the ^{13}C should still be detectable. The failure to detect any peaks of ^{13}C on the IRMS did not assist in differentiating whether a suboptimal amount of RNA had been loaded or there was insufficient label in the samples, but indicates either that insufficient label had incorporated into the RNA to enable detection or that the underlying methodology, from culturing through RT-PCR, was in some way flawed.

Since completion of the experiments described here, SIP has been more widely utilised as a tool for degradations studies including, for example, anaerobic ^{13}C-benzene degradation (Kunapuli *et al.*, 2007). These authors reported that although organisms maintained their populations during enrichment, there was large variation within the microbial consortia involved in benzene degradation, revealed

by the uptake of labelled carbon. Manefield *et al.* (2007) added $^{13}C_6$ phenol to an activated sludge micro-reactor to examine the resulting distribution of the labelled C. They found that within the first 100 minutes after addition, most of the phenol had been metabolically converted, with 49% being incorporated into microbial biomass and 6% respired as CO_2. Interestingly, less than 1% of the total ^{13}C labelled C supplied was incorporated into microbial RNA and DNA, with RNA labelling occurring 6.5 times faster than DNA, confirming that whilst RNA incorporated the label more efficiently that DNA, only a very small percentage (less than 1%) was incorporated into nucleic acids. It is clear that, for detection of the label incorporated into nucleic material, the level of enrichment has to be significant.

However, even with highly labelled *E. coli* RNA the labelled RNA, at a range of differing amounts, was undetectable using the highly sensitive IRMS. The dilution of the ^{13}C carbon by the acetate in the gradient may have obscured the isotope signal, which would be much less of a problem with an inorganic gradient matrix, such as CsCl used in DNA ultracentrifugation (see Manefield *et al.*, 2002). It is likely that the material was not enriched to a sufficiently high degree meaning that RT-PCR failed to produce the appropriate amplifications. However, given the failure to amplify fully labelled *E. coli* it seems likely that it was neither of the reasons suggested above that totally accounted for the inability to detect any RNA after ultra-centrifugation; indeed, it would have been more cautious to have attempted to repeat the technically less-demanding DNA SIP work before using RNA. Stable isotope probing of nucleic acids is clearly a technique which, while elegant and precise, is still an emerging technology and one which requires a considerable amount of protocol development and manipulation before becoming routine.

4.4.2 Sourhope 2004 PLFA analyses

The addition of lime to plots at Sourhope significantly affected the pH of the upper section of the soil profile, raising it a mean value of 2.1 over 4 years (Burt-Smith, 2003). The rise in the upper soil profile pH in the lime treatments at Sourhope was also strongly positively correlated with changes in biomass productivity (Burt-

Smith, 2003). It was surprising, given that Grayston *et al.* (2001) had reported that a raised pH (from pH 4.1 to pH 6.0) for a similar soil, had resulted in an increase in both soil microbial biomass and soil microbial activity, that the total PLFA concentrations were significantly lower in the L treatments in the current work, which was seen in both the fungal and bacterial concentrations. This may have been a result, for the LV treatment, of differing changes in vegetation associated with the liming, resulting in lower soil moisture amongst other effects (Burt-Smith, 2003).

The timing and pattern of incorporation of the isotopic label into six distinct PLFAs was apparent after 24 hours. This provides a major indication that the specific groups of organisms containing these PLFAs were in fact degrading the phenol, rather than being secondary degraders, which were mineralizing substrates from phenol-degrading microorganisms. The time at which the isotopic label can be seen varied greatly between substrates, for example when Treonis *et al.* 2004 pulsed grassland soils *in situ* with $^{13}CO_2$ for 5 hours, the enrichment in the PLFAs was seen after 4 and 8 days post pulse. Interestingly, out of the six PLFAs which incorporated the ^{13}C label, four (the fungal and Gram-negative lipid biomarkers) were also reported by Treonis *et al.* (2004) as showing the highest enrichment, turning over more rapidly than the Gram-positive biomarkers, attributing 16:0 as a PLFA assigned by Phillips *et al.* (2002) as a general bacteria biomarker lipid. Whilst Treonis *et al.* (2004) concluded that liming had not affected the turnover rates of ^{13}C labelled C, or which organisms utilised the photo-assimilate, the results presented here in Chapter 4 concluded that liming had significantly increased the rate of incorporation of ^{13}C labelled C from phenol into PLFAs. This finding is supported by Grayston *et al.* (2001) and Fuentes *et al.* (2006) who attributed greater respiration rates and microbial biomass C to the increase in pH caused by the liming and also found that, when compared to unlimed soil, limed soil had faster C turnover rates and increased mineralization of organic matter.

The difference in incorporation of the ^{13}C from phenol into the PLFAs over time between the two lime treatments was of interest. It is possible that, in the LV treatment, after the initial rise in incorporation between 24 and 26 hours post phenol addition, other C substrates such as plant root exudates are comparatively more

abundant, and easier to degrade than the phenol and so resulting in the decrease in assimilation, In contrast, in the LB treatment soil in the absence of plants, resulting in the removal of an important competing C source, resulted in the increased assimilation of phenol.

In conclusion, Gram-negative and fungal lipid biomarkers were the primary degraders of phenol. Known phenol degraders include Gram-negative bacteria (Sakia *et al.,* 2003) namely 5 species of *Pseudomonas*, and a species of *Ralstonia.* van Schie and Young, 2000) and, from ^{13}C incorporation into the fungal biomarker 18:2(n-6), fungi have been found dominate the phenol degradation in one soil microbial community (Brant *et al.,* 2006). Liming is known to increase the leaching of dissolved organic carbon (DOC) (Andersson and Nilsson, 2001) and so, as limed soils may be more limited in readily available C than the in the control soils, liming may dominate the assimilation of the C from phenol through indirect effects. The significant effect on the rate at which phenol is assimilated in both the vegetated and bare treatments may be as a result of C limitation.

The Gram-negative PLFA 16:1(n-7), whilst being present at a higher concentration in the control treatments, incorporated a significantly higher amount of ^{13}C in the limed treatments, indicating that it is not all Gram-negative bacteria with the PLFA 16:1(n-7) that are assimilating the phenol. The amount of phenol assimilated is small, with a maximum amount of ca. 40 ng g^{-1} dw soil incorporated in the LB treatment after 48 hours.

In order to gain a better understanding of the different destinations of ^{13}C from the phenol, the current results need to be combined with the results described in Chapters 3 and 4 to provide an overview of the allocations of ^{13}C derived from the phenol to the different parts of the soil system and this is discussed further in Chapter 6.

Chapter 5. Combining gas mass-spectrometry with PLFA SIP in the laboratory to examine phenol degradation in soils

5.1 Introduction

The mobile mass spectrometer has enabled the *in situ* monitoring of labeled ^{13}C substrates under natural conditions, as shown in Chapters 2 and 3. *In situ* monitoring in this way creates minimal disturbance to the treated plots and so has the advantages over laboratory-based studies where cores are taken and the system potentially disturbed. There are situations, however, when field testing is impracticable, for example when a substrate's toxicity is too high to be permitted in the field, when the terrain is not compatible with access by a mobile laboratory or when the treatments cannot be controlled efficiently in the field. Laboratory incubations themselves also have a number of advantages over field-based studies, with the potential for more treatment options, frequent monitoring, removing potentially confounding factors (e.g. moisture and temperature) and reducing the variability between replicate units. For this purpose the field experiment described in Chapter 3 was repeated in the laboratory. Cores from the field site were placed into a specially constructed laboratory incubator, held at a constant temperature in the dark with either phenol or water being added to examine whether phenol, at the same concentration used in the field, affected the rate of soil respiration. Following this initial laboratory experiment, a second set of cores from the Sourhope field site were placed into the same incubator system and ^{13}C-labeled phenol applied at the same concentration and to the same treatments as for the field experiment described in Chapter 3. This would demonstrate whether effects witnessed in the laboratory really represented the *in situ* behaviour and, if so, enable a more efficient and rapid turnaround of experimental designs.

5.2 Methods

The laboratory work described here used cores from the same treatments described Chapter 3, taken from the Sourhope field site. Cores (diameter 6.5 cm, depth 10 cm) were taken in mid March '05 and transported to the laboratory where they were kept under cover out of doors prior to being placed in the laboratory respiration system.

5.2.1 *Ex situ* degradation of phenol monitored using ^{12}C phenol

The laboratory measurements were made using a flow-through system similar to that used in the field. Compressed air was introduced into the system, passing through Nalgene tubing into a 45 gallon drum to ensure the air was thoroughly mixed and to dampen any fluctuations in concentration in the source air. From there, the air was passed into a 24 way manifold, below a set water level in the manifold (controlled to be 5 °C warmer than the chamber incubator to minimise water loss from the soil) with an outlet above the water level, acting as a 'constant head' device. This ensured that air at a constant pressure was being delivered to the incubation chambers and that the volume of air drawn through the lines by the pump in the mobile laboratory did not exceed that being delivered by the compressed air supply, which would result in a negative pressure being developed within the chambers. The air left the manifold via 24 Nalgene tubes, each line entering a dark, sealed chamber. The sealed chambers, capacity 2 l, used for the experiment were made from plastic, and held precisely at 15 °C in an incubator. The inlet hole was situated on the top of the chamber, the outlet hole was on the top of the chamber, away from the inlet, to which PTFE tubing, with an internal diameter smaller than the inlet tube, was connected, which ran to the 24 channel gas handler unit. Air from all 24 chambers, at a flow rate of 50 cm^3 min^{-1} per line, was drawn through PTFE lines to the 24 channel gas handler and subsequently into an infra red gas analyser (IRGA) for 5 minutes in sequence (see Fig. 5.1) The data were collected and stored using a PICOLOG analogue-digital converter and software (Pico Technology Ltd. Cambridgeshire, UK) connected to a laboratory computer.

To measure the degradation of phenol in the laboratory, phenol (30 cm^3, 50 ppm aqueous solution) was applied to a soil core (33 cm^2) from each of the 12 treated plots, with four different treatments and three replicates of each treatment. The treatments to which phenol was added were; control vegetated (CVP), control non-vegetated or 'bare' (manual removal of vegetation and prevention of regrowth over a year prior to the experiment) (CBP), lime (600 g m^{-2} y^{-1}) vegetated (LVP) and lime non-vegetated (LBP). Water, 30 cm^3, was added to two each of the 12 treated plots, across the four different treatments (CVW, CBW, LVW, LBW). Four chambers did not contain soil cores, enabling the CO_2 concentration of the inlet air to be measured.

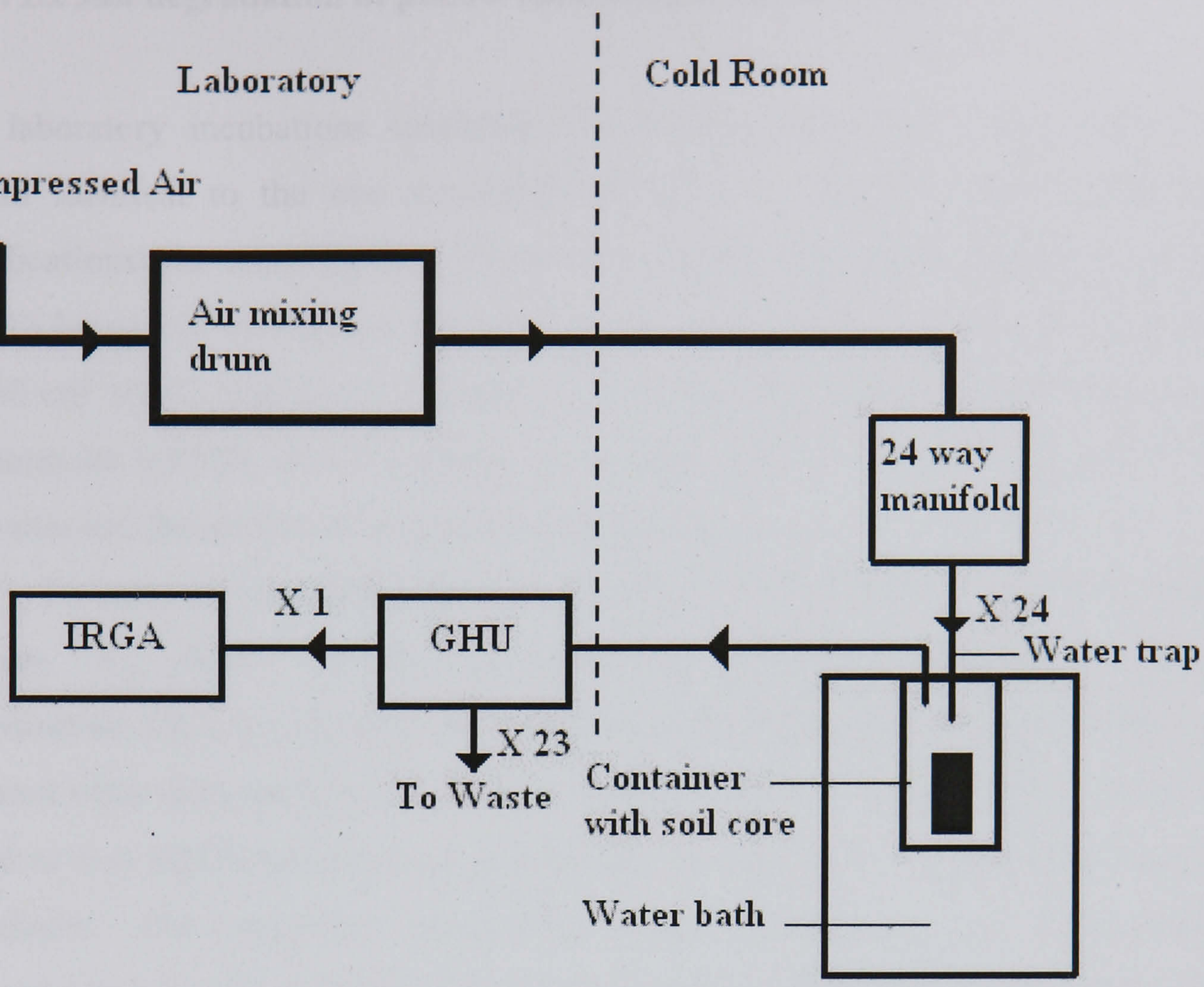

Figure 5.1 Schematic diagram of the laboratory incubation system. Air from a compressor passed into a 45 gallon drum and into a 24 way manifold, maintained at a slight positive pressure and 5 degrees warmer than the water bath which hold the soil cores. 24 lines left the manifold and each passed through a water trap and into a sealed container containing a soil core in a 3-compartment water bath, with each compartment holding 8 containers, controlled at the same temperature. Air from the containers then entered a gas handling unit (GHU) where the line was either diverted to waste or the infra red gas analyzer (IRGA). The GHU cycled through the lines with each line being diverted to the IRGA for 5 minutes per cycle.

5.2.2. *Ex situ* degradation of phenol monitored using ^{13}C phenol

The laboratory incubations involving ^{13}C labelled phenol used a flow-through system identical to the one described in Section 5.1 except for the following modifications: the manifold was 15 port (rather than 24; since the mobile lab has only 15 lines), not including a standard, and air from all 15 chambers, at a flow rate of 100 cm^3 min^{-1}, was drawn through PTFE lines to the mobile isotopic ratio mass spectrometer (IRMS) for semi-continuous measurement of $^{13}CO_2$, enabling both the ^{13}C value and the ppm CO_2 to be measured (Fig 5.2).

To measure the degradation of phenol in the laboratory 30 cm^3 of a 50ppm solution $^{13}C_6$ phenol was applied (99% atm enrichment, Cambridge Isotope Laboratories, UK), to soil cores (33 cm^2) from each of the 12 treated plots, with four different treatments and three replicates of each treatment. Water, 30 cm^3, was also added to two additional chambers to provide the signal of soil respiration "natural abundance". The treatments were; control vegetated (CV), control non-vegetated (manual removal of vegetation and prevention of regrowth over a year prior to the experiment, CB), lime (600 g m^{-2} y^{-1}) vegetated (LV) and lime non-vegetated (LB). A fifteenth chamber remained empty, allowing the $\delta^{13}C$ value and CO_2 concentration of the incoming air to be measured. The degradation of phenol was measured as $^{13}CO_2$ evolved from treated cores using the sealed chambers connected to the mobile laboratory.

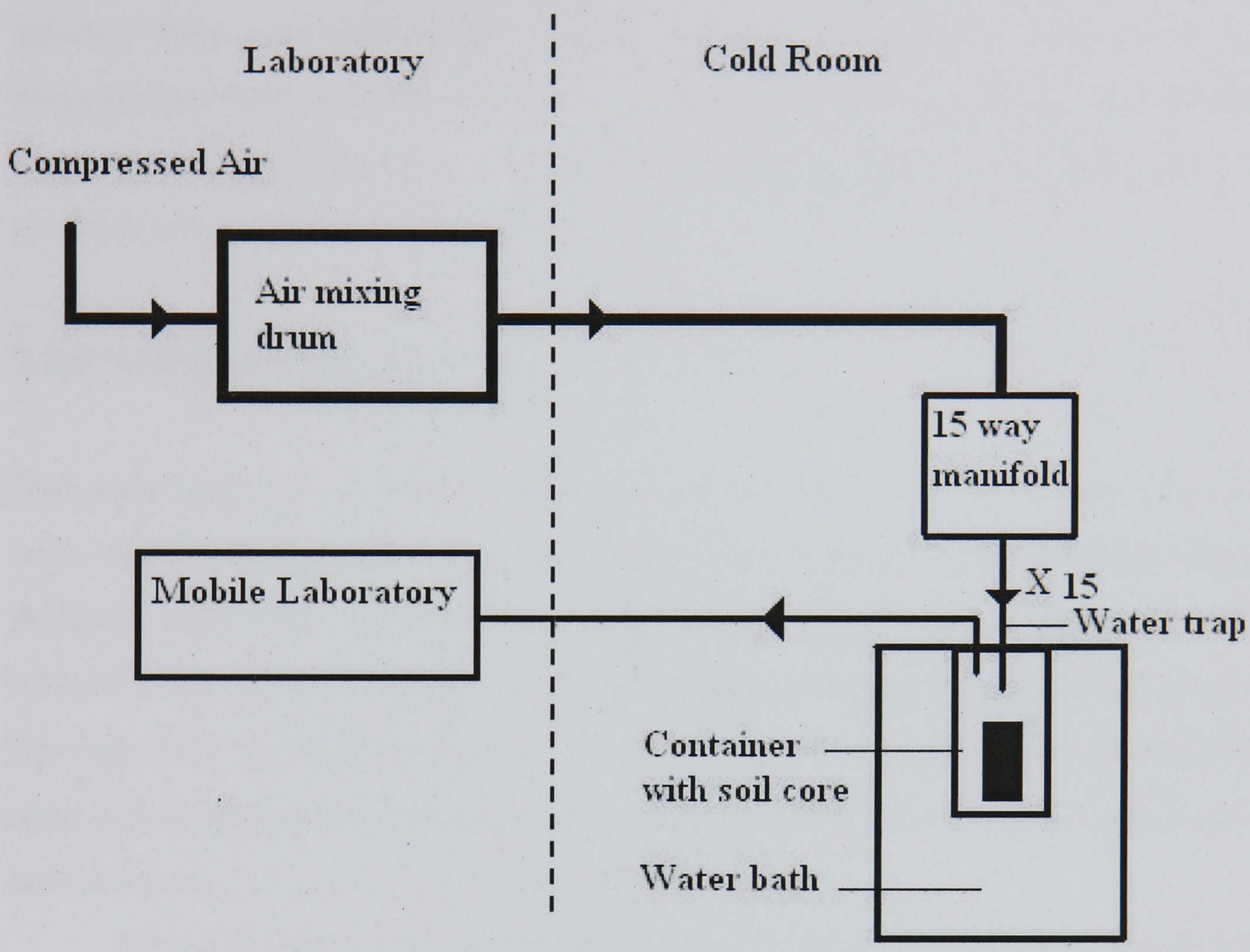

Figure 5.2 Schematic diagram of the laboratory incubation system used in conjunction with the mobile laboratory. See Fig. 5.1 for details. Air from the chambers entered the mobile laboratory, where they sequentially pass into the IRMS for $^{13}CO_2$ analysis.

5.2.3 PLFA analysis

The cores used in the experiment described in Section 5.2.2 were removed from the incubator after 48 hours and placed directly into a -80°C freezer to halt microbial activity. They were subsequently freeze-dried and PLFAs were extracted using the method described in Section 4.2.5, with 4 treatments (CV, CB, LV and LB) and 3 replicates of each treatment. The PLFAs were assigned, as in Chapter 4, to the groupings reported by Phillips *et al*. (2002).

5.2.4 Statistical analysis

Statistical analyses were performed using SPSS (v.14.0 2005 SPSS. Inc). ANOVA with repeated measures was used to compare the δ and flux measurements from the different treatments, followed by *a posterori t* tests, where appropriate. One-way ANOVA was used to compare the final cumulative fluxes, followed by a *post hoc* Duncan's test. A factorial ANOVA was also used to compare all the grouped PLFA data across treatments with the data being transformed (log_{10}), if necessary, for normalisation; a *post hoc* Tukey test was then applied.

SAS (V8 2000 SAS Institute Inc) was used to perform ANOVAs on each of the individual PLFAs for the compositions, $\delta^{13}C$ and ng. It is recognised that these high numbers of ANOVA comparisons (> 100) will result in Type II statistical errors (i.e. the likelihood of five false positive significant treatment impacts out of every 100 ANOVAs performed), but any consistent significant treatment effects would be detected.. Principal components analyses (PCA) was also applied to the PLFA data, both concentrations and $\delta^{13}C$ content, using SAS.

5.3 Results

5.3.1 *Ex situ* degradation of phenol monitored using ^{12}C phenol

Fig. 5.3 compares the CO_2 flux between CV and LV treatments after the addition of either phenol (CVP / LVP) or water (CVW / LVW). The mean flux from the CVW treatment was slightly higher than for the CVP treatment and remained consistent after the phenol and water were added, and then throughout the remaining experiment. Whilst the LVW treatment had a higher CO_2 flux than the LVP treatment, the increase in the flux began before the phenol was added and an ANOVA with repeated measures found no significant differences between any of the treatments.

The CO_2 fluxes from the bare treatments after the addition of phenol (CBP / LBP) or water (CBW / LBW) are shown in Fig. 5.4. Although the mean CO_2 flux from the CVW treatment flux appeared higher than the mean CVP flux, whilst the LVW mean flux appeared lower than the LVP flux, there were no significant differences between the four treatments.

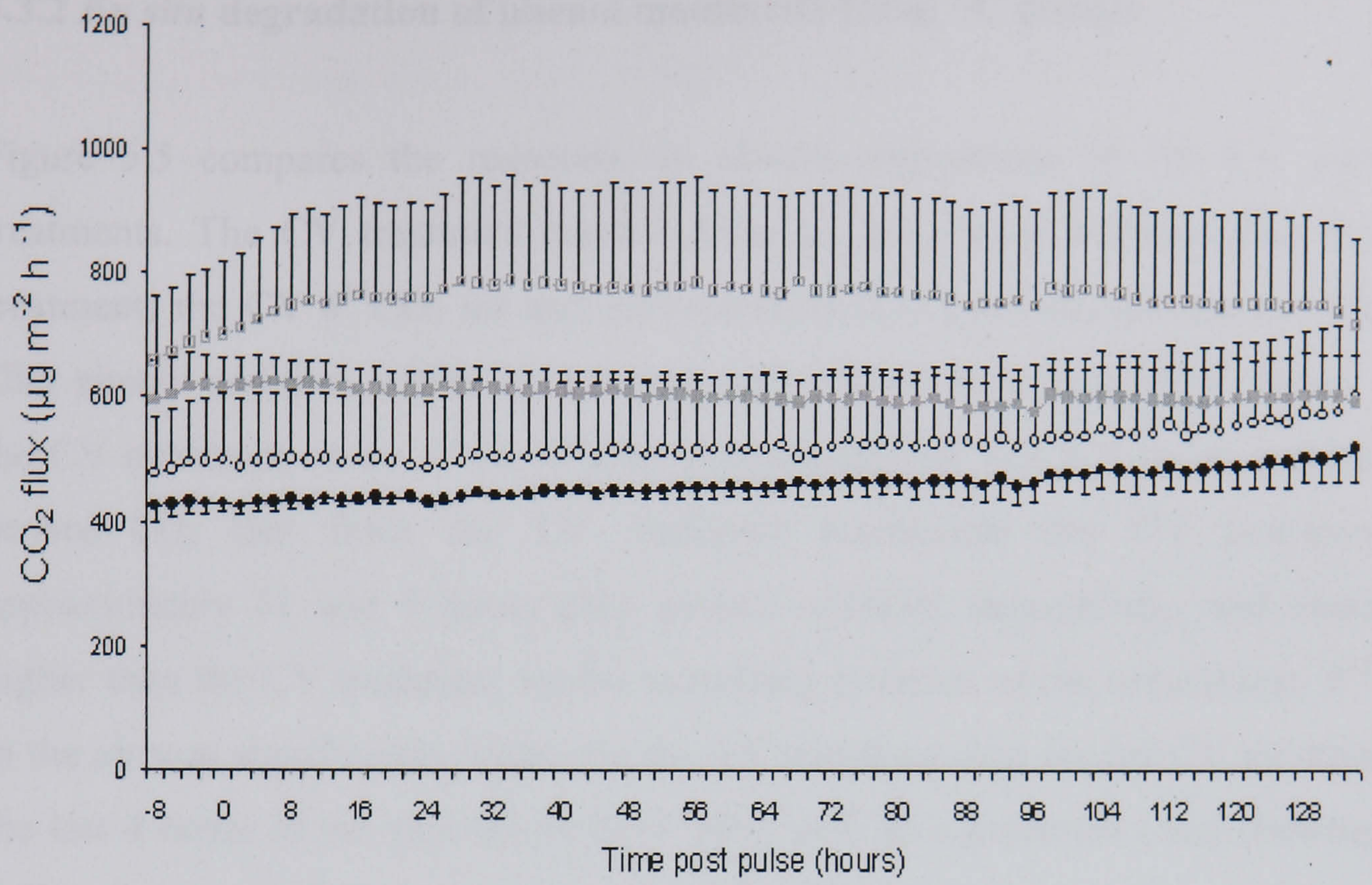

Figure 5.3 CO_2 flux following the application of 30 cm^3 phenol [50 ppm]. Error bars are one standard error of the mean and shown in one direction , for clarity. ●—● CVP ○- -○ CVW ■—■ LVP □- -□ LVW

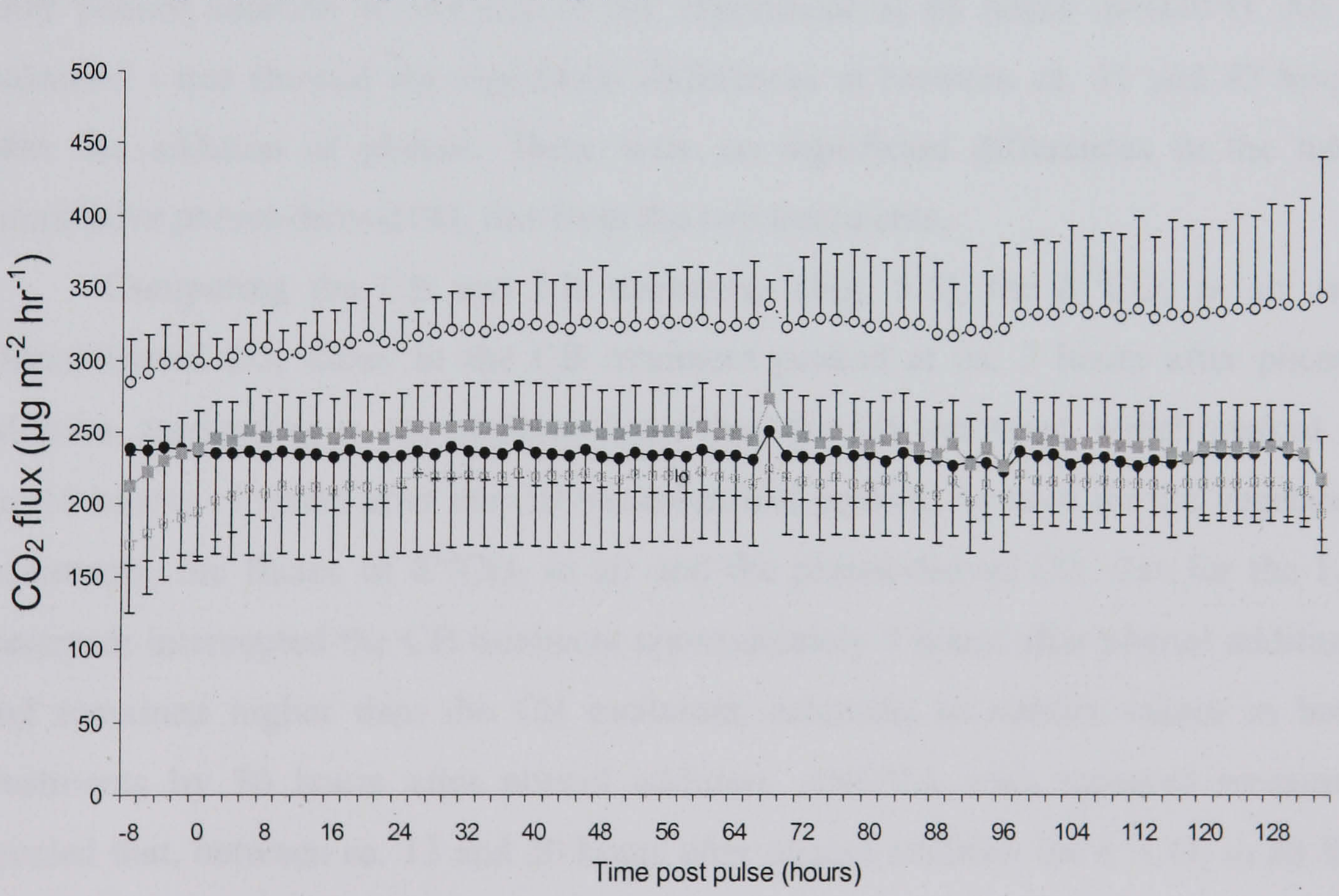

Figure 5.4 CO_2 flux following the application of 30 cm^3 phenol [50 ppm]. Error bars are one standard error of the mean. ●—● CBP ○- -○ CBW ■—■ LBP □- -□ LBW

5.3.2 *Ex situ* degradation of phenol monitored using ^{13}C phenol

Figure 5.5 compares the responses in phenol degradation in the CV and LV treatments. The CV treatment reacted faster to the phenol addition than the LV treatment; the CV $\delta^{13}CO_2$ air and phenol-derived CO_2 flux both peaked ca. 4 hours after phenol addition, whilst the LV treatment peaked approximately 11 hours after the CV treatment, at ca. 15 hours after phenol addition. The $\delta^{13}CO_2$ air and phenol-derived CO_2 flux from the LV treatment intercepted the CV treatment at approximately 11 and 9 hours after phenol addition, respectively, and remained higher than the CV treatment for the remaining duration of the experiment. $\delta^{13}CO_2$ in the air was significantly higher for the LV treatment than for the CV treatment in the last 4 hours of the experiment ($p=0.048$), with an *a posterori t* test showing the differences occurring at 42 hours after the addition of phenol. The analyses also revealed that the phenol-derived CO_2 flux under the LV treatment was significantly higher than for the CV treatment in the second half of the experiment, from 30 hours after phenol addition to the end of the experiment at 46 hours ($p=0.014$). An *a posterori t* test showed the significant differences at between ca. 31 and 43 hours after the addition of phenol. There were no significant differences in the total cumulative phenol-derived CO_2 flux from the two treatments.

Comparing the CB and LB treatments (Fig. 5.6), the $\delta^{13}CO_2$ in air and phenol-derived CO_2 fluxes in the CB treatment peaked at ca. 3 hours after phenol addition, responding to the addition faster than the LB treatment, which peaked at ca. 15 hours, 11 hours after the CB treatment had peaked. As seen for the vegetated treatments, the fluxes of $\delta^{13}CO_2$ in air and the phenol-derived CO_2 flux for the LB treatment intercepted the CB treatment approximately 9 hours after phenol addition, and remained higher than the CB treatment, returning to similar values in both treatments by 30 hours after phenol addition. ANOVA with repeated measures reveled that, between ca. 13 and 20 hours after phenol addition the $\delta^{13}CO_2$ in air for the LB treatment was significantly higher than for the CB treatment ($p=0.045$) and that between ca.13 and 23 hours after phenol addition the LB treatment phenol-derived CO_2 flux was significantly higher than the CB treatment ($p=0.016$). *A*

posterori t tests found the significant differences to be between ca. 14 and 19 hours after phenol addition. There were no significant differences in the total cumulative phenol-derived CO_2 flux between the CB and LB treatments.

a

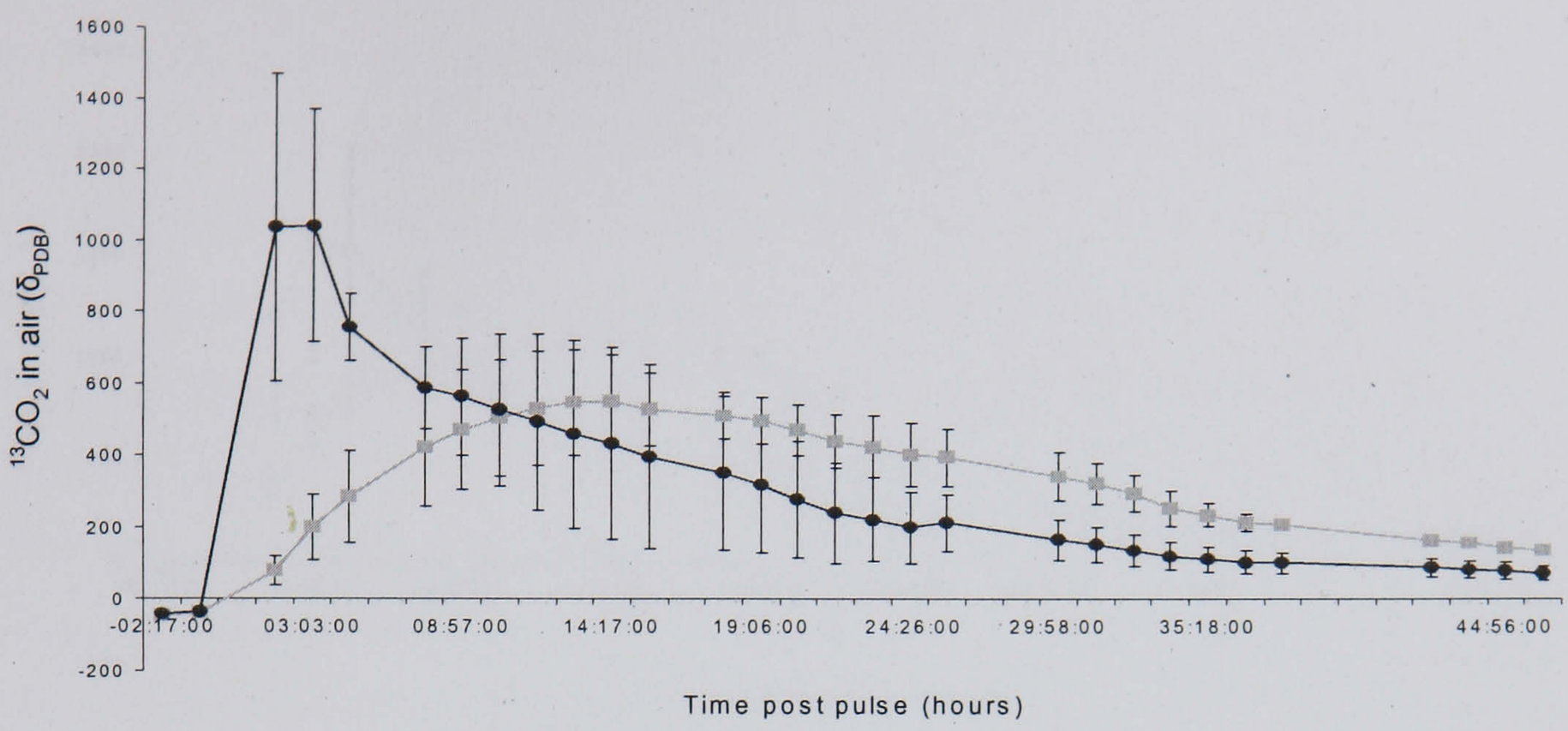

b

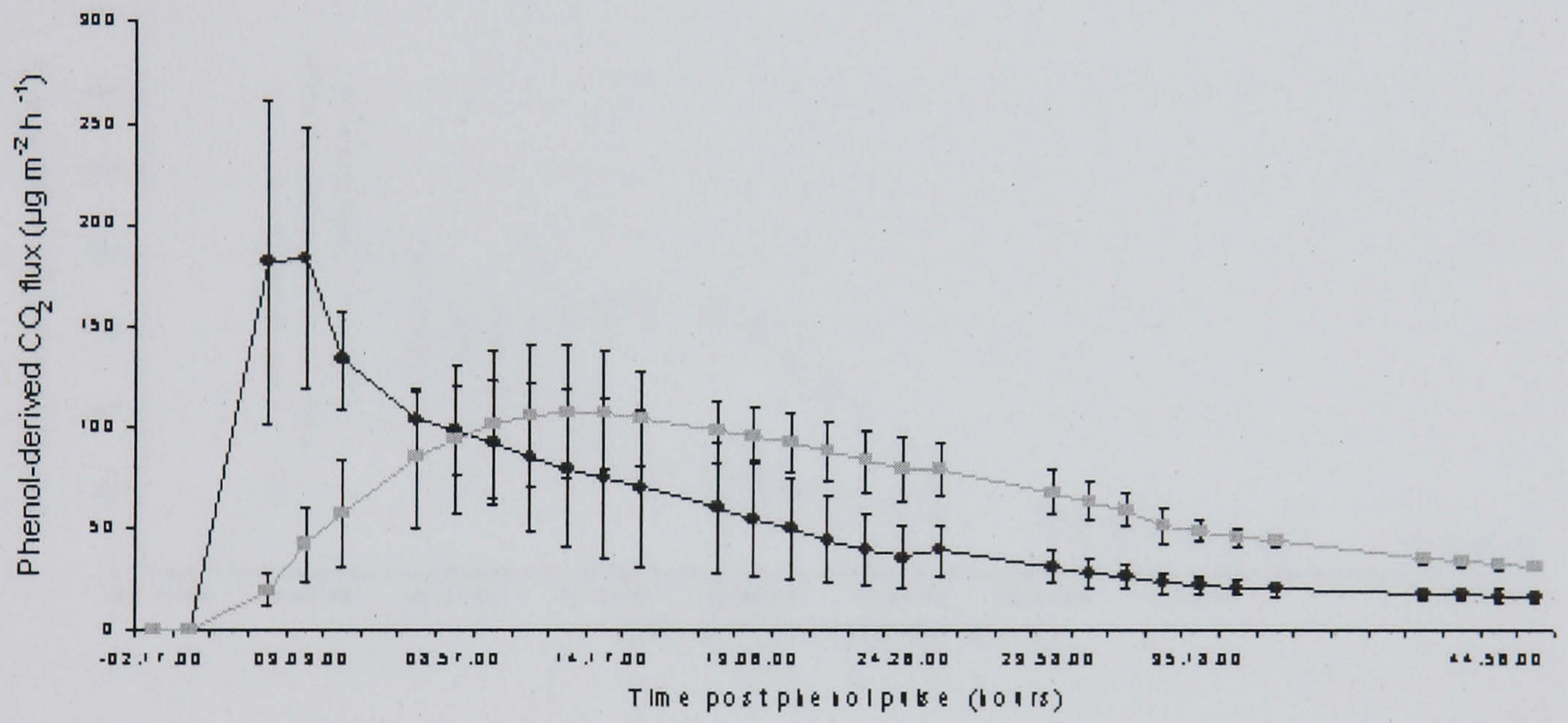

c

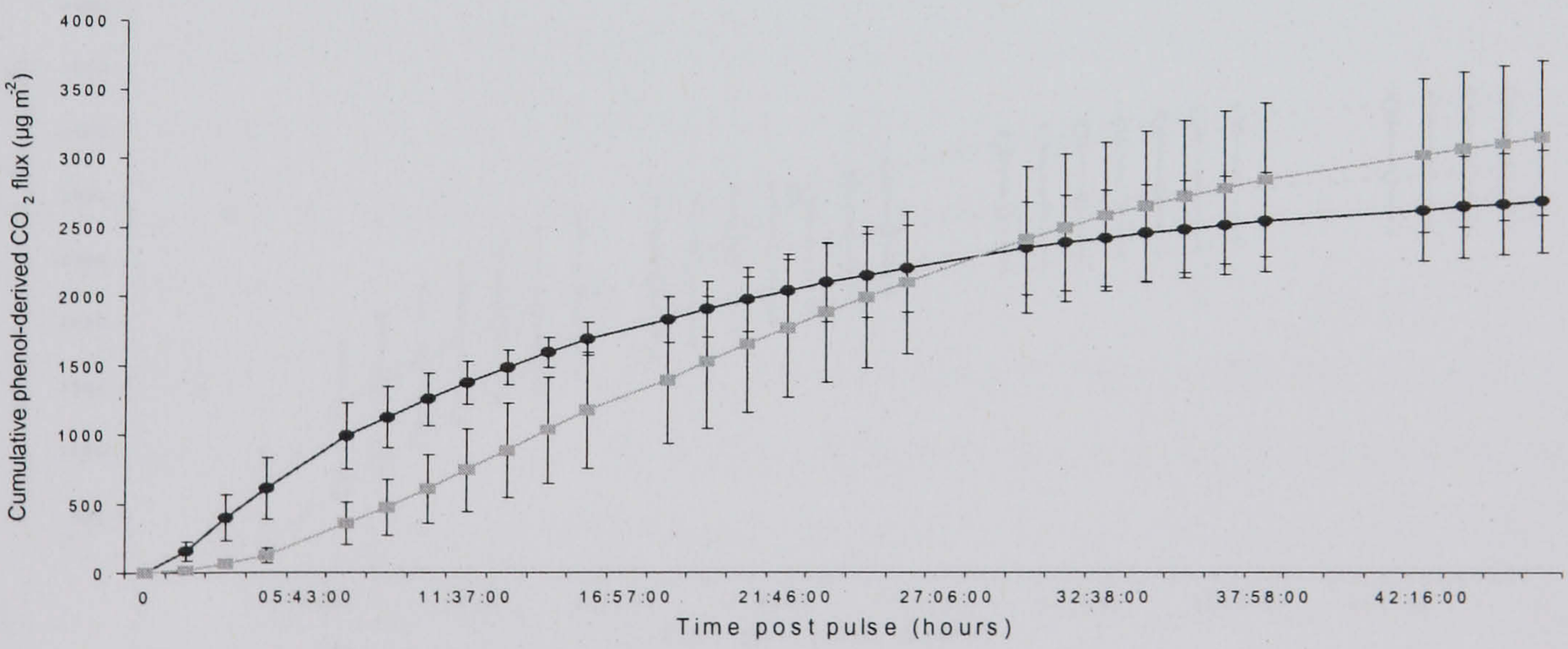

Figure 5.5 a, b, c $\delta^{13}CO_2$ air values, phenol-derived CO_2 flux values and cumulative phenol-derived CO_2 values following the application of 30 cm^3 $^{13}C_6$ phenol [50 ppm] to the control (●—● CV), and limed (■—■ LV) vegetated plots. Error bars are one standard error of the mean.

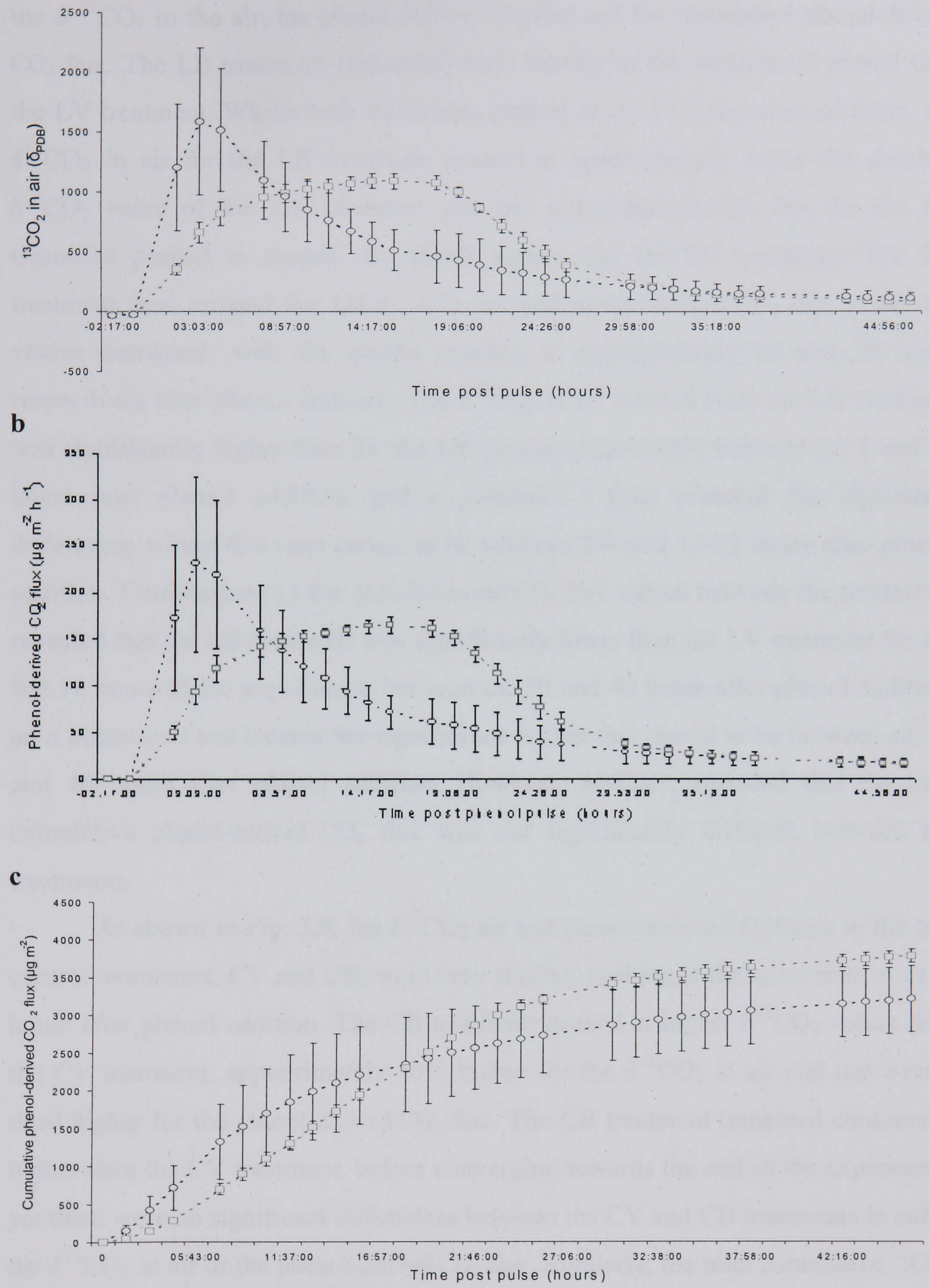

Figure 5.6 a, b, c $\delta\ ^{13}CO_2$ air values, phenol-derived CO_2 flux values and cumulative phenol-derived CO_2 values following the application of 30 $cm^3\ ^{13}C_6$ phenol [50 ppm] to the control (○- -○ CB), and limed (□- -□ LB) bare plots. Error bars are one standard error of the mean.

Figure 5.7 compares the impact of the two lime treatments, LV and LB, on the $\delta\ ^{13}CO_2$ in the air, the phenol-derived CO_2 flux and the cumulative phenol-derived CO_2 flux. The LB treatment responded more rapidly to the addition of phenol than the LV treatment. Whilst both treatments peaked at ca. 15 hours after addition, the $\delta^{13}CO_2$ in air for the LB treatment peaked at approximately twice the absolute $\delta^{13}CO_2$ value of the LV treatment and the phenol-derived CO_2 flux for the LB treatment peaked at around two thirds higher that the LV treatment. The LV treatment then crossed the LB $\delta\ ^{13}CO_2$ air and phenol-derived CO_2 flux as the LB values decreased, with the graphs crossing at approximately 26 and 24 hours respectively after phenol addition. The $\delta^{13}CO_2$ in air derived from the LB treatment was significantly higher than for the LV treatment ($p=0.009$) between ca. 2 and 24 hours post phenol addition, and *a posterori t* tests revealed the significant differences within this time period to be between 2-4 and 14-22 hours after phenol addition. Comparisons of the phenol-derived CO_2 flux values between the treatments revealed that the LB treatment was significantly lower than the LV treatment for the last 16 hours of the experiment, between ca. 30 and 46 hours after phenol addition; an *a posterori t* test located the significance within this period to be between ca. 35 and 46 hours after phenol addition. However, ANOVA revealed that the total cumulative phenol-derived CO_2 flux was not significantly different between the treatments.

As shown in Fig. 5.8, the $\delta^{13}CO_2$ air and phenol-derived CO_2 fluxes in the two control treatments, CV and CB, were very similar, peaking at the same time of ca. 3 hours after phenol addition. The CB treatment peaked at higher $\delta^{13}CO_2$ values than the CV treatment, approximately 50% higher for the $\delta^{13}CO_2$ in air and just over a third higher for the phenol-derived CO_2 flux. The CB treatment remained continually higher than the CV treatment, before converging towards the end of the experiment, yet there were no significant differences between the CV and CB treatments in either the $\delta^{13}CO_2$ in air or the phenol-derived CO_2 flux. Similarly, the total cumulative $^{13}CO_2$ flux was not significantly different between treatments (shown for all treatments in Fig.5.9).

A mass balance was calculated to determine the percentage of ^{13}C in the substrate that was mineralised to CO_2 in each of the four treatments and this is presented in Table 5.1, showing the variation between treatments from 0.22% in CV to 0.31% in LB.

Table 5.1 Mass balance showing percentage ^{13}C phenol mineralised to $^{13}CO_2$. No significant differences were found between treatments.

Treatment	% of ^{13}C phenol mineralised to $^{13}CO_2$
CV	0.22
CB	0.26
LV	0.26
LB	0.31

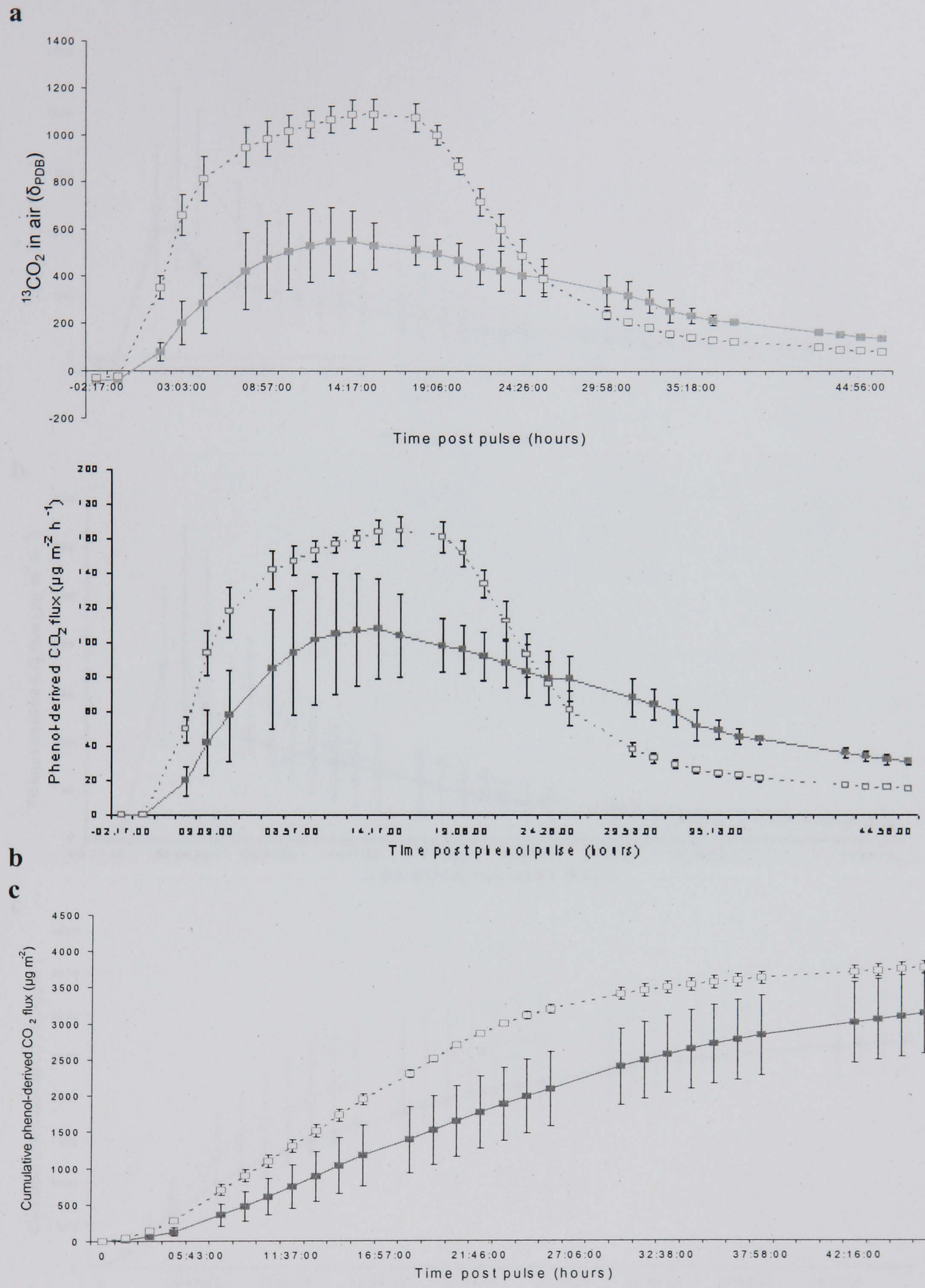

Figure 5.7 a, b, c $\delta^{13}CO_2$ air values, phenol-derived CO_2 flux values and cumulative phenol-derived CO_2 values following the application of 30 cm^3 $^{13}C_6$ phenol [50 ppm] to the vegetated (■—■ LV), and bare (□- -□ LB) limed plots. Error bars are one standard error of the mean.

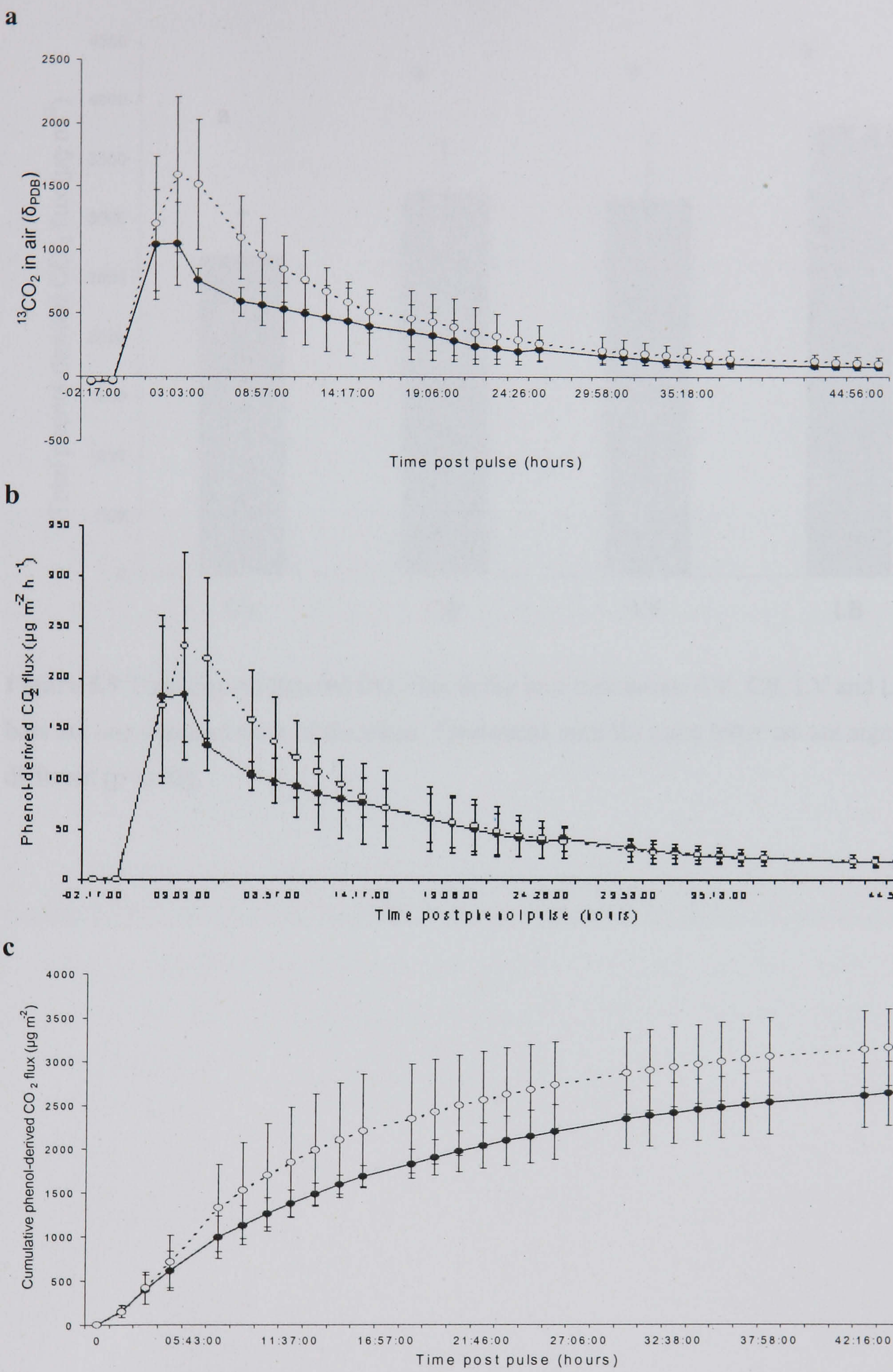

Figure 5.8 a, b, c $\delta^{13}CO_2$ air values, phenol-derived CO_2 flux values and cumulative phenol-derived CO_2 values following the application of 30 cm^3 $^{13}C_6$ phenol [50 ppm] to the vegetated (●—● CV), and bare (○- -○ CB) control plots. Error bars are one standard error of the mean.

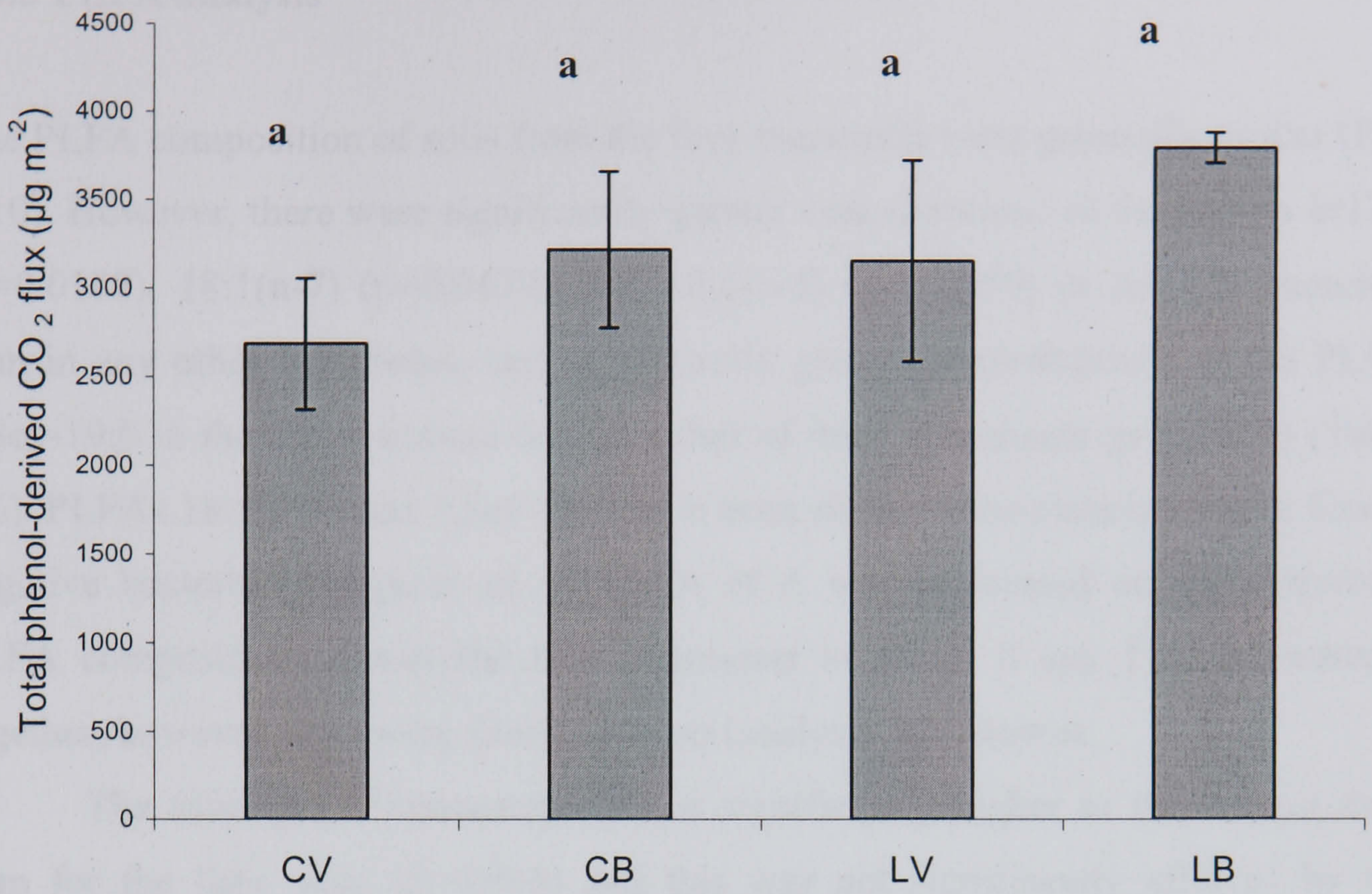

Figure 5.9 Total phenol-derived CO_2 flux in the four treatments: CV, CB, LV and LB. Error bars are one standard error of the mean. Treatments with the same letter are not significantly different ($p<0.05$).

5.3.3 PLFA analysis

The PLFA composition of soils from the four treatments were generally similar (Fig. 5.10). However, there were significantly greater concentrations of the PLFAs br17:0 ($p=0.0182$), 18:1(n-7) ($p=0.0439$), and 18:1(n-5) ($p=0.0050$) in the CB treatment than in any other treatments, and significantly greater concentrations of the PLFA 7,8cy-19:0 in the CB treatment than in either of the L treatments ($p=0.0433$) (Table 5.6). PLFAs 18:1(n-7) and 7,8cy-19:0 have been shown to be associated with Gram-negative bacteria (Philips *et al.* 2002). A PCA was performed on the individual PLFA compositions across the four treatments to reveal if any PLFAs clustered together, however none were found to do so (analyses not shown).

The total PLFA concentration was significantly higher in the control soils than for the lime soils ($p=0.036$) and this was not significantly affected by the presence or absence of vegetation (Fig. 5.11; Table 5.3). There were no significant differences in the concentrations of fungal PLFA across any of the treatments (Fig. 5.12, Table 5.4). However, the bacterial PLFA concentrations (Fig. 5.13, Table 5.5) were significantly higher in the control treatments than in the lime, ($p=0.027$), yet the difference was not sufficient to cause a significant change in the bacterial / fungal PLFA ratios (Fig. 5.14, Table 5.6). Therefore, whilst the total amount of PLFA was significantly higher in the control soils than the lime soils, this was dominated by the significantly higher concentrations of bacterial PLFAs in the control treatments.

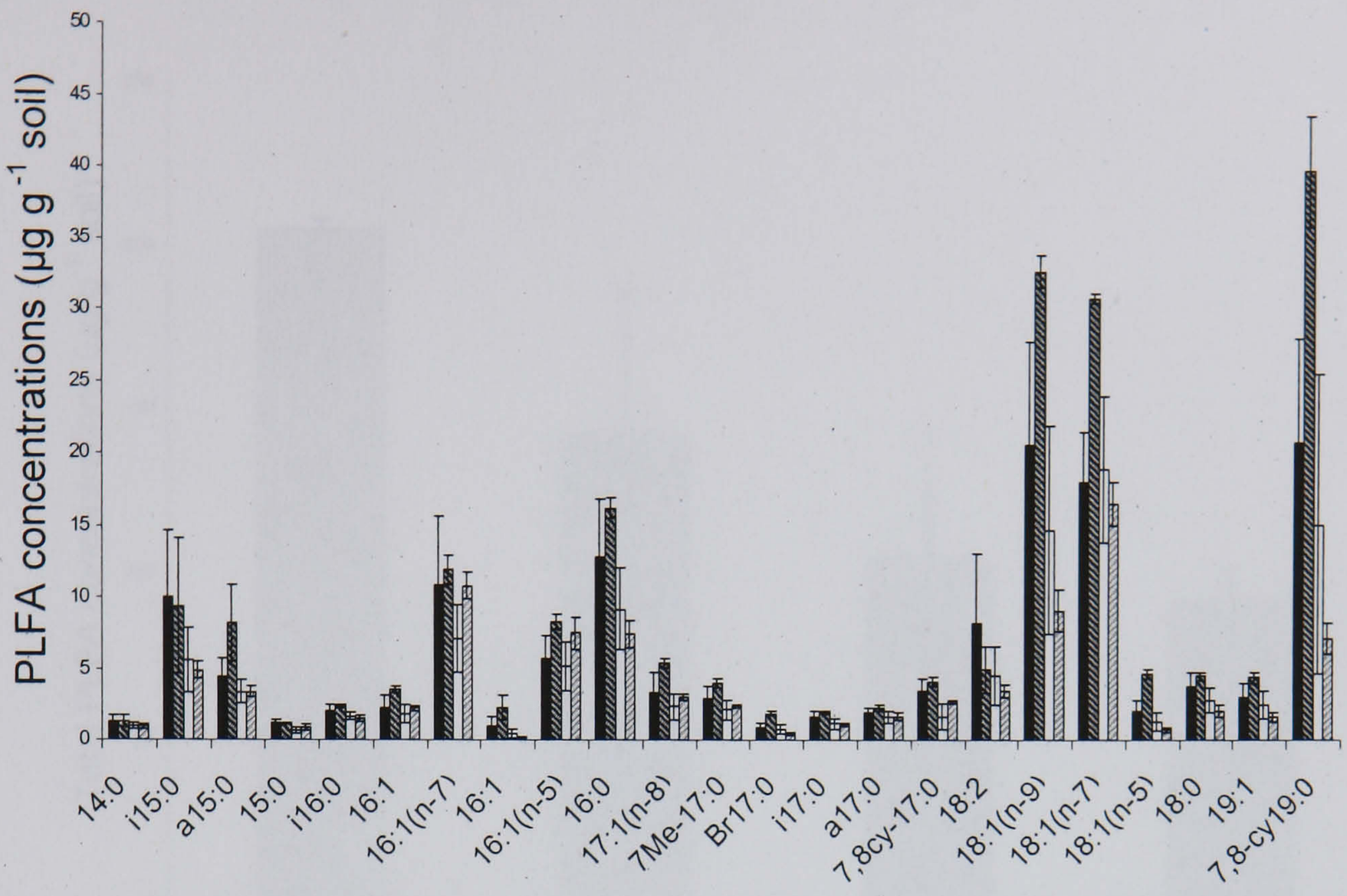

Figure 5.10 PLFA composition in the four treatments. Error bars are one standard error of the mean. (■= CV, ■=CB, □ = LV, ■ = LB).

Table 5.2 ANOVA and *post hoc* Duncan's of logged PLFA compositions (log_{10} transformed) in the four treatments. Treatments with different letters across a row denote significant treatment differences.

		Duncan's Multiple Range Test			
PLFA	P	CV	CB	LV	LB
14:0	0.6895				
i15:0	0.6729				
a15:0	0.1742				
15:0	0.3446				
i16:0	0.2554				
16:1	0.2098				
16:1(n-7)	0.6382				
16:1(n-5)	0.3526				
16:0	0.1406				
17:1(n-8)	0.1282				
7me-17:0	0.2143				
br17:0	**0.0182**	**a**	**b**	**a**	**a**
i17:0	0.1938				
a17:0	0.4617				
7,8cy-17:0	0.1285				
18:2(n-6)	0.6544				
18:1(n-9)	0.0574				
18:1(n-7)	**0.0439**	**a**	**b**	**a**	**a**
18:1'	**0.0050**	**a**	**b**	**a**	**a**
18:0	0.1410				
19:1	0.1348				
'7,8cy-19:0	**0.0433**	**ab**	**b**	**A**	**a**

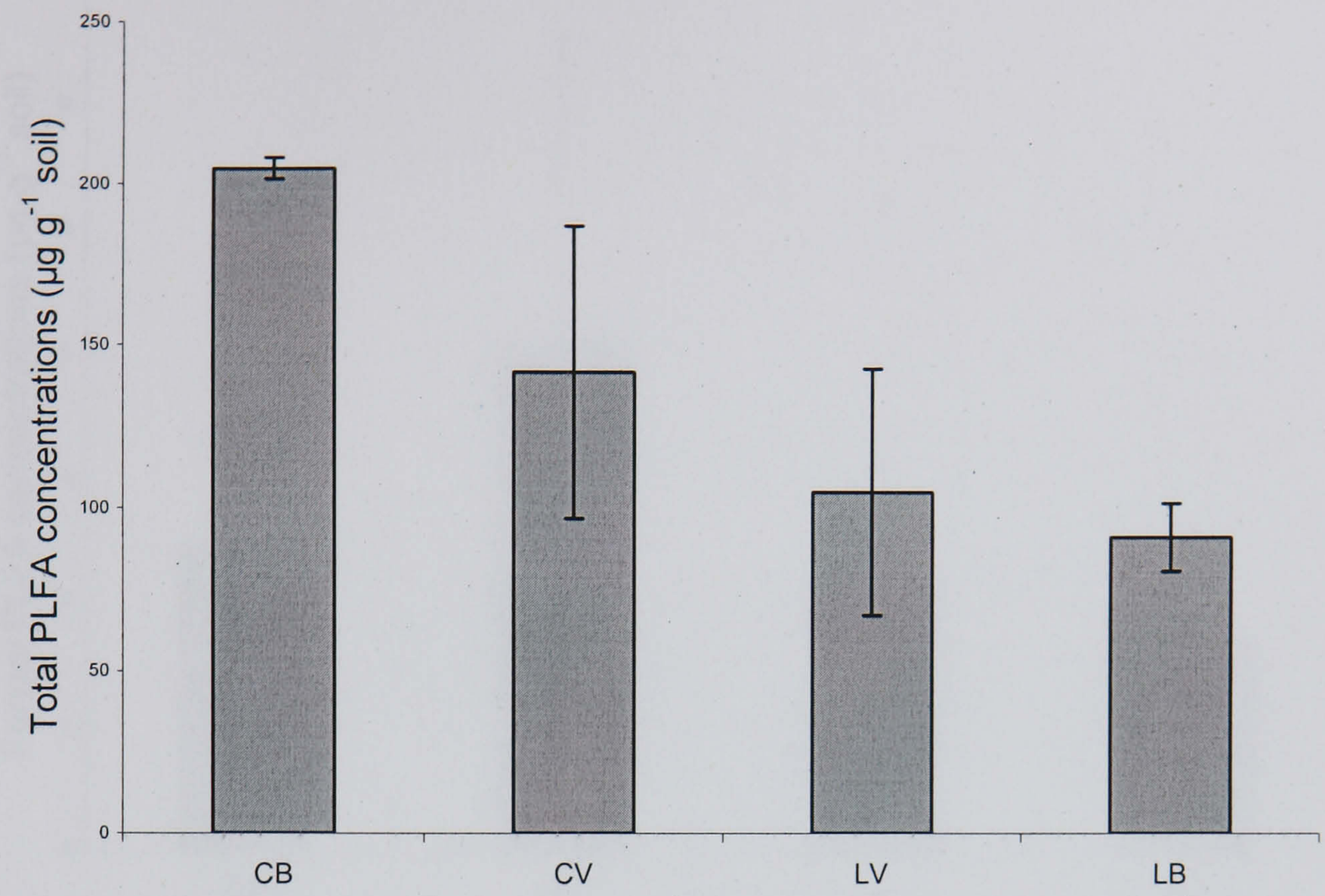

Figure 5.11 Total PLFA concentrations in the four treatments (CB = control bare, CV = control with vegetation, LV = lime with vegetation, LB = lime bare).

Table 5.3 ANOVA table for total PLFA concentrations, comparing the four treatments.

Source	Type III Sum of Squares	df	Mean Square	F	Sig.
Corrected Model	23259.505(a)	3	7753.168	2.885	.103
Intercept	220974.890	1	220974.890	82.214	.000
Vegetation	1819.424	1	1819.424	.677	.434
Lime	**16994.796**	**1**	**16994.796**	**6.323**	**.036**
Vegetation * Lime	4445.285	1	4445.285	1.654	.234
Error	21502.372	8	2687.797		
Total	265736.767	12			
Corrected Total	44761.877	11			

a R Squared = .520 (Adjusted R Squared = .339)

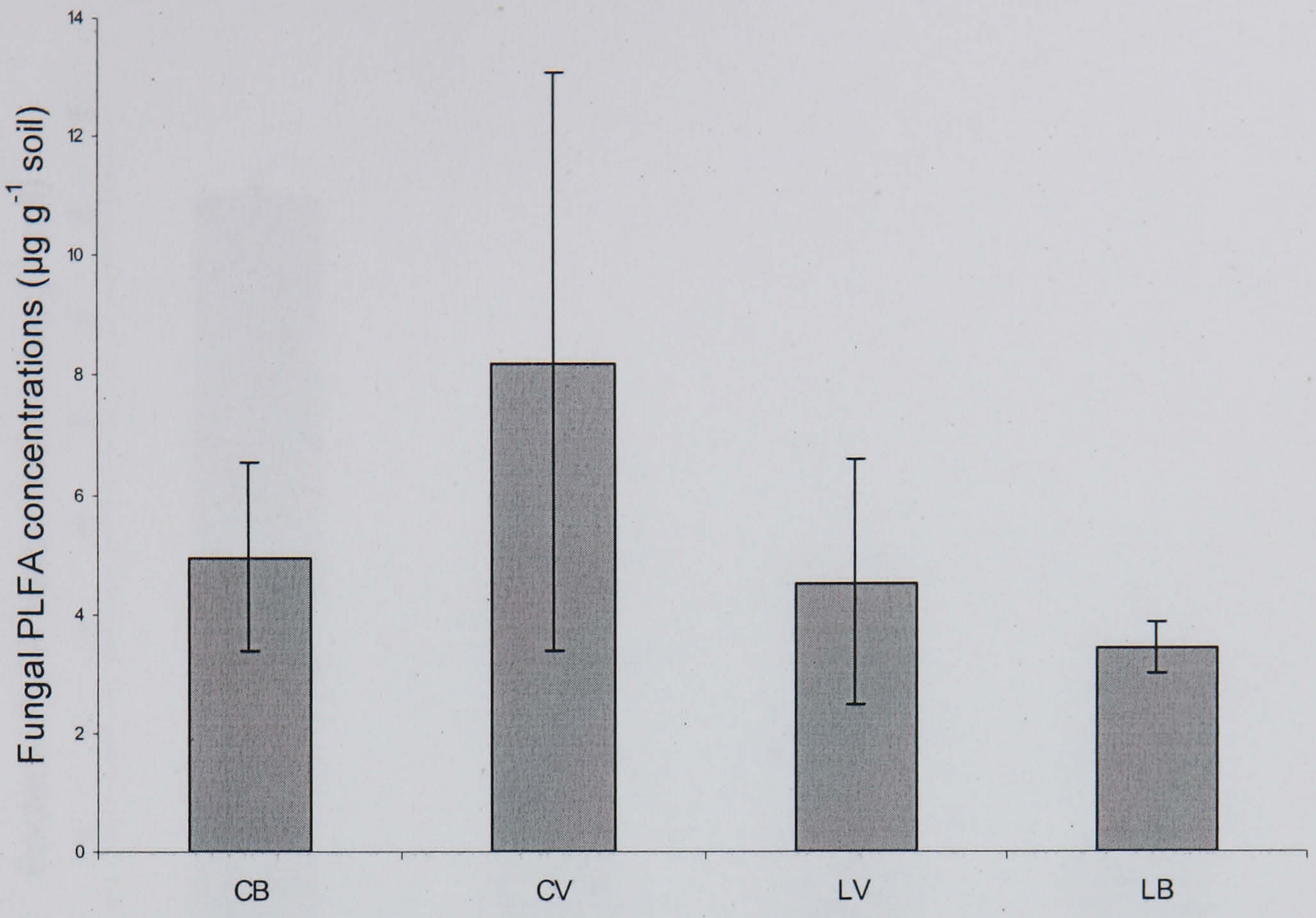

Figure 5.12 Fungal PLFA concentrations in the four treatments. Error bars are one standard error of the mean. (CB = control bare, CV = control with vegetation, LV = lime with vegetation, LB = lime bare).

Table 5.4 ANOVA table of fungal PLFA concentrations comparing the four treatments.

Source	Type III Sum of Squares	df	Mean Square	F	Sig.
Corrected Model	38.167(a)	3	12.722	.563	.654
Intercept	334.345	1	334.345	14.799	.005
Vegetation	14.241	1	14.241	.630	.450
Lime	20.484	1	20.484	.907	.369
Vegetation * Lime	3.442	1	3.442	.152	.706
Error	180.742	8	22.593		
Total	553.254	12			
Corrected Total	218.909	11			

a R Squared = .174 (Adjusted R Squared = -.135)

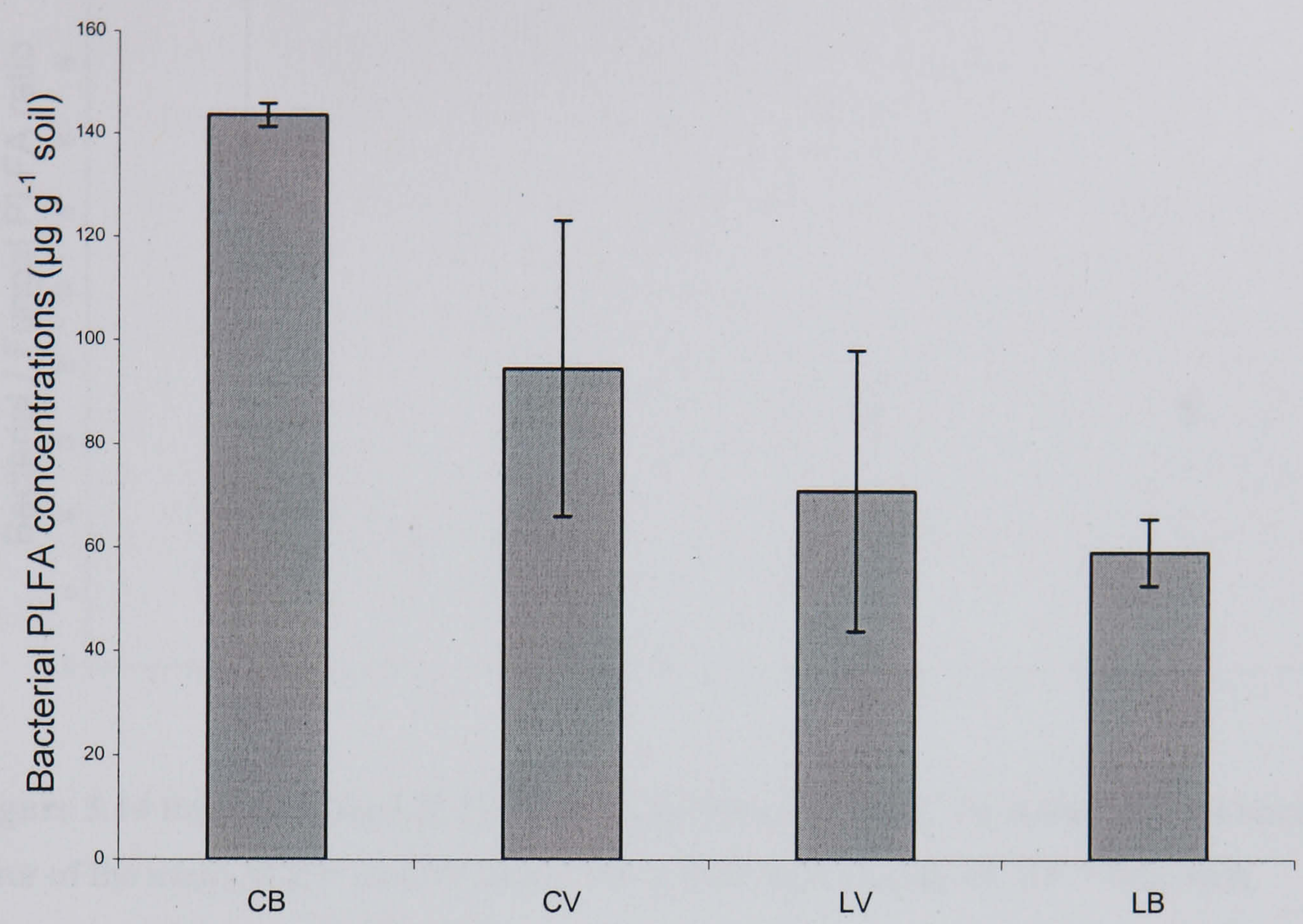

Figure 5.13 Bacterial PLFA concentrations in the four treatments. Error bars are one standard error of the mean, (CB = control bare, CV = control with vegetation, LV = lime with vegetation, LB = lime bare).

Table 5.5 ANOVA table for bacterial PLFA concentrations, comparing the four treatments.

Source	Type III Sum of Squares	df	Mean Square	F	Sig.
Corrected Model	12537.059(a)	3	4179.020	3.491	.070
Intercept	102051.688	1	102051.688	85.252	.000
Vegetation	1044.241	1	1044.241	.872	.378
Lime	**8710.928**	**1**	**8710.928**	**7.277**	**.027**
Vegetation * Lime	2781.890	1	2781.890	2.324	.166
Error	9576.436	8	1197.054		
Total	124165.182	12			
Corrected Total	22113.494	11			

a R Squared = .567 (Adjusted R Squared = .405)

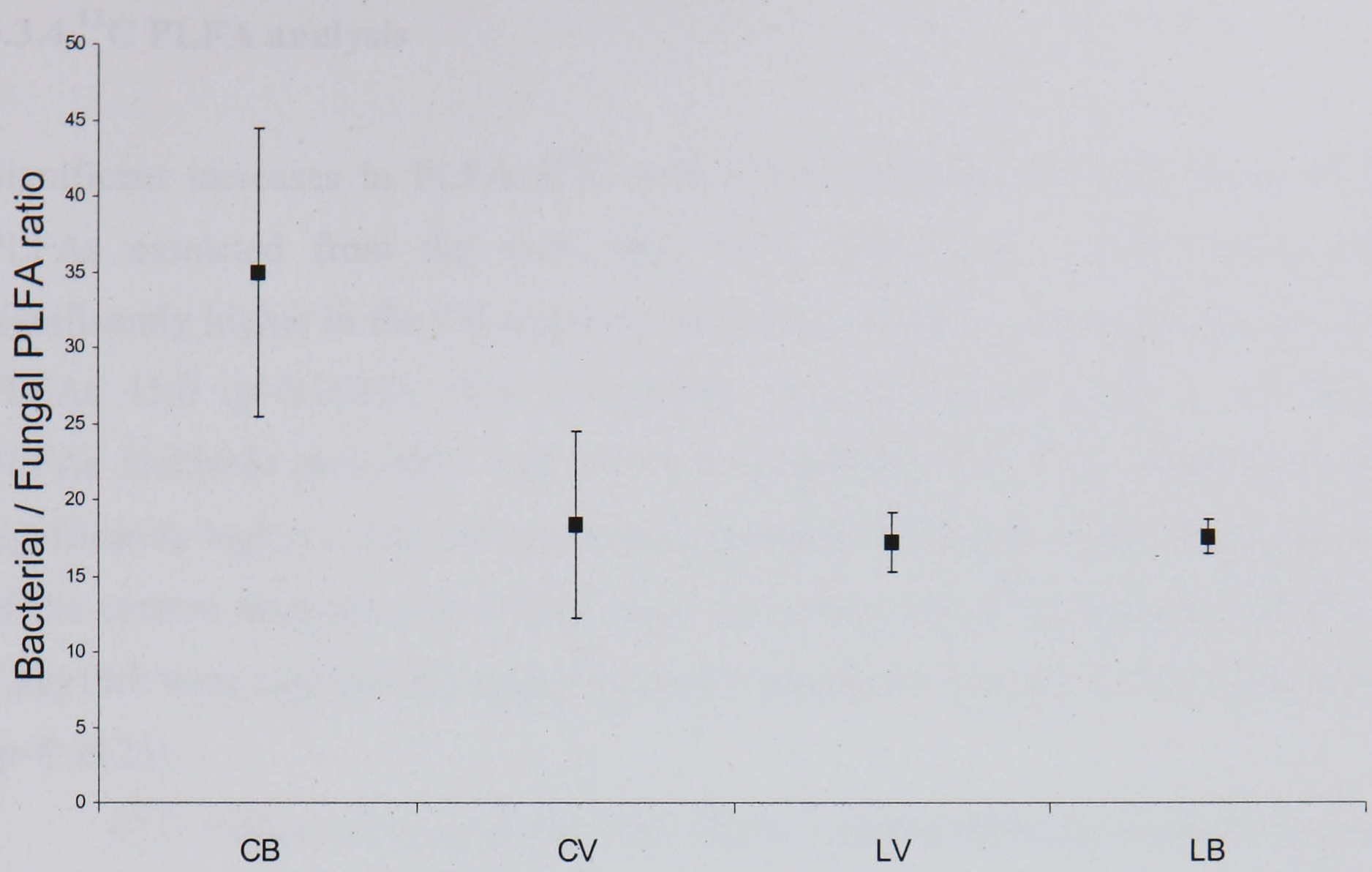

Figure 5.14 Bacterial/fungal PLFA ratios in the four treatments. Error bars are one standard error of the mean, (CB = control bare, CV = control with vegetation, LV = lime with vegetation, LB = lime with bare).

Table 5.6 ANOVA table for bacterial/fungal PLFA ratios in the four treatments.

Source	Type III Sum of Squares	df	Mean Square	F	Sig.
Corrected Model	670.607(a)	3	223.536	2.245	.160
Intercept	5800.781	1	5800.781	58.246	.000
Vegetation	213.264	1	213.264	2.141	.182
Lime	259.499	1	259.499	2.606	.145
Vegetation * Lime	197.844	1	197.844	1.987	.196
Error	796.725	8	99.591		
Total	7268.113	12			
Corrected Total	1467.332	11			

a R Squared = .457 (Adjusted R Squared = .253)

5.3.4 ^{13}C PLFA analysis

Significant increases in PLFA $\delta^{13}C$ values were observed for only some of the PLFAs extracted from the soils (Fig. 5.15; Table 5.7). $\delta^{13}C$ values were significantly higher in the LB treatment than for any other treatment in the bacterial PLFAs 15:0 ($p=0.0032$), 16:0 ($p=0.0139$), a17:0 ($p=0.0195$) and in the fungal PLFAs 18:2(n-6) ($p=0.0007$) and 18:1(n-9) ($p=0.0098$). The $\delta^{13}C$ values were also significantly higher in the LB treatment in the bacterial PLFA 16:1(n-7) that for any of the control treatments ($p=0.0347$) but, conversely, the $\delta^{13}C$ values in the PLFA 7,8cy19:0 were significantly higher in the CV treatment than any of the L treatments ($p=0.0125$).

$\delta^{13}C$ values were combined with PLFA concentrations to estimate the total amount of phenol-derived ^{13}C present in the PLFAs (Fig. 5.16; Table 5.8). The total amount of ^{13}C in the PLFAs was not affected by the presence or absence of vegetation, or the presence or absence of lime. However, the interaction between vegetation and liming tended towards significance ($p=0.058$), with a pattern of removal of the vegetation resulting in a decrease of ^{13}C in PLFAs in the control treatments, with a mean decrease of ca. 3 fold, whilst having the opposite effect in the lime treatments, with a mean increase of ca. 3 fold.

Further statistical analyses were carried out on the PLFAs for which increases in $\delta^{13}C$ values were observed (Fig. 5.17). Within this smaller number of PLFAs, there were significant differences in the amount of phenol-derived ^{13}C in the different PLFAs. Five distinct PLFAs, namely the bacterial PLFA 16:0, the Gram-negative bacterial PLFAs 16:1(n-7) and 18:1(n-7) and the fungal PLFAs, 18:2(n-6) and 18:1(n-9), incorporated significantly more ^{13}C than all other PLFAs. Within these five PLFAs, there was a significantly greater amount of ^{13}C in the fungal PLFA 18:2(n-6) in the LB treatment than in any other treatments ($p=0.024$). The LB treatment also incorporated significantly more ^{13}C than any other treatments in the Gram-positive PLFA 15:0 ($p=0.005$), although this incorporation was very small.

A PCA was performed on the PLFA $\delta^{13}C$ values across the four treatments and the amount of incorporation of ^{13}C however, yet it did not reveal any significant treatment clusters for PLFAs (analyses not shown).

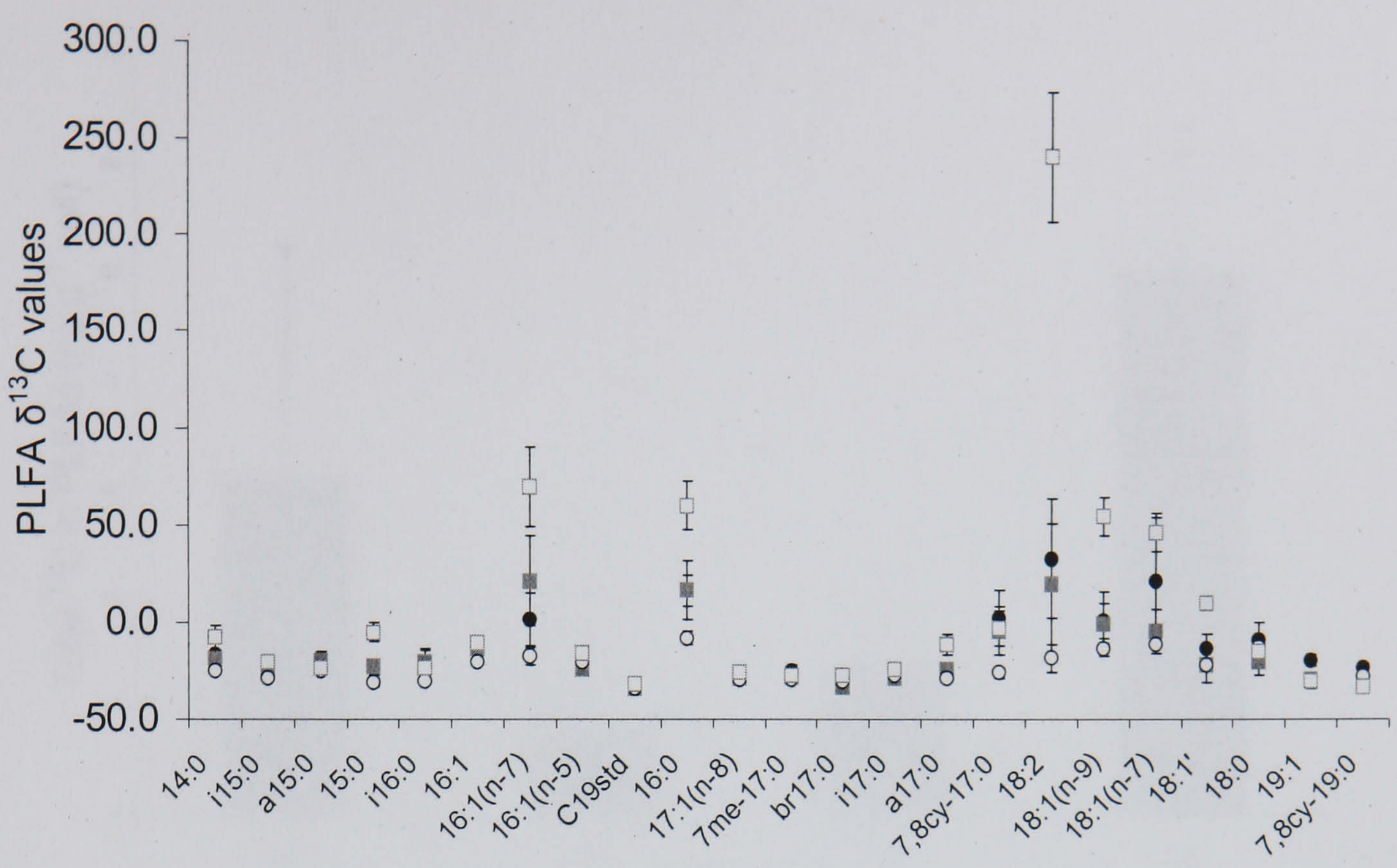

Figure 5.15 PLFA $\delta^{13}C$ values in the four treatments. Error bars are one standard error of the mean, (●—● CV ○- -○ CB ■—■ LV □- -□ LB).

Table 5.7 ANOVA and post hoc Duncan's of individual PLFA $\delta^{13}C$ values across the four treatments. Treatments with different letters across a row denote significant treatment differences.

		Duncan's Multiple Range Test			
PLFA	P	CV	CB	LV	LB
14:0	0.0798				
i15:0	0.3126				
a15:0	0.6655				
15:0	**0.0032**	**a**	**a**	**a**	**b**
i16:0	0.4772				
16:1	0.4512				
16:1(n-7)	**0.0347**	**a**	**a**	**ab**	**b**
16:1(n-5)	0.0669				
16:0	**0.0139**	**a**	**a**	**a**	**b**
17:1(n-8)	0.1955				
7me-17:0	0.3029				
br17:0	0.8914				
i17:0	0.3516				
a17:0	**0.0195**	**a**	**a**	**a**	**b**
7,8cy-17:0	0.3264				
18:2(n-6)	**0.0007**	**a**	**a**	**a**	**b**
18:1(n-9)	**0.0098**	**a**	**a**	**a**	**b**
18:1(n-7)	0.1729				
18:1'	**0.0184**	**a**	**a**	**a**	**b**
18:0	0.5879				
19:1	0.0524				
'7,8cy-19:0	**0.0125**	**a**	**ab**	**b**	**b**

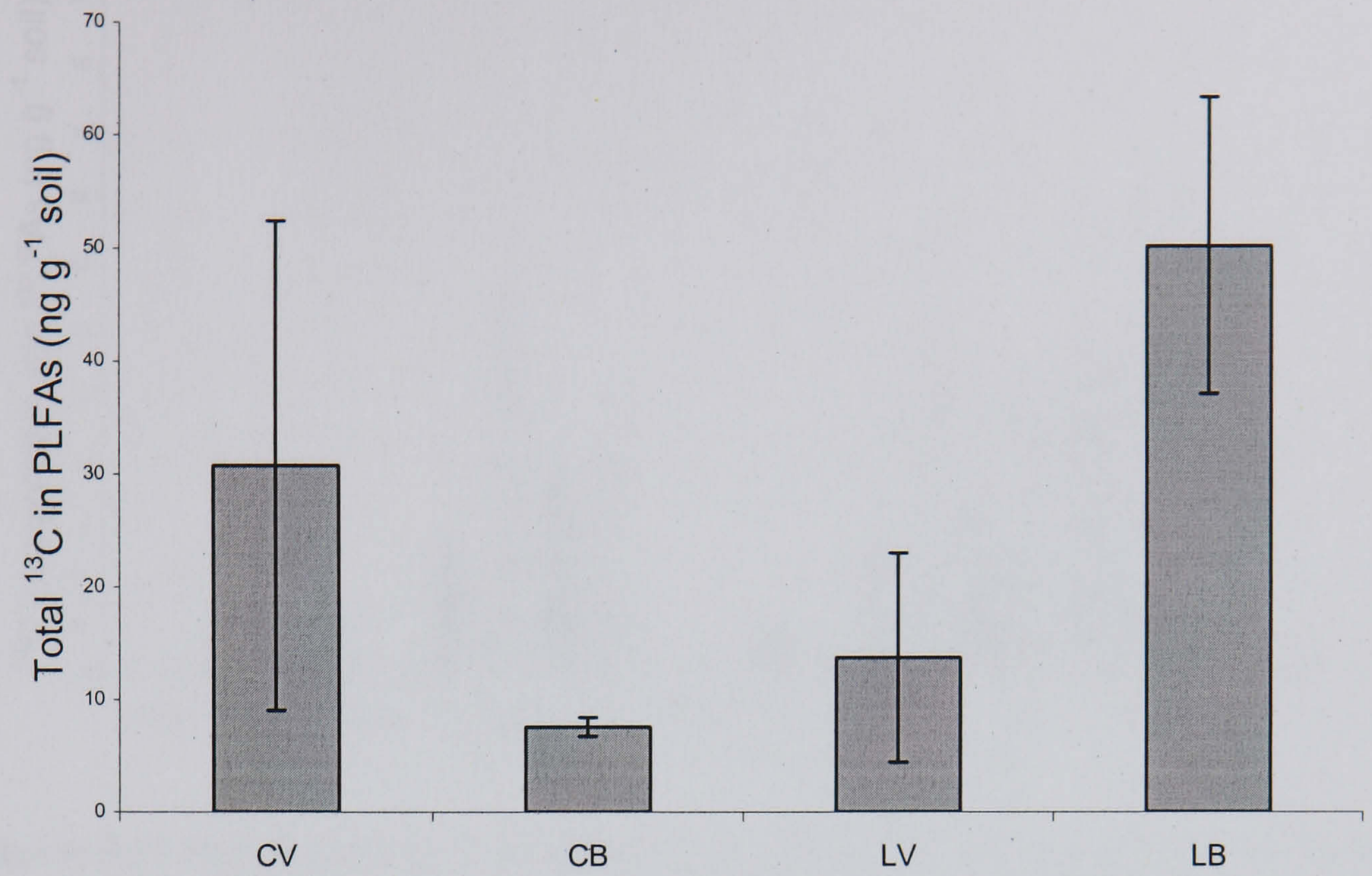

Figure 5.16 Total phenol-derived ^{13}C in PLFAs in the four treatments. Error bars are one standard error of the mean, (CB = control bare, CV = control with vegetation, LV = lime with vegetation, LB = lime bare).

Table 5.8 Results of the ANOVA of total phenol-derived ^{13}C in PLFAs across the four treatments.

Source	Type III Sum of Squares	df	Mean Square	F	Sig.
Corrected Model	3263.949(a)	3	1087.983	1.999	.193
Intercept	**7806.323**	**1**	**7806.323**	**14.342**	**.005**
Lime	484.126	1	484.126	.889	.373
Vegetation	129.717	1	129.717	.238	.639
Lime * Vegetation	2650.107	1	2650.107	4.869	.058
Error	4354.474	8	544.309		
Total	15424.746	12			
Corrected Total	7618.424	11			

a R Squared = .428 (Adjusted R Squared = .214)

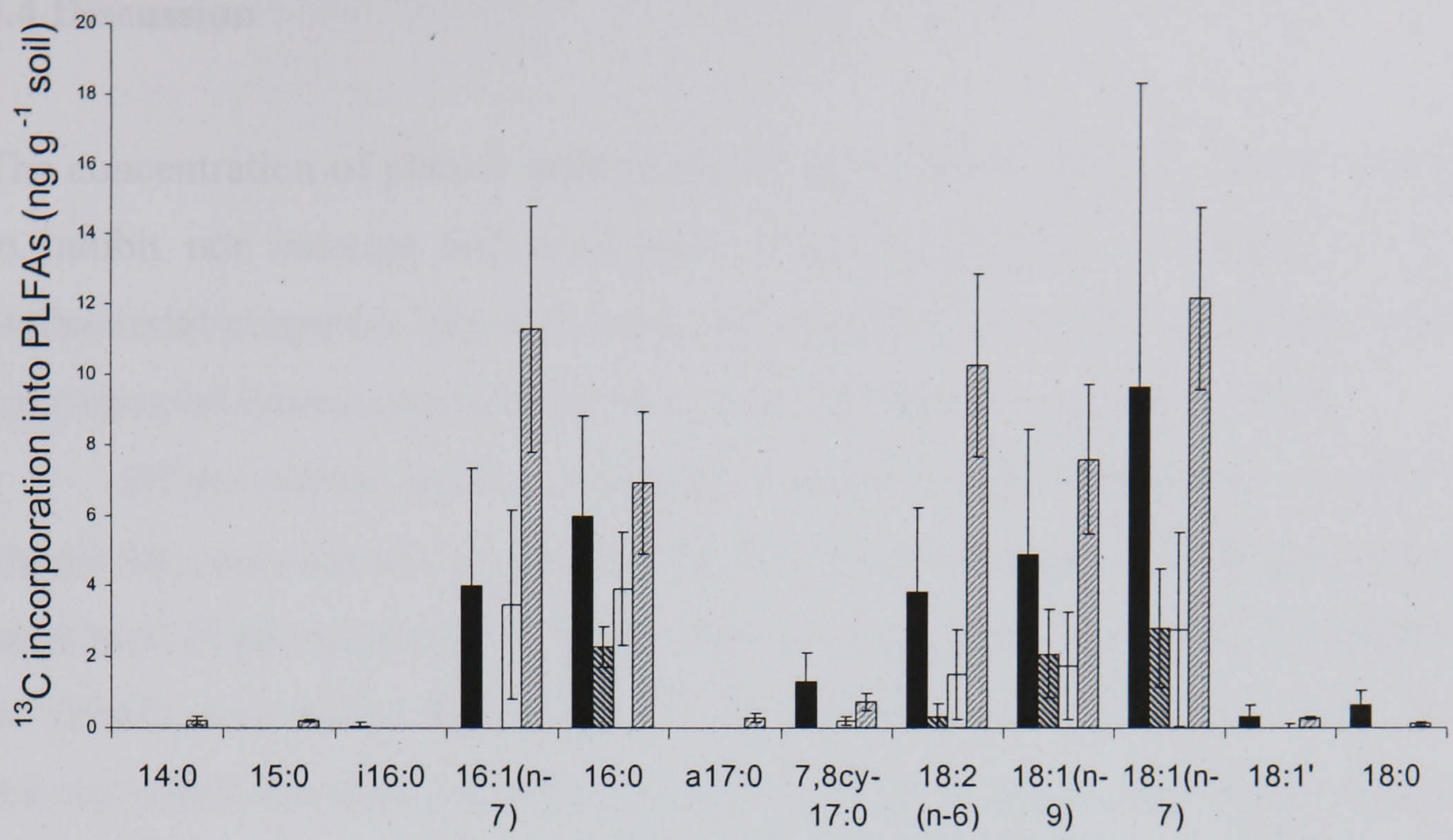

Figure 5.17 Phenol-derived ^{13}C incorporation into those PLFAs observed to show increases in d^{13}C values across the four treatments. Error bars are one standard error of the mean, (■= CV, ■=CB, □ = LV, ■ = LB).

Table 5.9 ANOVA and post hoc Duncan's for normalised PLFA compositions across the four treatments. Treatments with different letters across a row denote significant treatment differences.

		Duncan's Multiple Range Test			
PLFA	P	CV	CB	LV	LB
14:0	0.3197				
i15:0	0.3239				
a15:0	0.7276				
15:0	**0.0046**	**a**	**a**	**a**	**b**
i16:0	0.3875				
16:1	0.3486				
16:1(n-7)	0.1180				
16:1(n-5)	0.1720				
16:0	0.3869				
17:1(n-8)	0.1261				
7me-17:0	0.3033				
br17:0	0.6879				
i17:0	0.4267				
a17:0	0.0525				
7,8cy-17:0	0.2810				
18:2(n-6)	**0.0236**	**a**	**a**	**a**	**b**
18:1(n-9)	0.3001				
18:1(n-7)	0.4346				
18:1'	0.5539				
18:0	0.4006				
19:1	0.0820				
'7,8cy-19:0	0.1181				

5.4 Discussion

The concentration of phenol used in all the experiments (50 ppm) neither appeared to inhibit nor increase soil respiration. Although phenol is well-known for it's antibacterial properties, the concentrations used here are well beneath the published laboratory inhibitory concentrations (e.g. ca. 500 ppm, Kumar *et al.,* 2005).

Of the phenol applied, across all treatments described above, ca. 99.7% of phenol was not mineralised to CO_2. This is a high percentage and suggests there is a large pool of phenol derived C in the chamber. Looking at the work by Manefield *et al.* (2007), they found that, of the $^{13}C_6$ phenol added to a activated sludge micro-reactor within the first 100 minutes after addition, most of the phenol added had been metabolically converted, with 49% being incorporated into microbial biomass, 6% respired as CO_2 and less than 1% of the total ^{13}C labelled C incorporated into nucleic acids. The remainder of the added ^{13}C was adsorbed and/or complexed to suspended solids within the sludge. This would suggest that the amount incorporated into nucleic acids in this experiment would be negligible with the two largest pools being in microbial biomass and adsorbed to the soil. The percentage mineralised in the experiment in Chapter 5 is noticeably less that that cited by Manefield *et al.* (2007), however, there are several explanations for this. Firstly, the method of application. In Manefield *et al.* (2007) inlet liquor with phenol was added the activated sludge and then labelled phenol added after, allowing a priming effect, whereby a soil previously challenged with a substrate will respond faster to that substrate if exposed a second time than a naïve soil, (Betts 1991) such as the cores from Sourhope. Secondly the soils from Sourhope were exposed once in a relatively large volume of water, thus promoting both increased volatilisation than if added in small quantities, as in Manefield *et al.* (2007). Also, as mentioned in Chapter 1, phenol is highly mobile leaches readily into groundwater, thus making it likely that much of the phenol went through the cores to the bottom of the core, below the active organic layer where the sampling occurred. Finally, in the study by Manefield *et al.* (2007) the bioreactors were incubated overnight initially at 30 °C and subsequently maintained at 25 °C throughout the incubation and sampling periods,

which is around twice the temperature that the cores were incubated in this Chapter. The small percentage mineralised and detected as CO_2 again demonstrates the sensitivity of the GC-IRMS.

At the time of the experiment the question posed related purely to mineralisation and assimilation of the labelled substrate between the four treatments under investigation, and it was considered, primarily when conducting the experiments in the field, that the error term associated with calculating a mass balance, due to the leaching and volatilisation, would have greatly reduced the validity of the results. On reflection, a mass balance of the work carried out in the laboratory would have been interesting, and should the study be repeated or developed then it would be an area to be considered.

Somewhat surprisingly, it is clear that the results from the current experiment in the laboratory utilising labelled phenol were not the same as those found in the field experiments described in Chapter 3. In the laboratory, both the limed bare and the vegetated treatments showed a $^{13}CO_2$ cumulative flux which rose above that of the control whilst for the same experiment performed in the field, the limed flux remained lower than the control at all times. The total phenol-derived flux in the field experiments was significantly different between the treatments, with the LB treatment being significantly lower than the CB treatment and the LV being lower than the CV, tending toward significance. This could be as a result of the cores in the laboratory experiment being incubated at a higher temperature of 15°C rather than the field temperature during the experiment in Chapter 3, which was ca. 10°C. However, a more likely explanation for the differences between the responses to phenol in the field and the laboratory is disturbance.

The cores taken for the laboratory incubation will have resulted in severed roots and the leaching of carbon. Since limed soils tend to being more strongly C limited (Andersson and Nilsson, 2001) the addition of an available C source may have increased microbial respiration and turnover in the limed soils in the time between the cores actually being removed from the field and subsequently incubated, which was several days. The total cumulative phenol-derived $^{13}CO_2$ in the LB treatment was ca. twice as high in the laboratory when compared to the field

data, with the respective increase in total cumulative phenol-derived $^{13}CO_2$ in the LV treatments being ca. 6 fold. These discrepancies between the results of the field and laboratory experiments were only seen in the limed soils, supporting the above theory.

This change in behaviour of the limed soils sounds a cautionary note when extrapolating data obtained in the laboratory into the field. For example, Padmanabham *et al.,* (2003) removed samples from the field, sieved them and added substrates in the laboratory and extrapolated the results to *in situ* additions. If the level of disturbance experienced by the samples in the study described here in Chapter 5 resulted in up to a. 6 fold increase in mineralization of a substrate, then this should not be ignored when constructing microcosm experiments.

The PLFA composition in the soils from Sourhope had been significantly affected by the liming treatment, with a significant reduction in the bacterial population, whilst no significant change in the fungal population was detected. In the field the lime resulted in a significant decrease in the fungal population and again, the differences may be attributed to the input of C from root exudates.

The vegetation removal appeared to have a reverse effect on the total amount of ^{13}C in PLFAs in the limed treatments compared to the control treatments with an increase in LB compared with LV, and the converse occurring in CB compared to CV. If control soils are not as available-C limited as limed treatments, and with the LV treatment receiving the products of root cutting during collection, LB will be the most C limited treatment and therefore may have greatest demand for the phenol, as an exogenous available C source. Parallel changes in the microbial communities underpinning the observed changes in phenol mineralisation are unlikely, given that the label was incorporated into the PLFAs 16:1 (n-7), 16:0, 18:2 (n-6), 18:1 (n-9), 18:1 (n-7), which were the same as those seen in the field. Again, the assimilation of phenol was dominated by Gram-negative bacteria and fungi, given the labelling profile of the PLFAs.

Chapter 6. General Discussion

The overall aim of this thesis was to examine the impact of different soil treatments on the ability of microorganisms within soil to degrade substrates, largely using stable isotope approaches under *in situ* conditions. This lead to a consideration of the importance of vegetation in influencing soil microbial communities and the ability to degrade added pollutants. This was achieved largely by focussing on phenol as a substrate and aimed to establish the extent to which the addition of lime and the manipulation of vegetation affected the mineralization and assimilation of added phenol.

The main findings of the study were that: (1) the developed mobile mass spectrometer was able to very successfully detect $^{13}CO_2$ enriched air following the application of 300 cm^3 $^{13}C_6$ phenol (99%, 50 ppm) and $^{13}C_6$ glucose solution, 500 cm^3 (5 g l^{-1}, 1.69%) to the soil surface under field conditions (Chapters 2, 3 & 5). (2) In the field, the addition of lime to the soil was the only treatment to have any major effect on the initial rate at which microorganisms mineralised phenol and glucose, with N and biocide showing no significant effect (Chapter 2). Also, from field experiments, it was shown that the addition of lime significantly reduced the initial rate of phenol mineralization whilst the lime treatment did not appear to have any short term significant effect on the total cumulative phenol-derived $^{13}CO_2$ produced. When the vegetation had been removed, there became a significant effect of the liming treatment not only on the dynamics but also the total cumulative phenol-derived $^{13}CO_2$ produced; lime reduced the overall rate of mineralization to $^{13}CO_2$ (Chapter 3). (3) Forty-eight hours after the addition of $^{13}C_6$ phenol in the field, a maximum of only 0.3% of the added had been mineralised to $^{13}CO_2$ (Chapter 3). (4) These changes in mineralisation were associated with a lower concentration of microbial PLFAs in limed soils (Chapters 4 & 5). (5) The assimilation of ^{13}C from phenol, and subsequent incorporation into microbial PLFAs in the field, was dominated by the liming treatments. (Chapter 4). (6) Both the rates of mineralization of phenol and the effects of the liming treatment were not the same when studied in compared *in situ* and in the laboratory (Chapters 3 & 5).

The world's first mobile IR spectrometer has successfully detected $^{13}CO_2$ from highly enriched substrates both in the field, and in the laboratory. This is an

important technical breakthrough and removes the constraint of laboratory incubations and the associated artefacts. Chapter 5 clearly demonstrated that the behaviour of soils *in situ* is not always the same as when samples are taken and the same experiment performed in the laboratory; thus the opportunity to measure systems with minimal disturbance in the field allows the nature of these laboratory artefacts to be thoroughly investigated. Since the construction of the mobile mass spectrometer used in this work, another mobile mass spectrometer has been constructed and successfully used to measure the $\delta^{13}C$ and $\delta^{18}O$ of air sampled above a grassland canopy (Schnyder *et al.,* 2004). The technique will become of increasing importance in years to come.

The field study at Sourhope showed that the addition of lime significantly affected the initial rate at which phenol and glucose were mineralised, though did not significantly affect the total cumulative amount of phenol mineralized (Chapter 2). This was surprising as lime treatments at Sourhope showed greater biomass productivity, (Burt-Smith, 2003) and Grayston *et al.* (2001) and Fuentes *et al.* (2006) have attributed greater respiration rates and microbial biomass C to the increase in pH caused by the liming. They have demonstrated that, when compared to control unlimed soil, limed soils had faster C turnover rates and increased mineralization of organic matter. In the current work the removal of vegetation resulted in the total cumulative-phenol derived $^{13}CO_2$ in the lime soil being significantly lower than that in the control soil after 48 hours. The total cumulative-phenol derived $^{13}CO_2$ in the LV treatments was also tending towards significance. A possible explanation for the slower response in the limed plots to the phenol addition is evidenced by the lower microbial PLFA concentrations in the limed treatments (Figs. 4.5, 5.11) suggesting that the observed delay in mineralizing phenol may be due to the relatively smaller population size of phenol degraders in the limed soils, possibly caused by C limitation, as L addition results in increased leaching of DOC (Andersson and Nilsson, 2000).

Only very small amounts of the ^{13}C applied to the soil as $^{13}C_6$-phenol were traced into either the respired CO_2 or assimilated into the PLFAs. A maximum of 0.31% was accounted for in the field treatment (Chapters 3 & 4, see Fig. 6.1) whilst the treatment least able to degrade phenol was the LV treatment, at 0.05%. Looking purely at the *in situ* study, conclusions may be drawn that liming is detrimental to phenol degradation. However, when a similar

comparison was performed in the laboratory (Chapter 5, Fig.6.2), the LB treatment showed the greatest rate of phenol degradation, with 0.37% being traced and the amount of label mineralized and assimilated having increased ca. 5 fold in the LV treatment. The removal of the cores and placement in the laboratory will have resulted in the release of C into the cores from damaged and cut roots; also, the limed treatments were the only ones to be affected. These observations, coupled with those of Andersson and Nilsson (2000) leads to the conclusion that it was not the shift in the microbial community, associated with the lime treatment that was responsible for the different response to phenol addition by the lime treatments, but rather the resulting C limitation caused by the liming.

The success of the mobile laboratory raises the possibility for use in future work at enriched levels. With further fine tuning of sensitivity, it will be possible for the laboratory to detect isotopic differences at natural abundance levels. This will enable the mobile laboratory to be use in a far wider range of studies.

RNA SIP was not achieved during this work, however at the time the technique was in its infancy. It is now more widely used, and in conjunction with the PLFA SIP and work using the mobile laboratory would be able to provide a fuller picture of the degradation of substrates, down to the genus level.

The differences in phenol degradation are robust between the L and control treatments. The success in detecting enrichment in both mineralised $^{13}CO_2$ and PLFAs demonstrates the possibility to develop the work further to include more compounds of interest, such as Dichloro-Diphenyl-Trichloroethane (DDT). Whilst it is known that there are some species of bacteria capable of degrading DDT (or it's derivative DDE) the identities of many of these bacteria are not known (Foght *et al.*, 2001). In future the mobile laboratory combined with the SIP technique could be used to identify the organisms responsible for the degradation of DDT, with a view to enhancing bioremediation. The ability to take the mobile lab anywhere where there is vehicular access in the world means that, in the above example of future work with DDT, the soils could be studied *in situ* in Africa, avoiding the 'lab artifact' and thus resulting in any findings being of greater relevance to the areas affected.

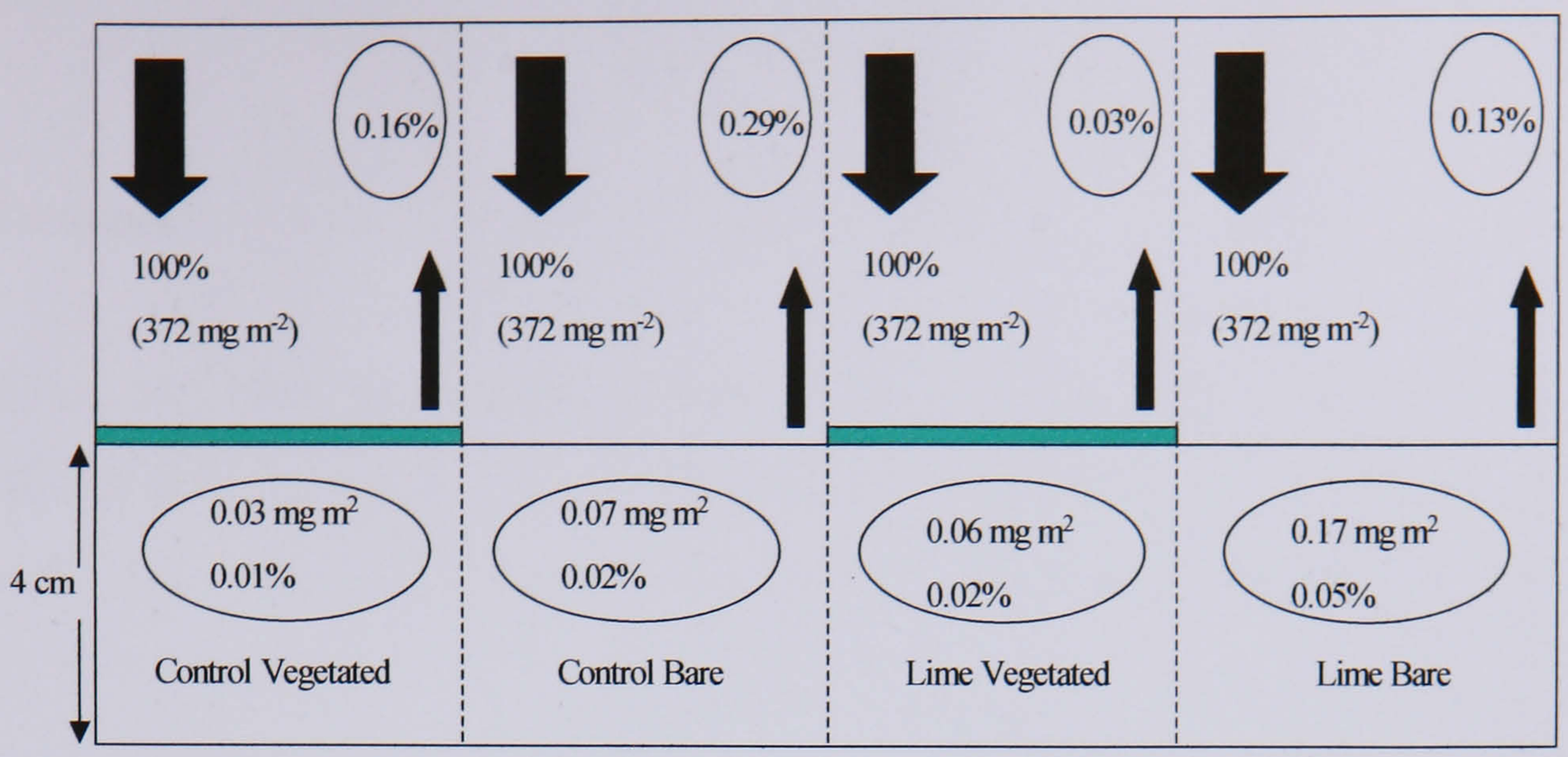

Figure 6.1 Field studies. Overview of the allocation of mineralised and assimilated ^{13}C following the application of 300 cm^3 $^{13}C_6$ phenol (99%, 50 ppm) to the soil surface of 4 treatments in the field.

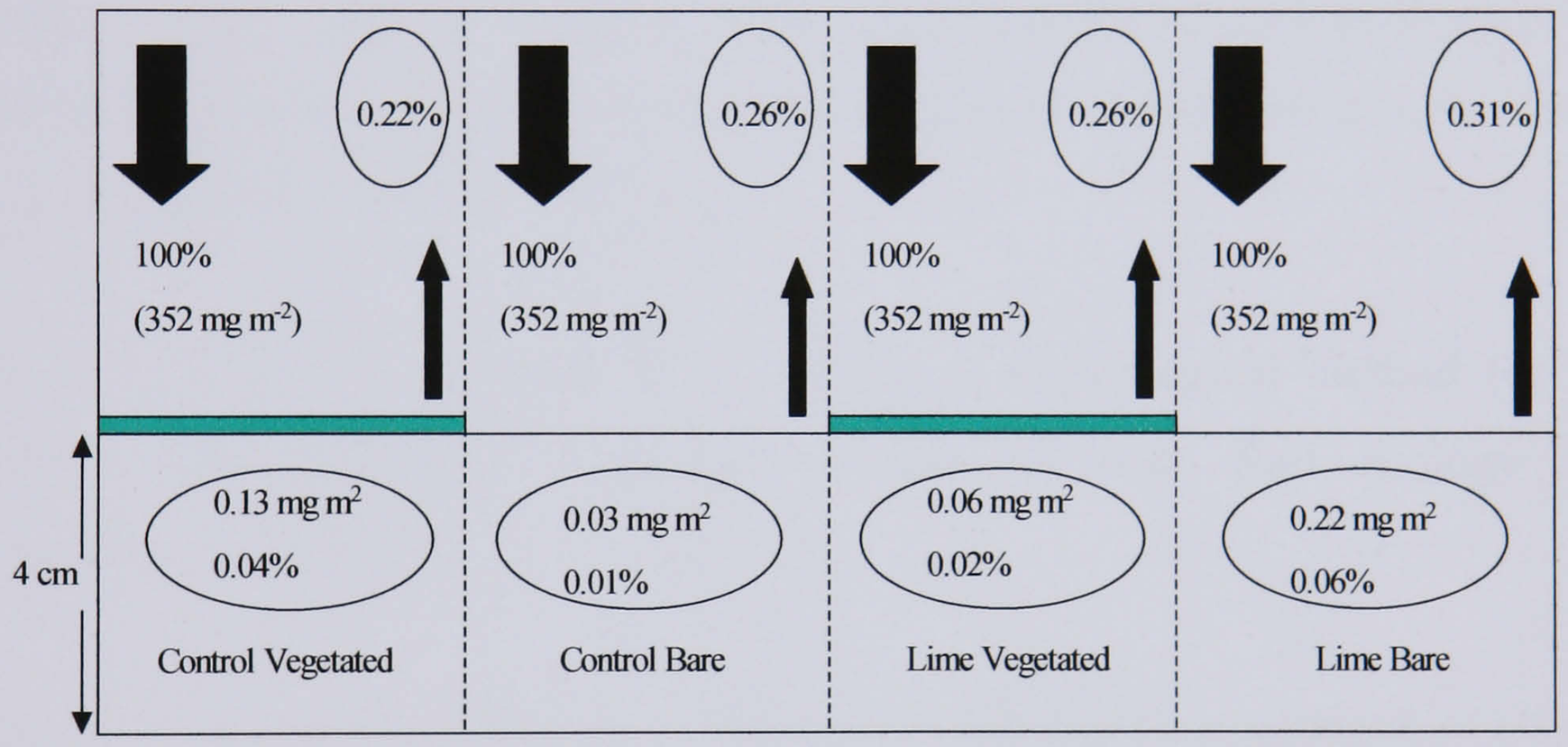

Figure 6.2 Laboratory study. Allocation of mineralised and assimilated ^{13}C following the application of 300 cm^3 $^{13}C_6$ phenol (99%, 50 ppm) to the soil surface of 4 treatments in the laboratory.

7. References

Alexander, M., 1965. Most probable number method for microbial populations. In: Methods of Soil Analysis. Part 2, Chemical and Microbiological Properties (Ed. Black, C. A.), 1467-1472. American Society of Agronomy, Madison, Wisconsin, USA.

Alexandrino, M., Knief, C., Lipski, A., 2001. Stable-isotope-based labeling of styrene-degrading microorganisms in biofilters. Applied and Environmental Microbiology 67, 4796-4804.

Anderson, J. P. E. and Domsch, K. H., 1974. Use of selective inhibitors in the study of respiratory activities and shifts in bacterial and fungal populations in soil. Annals of Microbiology 24, 189-194.

Anderson, J. P. E. and Domsch, K. H., 1978. A physiological method for the quantitative measurement of microbial biomass in soils. Soil Biology and Biochemistry 10, 215-221.

Annadurai, G., Juang, R. S., Lee, D. J., 2002. Microbiological degradation of phenol using mixed liquors of Pseudomonas putida and activated sludge. Waste Management 22, 703-710.

Atlas, R. M., 1982. In: Experimental Microbial Ecology (Eds. Burns, R. G. and Slater, J. H.), 84-102. Blackwell Scientific Publications. Oxford, U.K.

ATSDR, 1998. Toxicological Profile for Phenol, Agency for Toxic Substances and Disease Registry, Atlanta.

Bardgett, R. D., Hobbs, P. J., Frostegard,A., 1996. Changes in soil fungal:bacterial biomass ratios following reductions in the intensity of management of an upland grassland. Biology and Fertility of Soils 22, 261-264.

Bardgett, R. D., Leemans, D. K., Cook, R., Hobbs, P. J., 1997. Seasonality of the soil biota of grazed and ungrazed hill grasslands. Soil Biology & Biochemistry 29, 1285-1294.

Betts, W.D. (Ed), 1991. Biodegradation: Natural and Synthetic Materials. Springer-Verlag, Berlin, Germany

Boschker, H. T. S., Nold, S. C., Wellsbury, P., Bos, D., de Graaf, W., Pel, R., Parkes, R. J., Cappenberg, T. E., 1998. Direct linking of microbial populations to specific biogeochemical processes by C-13-labelling of biomarkers. Nature 392, 801-805.

Brant, J. B., Sulzman, E. W., Myrold, D. D., 2006. Microbial community utilization of added carbon substrates in response to long-term carbon input manipulation. Soil Biology & Biochemistry 38, 2219-2232.

Bull, I. D., Parekh, N. R., Hall, G. H., Ineson, P., Evershed, R. P., 2000. Detection and classification of atmospheric methane oxidizing bacteria in soil. Nature 405, 175-178.

Burt-Smith, G.. 2007. Sourhope Field Experiment Report IV (1999–2002). Ref Type: Report

Butler, J. L., Williams, M. A., Bottomley, P. J., Myrold, D. D., 2003. Microbial community dynamics associated with rhizosphere carbon flow. Applied and Environmental Microbiology 69, 6793-6800.

Chen, K. C., Lin, Y. H., Chen, W. H., Liu, Y. C., 2002. Degradation of phenol by PAA-immobilized Candida tropicalis. Enzyme and Microbial Technology 31, 490-497.

Clarke, F. E., 1965. Agar-plate method for total microbial count. In: Methods of Soil Analysis. Part 2, Chemical and Microbiological Properties (Ed. Black, C. A.), 1460-1466. American Society of Agronomy, Madison, Wisconsin, USA.

Crossman, Z. M., Ineson, P., Evershed, R. P., 2005. The use of C-13 labelling of bacterial lipids in the characterisation of ambient methane-oxidising bacteria in soils. Organic Geochemistry 36, 769-778.

Crossman, Z. M., Wang ,Z. P., Ineson, P., Evershed, R. P., 2006. Investigation of the effect of ammonium sulfate on populations of ambient methane oxidising bacteria by C-13-labelling and GC/C/IRMS analysis of phospholipid fatty acids. Soil Biology & Biochemistry 38, 983-990.

Davidson, D. A., Bruneau, P. M. C., Grieve, I. C., Young, I. M., 2002. Impacts of fauna on an upland grassland soil as determined by micromorphological analysis. Applied Soil Ecology 20, 133-143.

Environment Agency, 2002. The Effects of Contaminant Concentration on the Potential for Natural Attenuation, Technical Report P2 – 228/TR.

Environment Agency, 2005. Soil guideline values for phenol contamination. Science Report SGV 8

Finlay, B. J., Fenchel, T., 2001. Protozoan community structure in a fractal soil environment. Protist 152, 203-218.

Fitter, A. H., Gilligan, C. A., Hollingworth, K., Kleczkowski, A., Twyman, R. M., Pitchford, J. W., 2005. Biodiversity and ecosystem function in soil. Functional Ecology 19, 369-377.

Floyd,R., Abebe,E., Papert,A., Blaxter,M., 2002. Molecular barcodes for soil nematode identification. Molecular Ecology 11, 839-850.

Foght, J., April, T., Biggar, K., Aislabie, J., 2001. Bioremediation of DDT-Contaminated Soils: A Review. Bioremediation Journal 5, 225-246

Frostegard, A., Baath, E., Tunlid, A., 1993. Shifts in the Structure of Soil Microbial Communities in Limed Forests As Revealed by Phospholipid Fatty-Acid Analysis. Soil Biology & Biochemistry 25, 723-730.

Fuentes, J. P., Bezdicek, D. F., Flury, M., Albrecht, S., Smith, J. L., 2006. Microbial activity affected by lime in a long-term no-till soil. Soil & Tillage Research 88, 123-131.

Gavito, M. E., Olsson, P. A., 2003. Allocation of plant carbon to foraging and storage in arbuscular mycorrhizal fungi. Fems Microbiology Ecology 45, 181-187.

Gianazza, E., Eberini, I., Santi, O., Vignati, M., 1998. Denaturant-gradient gel electrophoresis: technical aspects and practical applications. Analytica Chimica Acta 372, 99-120.

Gornall, J. L.. Using density gradient ultra-centrifugation to recover ^{13}C labelled RNA from Escherichia coli: a method for use in soil ecology. 2000. University Of York. Ref Type: Thesis/Dissertation

Gray, N. D., Hastings, R. C., Sheppard, S. K., Loughnane, P., Lloyd, D., McCarthy, A. J., Head, I. M., 2003. Effects of soil improvement treatments on bacterial community structure and soil processes in an upland grassland soil. Fems Microbiology Ecology 46, 11-22.

Grayston, S. J., Griffith, G. S., Mawdsley, J. L., Campbell, C. D., Bardgett, R. D., 2001. Accounting for variability in soil microbial communities of temperate upland grassland ecosystems. Soil Biology & Biochemistry 33, 533-551.

Guerin, T. F., 1999. Bioremediation of phenols and polycyclic aromatic hydrocarbons in creosote contaminated soil using ex-situ land treatment. Journal of Hazardous Materials 65, 3, 305-315

Hanson, J. R., Macalady, J. L., Harris, D., Scow, K. M., 1999. Linking toluene degradation with specific microbial populations in soil. Applied and Environmental Microbiology 65, 5403-5408.

He, Z., Weigel, J., 1995. Purification and characterization of an oxygen-sensitive reversible 4-hydroxybenzoate decarboxylase from Clostridium hydroxybenzoicum. European Journal of Biochemistry 229, 77-82.

Heipieper, H. J., Diefenbach, R., Keweloh, H., 1992. Conversion of Cis Unsaturated Fatty-Acids to Trans, A Possible Mechanism for the Protection of Phenol-Degrading Pseudomonas-Putida P8 from Substrate Toxicity. Applied and Environmental Microbiology 58, 1847-1852.

Hinrichs, K. U., Hayes, J. M., Sylva, S. P., Brewer, P. G., Delong, E. F., 1999. Methane-consuming archaebacteria in marine sediments. Nature 398, 802-805.

Hinteregger, C., Leitner, R., Loidl, M., Ferschl, A., Streichsbier, F., 1992. Degradation of phenol and phenolic compounds by Pseudomonas putida EKII, Applied Microbiology and Biotechnology 37, 252–259

Hogberg, P., Ekblad, A., 1996. Substrate-induced respiration measured in situ in a C-3-plant ecosystem using additions of C-4-sucrose. Soil Biology & Biochemistry 28, 1131-1138.

Jenkinson, D. S. and Powlson, D. S., 1976. The effects of biocidal treatments on metabolism in soil - V. A method for measuring soil biomass. Soil Biology and Biochemistry 8, 209-213.

Jensen. J., 1996. Chlorophenols in the terrestrial environment. Reviews of Environmental Contamination and Toxicology 146, 25 - 51.

Johnson, D., Leake, J. R., Ostle, N., Ineson, P., Read, D. J., 2002. In situ (CO2)-C-13 pulse-labelling of upland grassland demonstrates a rapid pathway of carbon flux from arbuscular mycorrhizal mycelia to the soil. New Phytologist 153, 327-334.

Keweloh, H., Diefenbach, R., Rehm, H. J., 1991. Increase of phenol tolerance of Escherichia coli by alterations of the fatty-acid composition of the membrane-lipids. Archives of Microbiology 157, 49-53.

Killham, K., 1994. Soil Ecology. University Press, Cambridge, UK

Kuan, H. L., Fenwick, C., Glover, L. A., Griffiths, B. S., Ritz, K., 2006. Functional resilience of microbial communities from perturbed upland grassland soils to further persistent or transient stresses. Soil Biology and Biochemistry 38, 2300-2306.

Kumar, A., Kumar, S., Kumar, S., 2005. Biodegradation kinetics of phenol and catechol using Pseudomonas putida MTCC 1194. Biochemical Engineering Journal 22, 151-159.

Kunapuli, U., Lueders, T., Meckenstock, R.U., 2007. The use of stable isotope probing to identify key iron-reducing microorganisms involved in anaerobic benzene degradation. International Society for Microbial Ecology. 1, 643-653

Lack, A., Fuchs, G., 1994. Evidence that phenol phosphorylation to phenylphosphate is the first step in anaerobic phenol metabolism in a denitrifying Pseudomonas Sp. Archives of Microbiology 161, 132-139.

Lu, Y. H., Murase, J., Watanabe, A., Sugimoto, A., Kimura, M., 2004. Linking microbial community dynamics to rhizosphere carbon flow in a wetland rice soil. Fems Microbiology Ecology 48, 179-186.

Mackay D., Shiu W. Y., Ma, K. C., 2000. Physical-Chemical Properties and Environmental Fate Handbook on CD-ROM. CRC Press, Boca Raton, Florida

Manefield, M., Whiteley, A. S., Ostle, N., Ineson, P., Bailey, M. J., 2002a. Technical considerations for RNA-based stable isotope probing: an approach to associating microbial diversity with microbial community function. Rapid Communications in Mass Spectrometry 16, 2179-2183.

Manefield, M., Whiteley, A. S., Griffiths, R. I., Bailey, M. J., 2002b. RNA stable isotope probing, a novel means of linking microbial community function to Phylogeny. Applied and Environmental Microbiology 68, 5367-5373.

Manefield, M., Griffiths, R., McNamara, N. P., Sleep, D., Ostle, N., Whiteley, A., 2007. Insights into the fate of a 13C labelled phenol pulse for stable isotope probing (SIP) experiments. Journal of Microbiological Methods 69, 340-344

McCaig, A. E., Glover, L. A., Prosser, J. I., 2001. Numerical analysis of grassland bacterial community structure under different land management regimens by using 16S ribosomal DNA sequence data and denaturing gradient gel electrophoresis banding patterns. Applied and Environmental Microbiology 67, 4554-4559.

McDonald, I. R., Hall G. H., Pickup R. W., Murrell J. C., 1996. Methane oxidation potential and preliminary analysis of methanotrophs in blanket bog peat using molecular ecology techniques. FEMS Microbiol. Ecol. 21, 197–211

McNamara, N., Benham, D., Sleep, D., Grant, H., Stott, A., 2002. Development of a trace gas stable isotope capture system in a mobile laboratory for temporal and spatial sampling of field and laboratory experiments. Rapid Communications in Mass Spectrometry 16, 2165-2171.

Meselson, M., Stahl, F. W., 1958. The Replication of DNA. Cold Spring Harbor Symposia on Quantitative Biology 23, 9-12.

Mishra, V., Lal, R., Srinivasan, 2001. Enzymes and operons mediating xenobiotic degradation in bacteria. Critical Reviews in Microbiology 27, 133-166.

Neujahr, H. Y., Gaal, A., 1973. Phenol hydroxylase from yeast: purification and properties of the enzymes from Trichosporon cutaneum. European Journal of Biochemistry 35, 386–400

Ostle, N., Ineson, P., Benham, D., Sleep, D., 2000. Carbon assimilation and turnover in grassland vegetation using an in situ (CO2)-C-13 pulse labelling system. Rapid Communications in Mass Spectrometry 14, 1345-1350.

Padmanabhan, P., Padmanabhan, S., DeRito, C., Gray, A., Gannon, D., Snape, J. R., Tsai, C. S., Park, W., Jeon, C., Madsen, E. L., 2003. Respiration of C-13-labeled substrates added to soil in the field and subsequent 16S rRNA gene analysis of C-13-labeled soil DNA. Applied and Environmental Microbiology 69, 1614-1622.

Pelz, O., Chatzinotas, A., Zarda-Hess, A., Abraham, W. R., Zeyer, J., 2001. Tracing toluene-assimilating sulfate-reducing bacteria using C-13-incorporation in fatty acids and whole-cell hybridization. Fems Microbiology Ecology 38, 123-131.

Phillips, R. L., Zak, D. R., Holmes, W. E., White, D. C., 2002. Microbial community composition and function beneath temperate trees exposed to elevated atmospheric carbon dioxide and ozone. Oecologia 131, 236-244.

Picard, C., Ponsonnet, C., Paget, E., Nesme, X. and Simonet, P., 1992. Detection and enumeration of bacteria in soil by direct DNA extraction and polymerase chain reaction. Applied and Environmental Microbiology 58, 2717-2722.

Pombo, S. A., Pelz, O., Schroth, M. H., Zeyer, J., 2002. Field-scale C-13-labeling of phospholipid fatty acids (PLFA) and dissolved inorganic carbon: tracing acetate assimilation and mineralization in a petroleum hydrocarbon-contaminated aquifer. Fems Microbiology Ecology 41, 259-267.

Prosser, J. I., Rangel-Castro, J. I., Killham, K., 2006. Studying plant-microbe interactions using stable isotope technologies. Current Opinion in Biotechnology 17, 98-102.

Radajewski, S., Ineson, P., Parekh, N. R., Murrell, J. C., 2000. Stable-isotope probing as a tool in microbial ecology. Nature 403, 646-649.

Radajewski, S., McDonald, I. R., Murrell, J. C., 2003. Stable-isotope probing of nucleic acids: a window to the function of uncultured microorganisms. Current Opinion in Biotechnology 14, 296-302.

Rangel-Castro, J. I., Prosser, J. I., Scrimgeour, C. M., Smith, P., Ostle, N., Ineson, P., Meharg, A., Killham, K., 2004. Carbon flow in an upland grassland: effect of liming on the flux of recently photosynthesized carbon to rhizosphere soil. Global Change Biology 10, 2100-2108.

Raynaud, X., Lata, J. C., Leadley, P. W., 2006. Soil microbial loop and nutrient uptake by plants: a test using a coupled C : N model of plant-microbial interactions. Plant and Soil 287, 95-116.

Sakai, M., Miyauchi, K., Kato, N., Masai, E., Fukuda, M., 2003. 2-hydroxypenta-2,4-dienoate metabolic pathway genes in a strong polychlorinated biphenyl degrader, Rhodococcus sp strain RHA1. Applied and Environmental Microbiology 69, 427-433.

Schlegel, H. G., 1993. General Microbiology. Cambridge University Press.

Schnyder, H., Schaufele, R., Wenzel, R., 2004. Mobile, outdoor continuous-flow isotope-ratio mass spectrometer system for automated high-frequency C-13- and O-18-CO2 analysis for Keeling plot applications. Rapid Communications in Mass Spectrometry 18, 3068-3074.

Staddon, P. L., Ostle, N., Dawson, L. A., Fitter, A. H., 2003. The speed of soil carbon throughput in an upland grassland is increased by liming. Journal of Experimental Botany 54, 1461-1469.

Staddon, P. L., 2004. Carbon isotopes in functional soil ecology. Trends in Ecology & Evolution 19, 148-154.

Stenberg, M., Stenberg, B., Rydberg, T., 2000. Effects of reduced tillage and liming on microbial activity and soil properties in a weakly-structured soil. Applied Soil Ecology 14, 135-145.

Stotzky, G., Norman, A.G., 1961. Factors limiting microbial activities in soil. I. The level of substrate, nitrogen and phosphorus. Archiv fuer Mikrobiologie 40, 341–369.

Topp, E., Hendel, J. G., Lu, Z. X., Chapman, R., 2006. Biodegradation of caffeine in agricultural soils. Canadian Journal of Soil Science 86, 533-544.

Torsvik, V., Goksoyr, J., Daae,F. L., 1990. High Diversity in DNA of Soil Bacteria. Applied and Environmental Microbiology 56, 782-787.

Treonis, A. M., Ostle, N. J., Stott, A. W., Primrose, R., Grayston, S. J., Ineson, P., 2004. Identification of groups of metabolically-active rhizosphere microorganisms by stable isotope probing of PLFAs. Soil Biology & Biochemistry 36, 533-537.

Trott, D., Dawson, J. J. C., Killham, K. S., Miah, M. R. U., Wilson, M. J., Paton, G. I., 2007. Comparative evaluation of a bioluminescent bacterial assay in terrestrial ecotoxicity testing. Journal of Environmental Monitoring 9, 44-50.

USEPA, 1996. Soil Screening Guidance: Technical Background Document, EPA/540/R95/128.

USEPA, 1999. Aerobic Biodegradation of Organic Chemicals in Environmental Media: A Summary of Field and Laboratory Studies. Prepared by Environmental Science Center, Syracuse Research Corporation.

van Hees, P. A. W., Jones, D. L., Finlay, R., Godbold, D. L., Lundstomd, U. S., 2005. The carbon we do not see - the impact of low molecular weight compounds on

carbon dynamics and respiration in forest soils: a review. Soil Biology & Biochemistry 37, 1-13

van Schie, P. K., Young, L. Y., 2000. Biodegradation of phenol: Mechanisms and applications. Bioremediation Journal 4, 1-18.

Vandenkoornhuyse, P., Husband, R., Daniell, T. J., Watson, I. J., Duck, J. M., Fitter, A. H., Young, J. P. W., 2002. Arbuscular mycorrhizal community composition associated with two plant species in a grassland ecosystem. Molecular Ecology 11, 1555-1564.

Walker, N., 1973. Metabolism of chlorophenols by Rhodotorula glutinis. Soil Biology and Biochemistry 5, 525-530.

Wallis, G. W. and Wilde, S. A., 1957. Rapid method for the determination of carbon dioxide evolved from forest soil. Ecology 38, 359-361.

Watanabe, K., Baker, P. W., 2000. Environmentally relevant microorganisms. Journal of Bioscience and Bioengineering 89, 1-11.

Watanabe, K., 2001. Microorganisms relevant to bioremediation. Current Opinion in Biotechnology 12, 237-241.

White, D. C., Davis, W. M., Nickels, J. S., King, J. D., Bobbie, R. J., 1979. Determination of the sedimentary microbial biomass by extractable lipid phosphate. Oecologia 40, 51-62.

WHO, 1994. Phenol, Environmental Health Criteria Monograph 161, World Health Organization, Geneva.

Yoshitake, S., Sasaki, A., Uchida, M., Funatsu, Y., Nakatsubo, T., 2007. Carbon and nitrogen limitation to microbial respiration and biomass in an acidic solfatara field. European Journal of Soil Biology 43, 1-13.

Zelles, L., Bai, Q. Y., Beck, T. and Beese, F., 1992. Signature fatty acids in phospholipids and lipopolysaccharides as indicators of microbial biomass and community structure in agricultural soils. Soil Biology and Biochemistry 24, 317-323.

Zelles, L., 1999. Identification of single cultured micro-organisms based on their whole-community fatty acid profiles, using an extended extraction procedure. Chemosphere 39, 665-682.